2015

Mechanisms Controlling Stem Cell Differentiation

Tran Doan Ngoc Tran
Louisiana State University and Agricultural and Mechanical College, ngoctran2711@gmail.com

MECHANISMS CONTROLLING STEM CELL DIFFERENTIATION

A Dissertation

Submitted to the Graduate Faculty of the
Louisiana State University and
Agricultural and Mechanical College
in partial fulfillment of the
requirements for the degree of
Doctor of Philosophy

in

The Interdepartmental Program in
Veterinary Medical Science
through
The Department of Comparative Biomedical Sciences

by
Tran Doan Ngoc Tran
D.V.M, Nong Lam University, 2006
May 2015

ACKNOWLEDGMENTS

First of all, I would like to express my utmost gratitude to my mentor, Dr. Henrique Cheng for his continuously great support and guidance, strong knowledge in signaling, cell culture and ion channel electrophysiology. I always appreciate his sympathy, enthusiastic sharing research experience from not only himself but also other past graduate students, researchers, spontaneous guidance since the first day I came to his lab when everything was new. He also spent time teaching me how to criticize papers by practicing as a reviewer, caring for my private life and health. Without his help, my work and dissertation for this PhD degree at Louisiana State University would have not been possible.

In addition, I would like to thank my committee members for their guidance and help throughout my program. I am grateful to Dr. Shaomian Yao for his expertise in molecular biology, cell culture and his willingness to assist me. I would also like to express my gratitude to Dr. Jeffrey Gimble, the expert in stem cells who continuously supported my project by proposing wonderful ideas and providing stem cells for my studies. Likewise, I will never forget the invaluable guidance from Dr. Masami Yoshimura.

I appreciate very much the help from our collaborators, Dr. Arthur Penn and Dr. Rui Xiao for microarray analysis, Dr. Ji-Ming Feng for MTT assay, Dr. Marxa Figueiredo and Ms. Olga Zolochevska for generating TRPM4 knockdown stem cells, Dr. Li-Jun Yang and Dr. Hai Wang for western blot and RT-PCR of human adipose tissue, Dr. Bruce Allan Bunnell for providing human bone marrow-derived stem cells, and Dr. Walter Haw Hsu for providing reagents for experiments.

I convey my warm thanks to Drs. Hongzhi He, Dawen Liu, and Suidong Ouyang for the assistance with molecular techniques.

I would like to thank all instructors in the Department of Comparative Biomedical Sciences for their contribution to my knowledge. I also give my sincere thanks to Drs. Nguyen Ngoc Tuan, Tran Thi Dan, Nguyen Van Khanh, Tran Thanh Phong, Ho Thi Kim Hoa, Vo Tan Dai, and Nguyen Tat Toan at the Faculty of Animal Science and Veterinary Medicine, Nong Lam University, Ho Chi Minh City, Vietnam for their invaluable support during my studies.

I would like to extend my deepest gratitude to my parents, Mr. Tran Van Khanh and Mrs. Doan Thi Phuong Tra, my sister, Dr. Tran Doan Phuong Tran and my younger brother, Tran Doan Khanh Vu who devoted all of their life to my studies and countless hours listening to my work, Mr. Du Ba Thanh, MSc., Mr. Vo Van Cam for the continuous support.

I give my special thanks to Drs. Michael Brian Flanagan, Maryam Rezai Rad, and Ms. Chunhong Li for their friendship and support, especially, Dr. Bui Thi Thu Trang, my close friend.

Finally, I appreciate very much the CBS staff for all of their assistance during my time at the School of Veterinary Medicine.

TABLE OF CONTENTS

LIST OF TABLES

LIST OF FIGURES

LIST OF ABBREVIATIONS

ACTH	Adrenocorticotropic hormone
ADP	Adenosine diphosphate
AdSCs	Adult stem cells
ALDH6A1	Aldehyde dehydrogenase 6 family member A1
AMP	Adenosine monophosphate
AMP-PNP	Adenylyl-imidodiphosphate
aP2	Adipocyte protein 2
ASPN	Asporin
ARS	Alizarin Red S
AVP	Arginine vasopressin
BAT	Brown adipose tissue
BMI	Body mass index
BMP	Bone morphogenetic protein
cAMP	Cyclic adenosine monophosphate
CAN	Ca^{2+}-activated non-selective cation
CD	Cluster of differentiation
CDK6	Cyclin-dependent kinase 6
cDNA	Complementary deoxyribonucleic acid
C/EBPβ	CCAAT/enhancer-binding protein β
CITED1	Cbp/p300-interacting transactivator 1
Col3a1	Collagen alpha-1(III)
CRAC	Ca^{2+} release-activated Ca^{2+} channels
CSCs	Cancer stem cells

DAG	Diacylglycerol
DLX3	Distal-less homeobox 3
DPSCs	Dental pulp stem cells
ER	Endoplasmic reticulum
ERK	Extracellular signal-regulated kinase
ESCs	Embryonic stem cells
FAS	Fatty acid synthase
FIGF	c-fos induced growth factor
Flt1	FMS-like tyrosine kinase 1
Fura-2AM	Fura-2 acetoxymethyl ester
GAPDH	Glyceraldehyde-3-phosphate dehydrogenase
hASCs	Human adipose-derived stem cells
hBMSC	Human bone marrow-derived stem cells
IBMX	3-isobutyl-1-methylxanthine
IL-2	Interleukin 2
IL6R	Interleukin 6 receptor
IP_3R	Inositol-1,4,5-triphosphate receptor
iPSCs	Induced pluripotent stem cells
LPIN1	Lipin 1
LPL	Lipoprotein lipase
LUM	Lumican
MAPK	Mitogen-activated protein kinases
MEPE	Matrix extracellular phosphoglycoprotein
MGP	Matrix γ-carboxyglutamate protein

miRNA	Micro-ribonucleic acid
MMP3	Matrix metallopeptidase 3
MSCs	Mesenchymal stem cells
NFAT	Nuclear factor of activated T-cells
NFE2	Nuclear factor erythroid-derived 2
NMDG	N-methyl-D-glucamine
ORO	Oil Red O
PI3K/Akt/mTOR	Phosphoinositide-3-kinase/Akt/mammalian target of rapamycin
PIP_2	Phosphatidylinositol-4,5-biphosphate
PKA	Protein kinase A
PKC	Protein kinase C
PLC	Phospholipase C
PPARγ	Peroxisome proliferator-activated receptor γ
rDFSCs	Rat dental follicle stem cells
RGS2	G-protein signaling 2
RT-PCR	Reverse transcriptase polymerase chain reaction
Runx2	Runt-related transcription factor 2
SELENBP1	Selenium binding protein 1
SFRP1	Secreted frizzled-related protein 1
shRNA	Short hairpin ribonucleic acid
Smad1	Sma and Mad related family 1
SOCs	Store-operated Ca^{2+} channels
SPP1	Secreted phosphoprotein 1

STIM1	Stromal interaction molecule 1
TG	Thapsigargin
TRPA	Transient receptor potential ankyrin
TRPC	Transient receptor potential canonical
TRPM4	Transient receptor potential melastatin 4
TRPML	Transient receptor potential mucolipin
TRPN	Transient receptor potential *Drosophila* no mechano-potential C
TRPP	Transient receptor potential polycystin
TRPV	Transient receptor potential vallinoid
VDCCs	Voltage dependent Ca^{2+} channels
WIF1	WNT inhibitory factor 1

ABSTRACT

Mesenchymal stem cells are multipotent cells that can differentiate into many cell types. However, the molecular mechanism controlling this process remains unclear. We utilized rat dental follicle stem cells (rDFSCs) and human adipose derived stem cells (hASCs) to study the mechanisms controlling osteogenesis and adipogenesis. Elevations in the intracellular Ca^{2+} concentration are a phenomenon commonly observed during stem cell differentiation but cease after the process is complete. The Transient Receptor Potential Melastatin 4 (TRPM4) is an ion channel that controls Ca^{2+} signals in excitable and non-excitable cells. However, there are no studies on TRPM4 in stem cells. In another study, we investigate the mechanism by which arginine vasopressin (AVP), a neuropeptide hormone secreted mostly from the posterior pituitary gland increased Ca^{2+} signals and inhibited adipogenesis in hASCs.

The overall goal of our studies is to investigate the effect of TRPM4 and AVP on stem cell differentiation and Ca^{2+} signaling. First, we identified TRPM4 gene expression and its characteristics such as Ca^{2+}-activated, voltage dependent and monovalent conducting properties in rDFSCs. Molecular suppression of TRPM4 transformed the normal agonist-induced first and secondary phases of Ca^{2+} signals into a gradual and sustained increase which enhanced osteogenesis but inhibited adipogenesis in rDFSCs. Next, we examined TRPM4's impact on Ca^{2+} signals and adipogenesis in hASCs, which is a more suitable stem cell type for adipogenic studies. Suppression of the TRPM4 diminished the histamine-induced Ca^{2+} signals mainly via H1 receptors. The increases in

intracellular Ca^{2+} were due to influx via voltage-dependent Ca^{2+} channels of the L-type ($Ca_v1.2$) and release from the endoplasmic reticulum (ER). Lastly, we determined the role of AVP on adipogenesis in hASCs. These cells were responsive to AVP stimulation by increasing intracellular Ca^{2+} via V1a receptors, Gq-proteins and the PLC-IP_3 pathway. Both Ca^{2+} release from the ER and influx from the extracellular space contribute to the Ca^{2+} signals. AVP supplementation to the differentiation media decreased the number of adipocytes during adipogenesis. The effect of AVP on adipocyte formation was reversed by the V1a receptor blocker V2255. In conclusion, TRPM4 and AVP control Ca^{2+} signals which affect stem cell differentiation.

CHAPTER 1: STEM CELLS AND Ca^{2+} SIGNALING

1.1 STEM CELLS

Stem cells are cells that have capacity for self-renewal, clonogenic entity and potency [1]. Stem cell research is focused on tissue/adult stem cells, embryonic stem cells and induced pluripotent stem cells. Also, cancer stem cells are being used to develop diagnostic tests and effective anti-tumor therapy [1].

1.1.1 Embryonic stem cells

Embryonic stem cells (ESCs) are pluripotent cells derived from the inner cell mass of the blastocyst that can differentiate into all cell types except placenta [2]. They are promising for tissue engineering because of their proliferation capability and sustained potency. However, there are ethical issues preventing their use. In addition, they can cause tumors and immune rejection after transplanted into patients [3].

1.1.2 Induced pluripotent stem cells

Induced pluripotent stem cells (iPSCs) are somatic cells that are reprogrammed to become pluripotent like ESCs [4]. Yamanaka's group utilized retroviral expression of 4 transcription factors (Oct4, Sox2, Klf4 and c-Myc) in mouse fibroblast to generate embryonic stem cell-like cells [4]. Next, Yu's group utilized Lin-28 instead of c-Myc to induce iPSCs from human somatic cells [5]. Currently, there are various approaches to induce iPSCs such as RNA reprogramming (miRNAs, RNA virion, RNA replicon), protein, polycistron, and non-replicating plasmids (Figure 1.1) [6]. iPSCs have advantages because of the absence of ethical issues. Furthermore, they can differentiate into three germ layers,

proliferate continuously *in vitro*, and can be used for future disease treatment. These cells open new opportunities for regenerative medicine and stem cell modeling of human disease [7]. However, their disadvantages are low reprogramming efficiency, potential for genetic and epigenetic abnormalities, tumorigenicity, and immunogenicity of transplant cells [6-8].

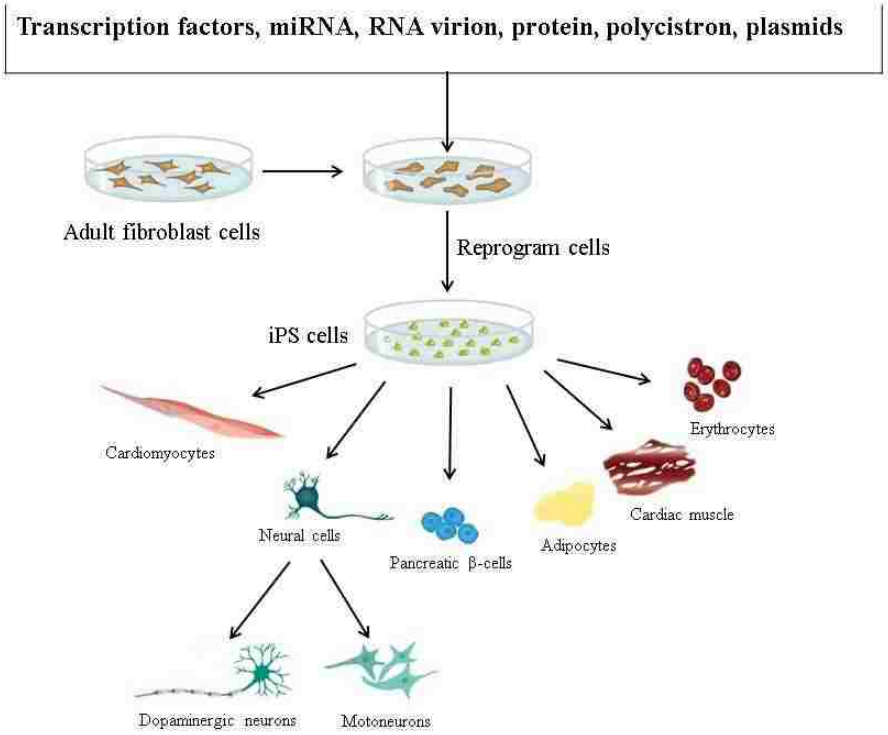

Figure 1.1 Reprogramming pluripotent stem cells (Modified from [9] and http://www.rndsystems.com/Cytokine_cb09i2_induced_pluripotent_stem_cells.aspx.)

1.1.3 Cancer stem cells

Cancer stem cells (CSCs) are derived from damaged or mutated stem cells/progenitor cells that have self-renewal, differentiation and tumor generating properties [1, 10]. Despite their limited numbers, CSCs are a major cause of tumors. They share some similar signaling pathways with normal stem cells like Bmi-1 and

Wnt signaling [10]. They are hereditary, unstable, and highly resistant to chemotherapy and radiotherapy. CSCs are thought to be responsive for tumor regrowth after conventional radiation treatment.

1.1.4 Adult stem cells

Adult stem cells (AdSCs) are cells derived from postembryonic stage tissue with self-renewal capability and multipotency [1]. They include hematopoietic, neural, epithelial, skin, and mesenchymal stem cells (MSCs). This last type is present in many tissues such as bone marrow, dental follicle and fat. DFSCs are isolated from medical waste, unerupted third molars and have advantages such as ease to collect with high efficiency, low morbidity, and good for bone regeneration in osteoporosis [11, 12]. hASCs from adipose tissue have minimal loss of differentiation potential after cryopreservation which make this kind of stem cell a potential source for tissue regeneration [13, 14]. As AdSCs are taken from patients, immune rejection and teratoma will not occur when transplanted back to the same patients. For example, bone marrow-derived stem cells (BMSCs) are used to treat leukemia, lymphoma, and several inherited blood disorders [15].

1.1.4.1 Dental follicle stem cells

The dental follicle is a loose connective tissue around the developing tooth and is composed of different cell populations derived from the cranial neural crest. Bovine dental follicle contains precursor cells that can differentiate into cementum matrix after being transplanted into mice [16, 17]. Dental follicle precursors/stem cells express putative stem cell markers such as nestin, Notch-1, STRO-1, Oct4, and Nanog as well as mesenchymal stem cell-related surface antigens like CD13,

CD29, CD44, CD73, and CD105 [18-20]. Hypoxia increases the growth and differentiation compared to normoxia [21]. DFSCs can proliferate, form colonies and be harvested at a large volume [20, 22, 23]. In addition, they differentiate into adipocytes better than dental pulp stem cells (DPSCs) but have lower potential to form chondrocytes, and osteoblasts [24]. The osteogenic potential of hDFSCs is higher than hASCs while the opposite is observed during adipogenesis [25]. After cryopreservation, many characteristics of DFSCs such as expression of stem cell markers, proliferation, differentiation, apoptosis and transcription-related genes are unchanged [26]. DFSCs lose their osteogenic properties about passage 11 [27]. Under heat-stress culture condition, there is increased cell proliferation, osteogenesis and expression of marker genes such as BMP2, BMP6, Col3a1, Flt1, Runx2 and SPP1 [28]. Under serum-free conditions, DFSCs form spheroid clusters through focal adhesion kinase signaling [29]. Cementoblast formation from DFSCs involves BMP2/7, MAPK and Smad1 pathway when stimulated by enamel matrix derivatives *in vitro* [30]. BMP-9 promotes osteogenesis by activating p38MAPK pathway and inhibiting ERK1/2 activity in rDFSCs [31]. Notch1 signaling is activated by DLX3 during proliferation and self-renewal in hDFSCs and impairs osteogenesis by downregulating BMP2/DLX3 [32, 33]. BMP4 and BMP6 are involved in osteogenic differentiation of DFSCs since they are upregulated after three days in osteogenic induction media [34]. High levels of BMP6 are required to maintain their osteogenic capability because knockdown reduces osteogenesis [27]. Transcription factors such as TP53 improves DFSC proliferation while SP1 stimulates osteogenesis [35]. Early growth response gene 1 increases osteogenesis

in hDFSCs by facilitating BMP2 and DLX3 expression [36]. Purinergic receptor P2X6, P2Y4 and P2Y14 receptors are also involved in osteogenic and adipogenic induction of hDFSCs and hASCs [37].

1.1.4.2 Human adipose-derived stem cells

The origin of hASCs is from the mesoderm layer of the embryo [38]. They are multipotent cells that can differentiate into adipocytes, chondrocytes, osteoblasts, hepatocytes, myocytes, and pancreatic cells [13]. They have fibroblastic morphology and colony-forming unit ability; they share similar surface antigens with other MSCs such as $CD44^+$, $CD73^+$, $CD90^+$, $CD105^+$, $CD45^-$, and $CD31^-$ [39]. The immunogenicity of hASCs after passage 2 fails to show T lymphocyte reaction during *in vitro* expansion [40]. In addition, hASCs can cause dendritic cell tolerance when being co-cultured by inhibiting $CD4^+$ T cell activation [41]. They have normal karyotype, reduced telomerase levels and cease proliferation at passage 30 [42]. hASCs from different donors vary in adipogenic capability [43]. Intracellular Ca^{2+} oscillations in undifferentiated hASCs may be involved in stem cell maintenance and are dependent on Ca^{2+} release and influx [44]. ERK suppression inhibits osteogenesis but induces adipogenesis [45, 46]. Endogenous Wnt signaling inhibits osteogenesis but has no effect on adipogenesis while Notch signaling inhibits adipogenesis [47, 48]. The Hedgehog signaling pathway is involved in adipocyte maturation by reducing C/EBPα and PPARγ expression and insulin sensitivity [49]. Nell-1 signaling crosstalks with the Hedgehog pathway to inhibit adipogenesis [50]. Epidermal and fibroblast growth factors facilitate proliferation and increase adipogenesis and insulin sensitivity [51].

miRNAs, such as miR-17-5p, miR-106a and miR-22 also regulate osteogenesis and adipogenesis [52, 53]. Hypoxia can invoke adipogenesis by stimulating the PI3K/Akt/mTOR pathway [54]. Autologous platelet-rich plasma and insulin treatment stimulate adipogenic differentiation via Akt [55]. Therefore, many signaling pathways control adipogenesis and osteogenesis in AdSCs but the role of Ca^{2+} signaling on differentiation remain largely unknown.

1.2 CALCIUM SIGNALING IN STEM CELLS

Intracellular Ca^{2+} signaling controls many processes such as fertilization, proliferation, development, differentiation, contraction, and secretion [56]. Stem cells have ion channels on their plasma membrane that regulate Ca^{2+} movement into cells. Below is an overview of different Ca^{2+} channels and signaling pathways.

1.2.1 Voltage dependent Ca^{2+} channels

Voltage dependent Ca^{2+} channels (VDCCs) are mostly expressed in excitable cells like neuron, skeletal muscle, and heart cells [57]. Due to the depolarization, VDCCs open to stimulate Ca^{2+} influx into the cells, leading to various cellular responses such as hormone secretion, neurotransmitter release, and muscle contraction [57]. However, there are reports of VDCCs in non-excitable cells such as microglial cells and T lymphocytes [58, 59]. VDCCs may play a role in histamine release from human basophils [60]. In stem cells, hBMSCs express functional L-type VDCCs of the $Ca_v1.2$ type [61, 62]. hASCs also have L-type VDCCs ($Ca_v1.2$) and T-type VDCCs ($Ca_v3.2$) [63]. In rDPSCs, the $Ca_v1.2$ is needed for neural differentiation as knockdown inhibits differentiation [64].

1.2.2 Store-operated Ca^{2+} channels

Store-operated Ca^{2+} channels (SOCs) also known as Ca^{2+} release-activated Ca^{2+} channels (CRAC) are activated by the phospholipase C (PLC) pathway which catalyzes phosphatidylinositol-4,5-biphosphate (PIP_2) to inositol-1,4,5-triphosphate (IP_3) that binds to the ER to promote Ca^{2+} release into the cytoplasm [65]. When the ER is exhausted of Ca^{2+}, stromal interaction molecule (STIM), a Ca^{2+} ER sensor, translocates to SOCs to promote Ca^{2+} influx [66]. This channel is the main Ca^{2+} entry pathway in non-excitable cells [67]. It is highly selective for Ca^{2+} ions and is only permeable to monovalent cations in divalent free cation extracellular solution [68, 69]. Mutation of two conserved negatively charged glutamate residues decreases the Ca^{2+} entry via SOCs in T lymphocytes [70]. The Orai1, Orai2, Orai3 are the main components of SOCs while the first is the pore of the channel [71-73]. Orai1 is a membrane protein with four transmembrane segments with intracellular C and N terminus [70, 71]. Orai1 or Orai2/Orai3 overexpression with STIM1 amplify CRAC currents; Orai1, not Orai2 or Orai3, is inhibited by intracellular Ca^{2+} [73, 74]. Orai1 and STIM1 are important for AVP-induced Ca^{2+} oscillations and entry in rat hepatocytes [75]. The CRAC channel is also regulated by pH because acidification diminishes while alkalization facilitates its activity [76].

1.2.3 The phospholipase C - Inositol triphosphate pathway

Phospholipase C was first reported from amylase secretion in the pancreas treated with acetylcholine and carbamylcholine [77]. Later, PLC was identified as the enzyme catalyzing PIP_2 to IP_3 and diacylglycerol (DAG) [78]. There are 13

PLC family members that are subdivided into 6 classes (β, γ, δ, ζ, ε, and η) [79]. PLCβ, PLCδ and PLCη are linked to Gq-couple receptors; however, PLCγ and PLCζ, are connected to tyrosine-kinase receptors while PLCε is attached to both receptors [79].

Inositol-1,4,5-triphosphate's function was determined when pancreatic acinar cells released ER Ca^{2+} during carbachol stimulation [80, 81]. There are 3 types of IP_3R: IP_3R1, IP_3R2 and IP_3R3 [82]. IP_3R is a major contributor to Ca^{2+} release from the ER in undifferentiated hBMSCs [62]. IP_3-induced Ca^{2+} release is crucial for spontaneous Ca^{2+} oscillations in stem cells [83-85]. Human preadipocytes have all three IP_3Rs that are involved in intracellular Ca^{2+} oscillations [86].

1.3 EFFECT OF TRPM4 ON Ca^{2+} SIGNALING

1.3.1 Overview of TRP channels

Transient receptor potential (TRP) ion channels were first reported in *Drosophila melanogaster* [87]. They are divided into 7 subfamilies: The canonical (TRPC), vallinoid (TRPV), melastatin (TRPM), ankyrin (TRPA), mucolipin (TRPML), polycystin (TRPP), and *Drosophila* no mechano-potential C (TRPN). All channels have six transmembrane segments with the pore region between the 5^{th} and 6^{th} segments and C- and N-terminal domains in the intracellular space (Figure 1.2).

TRPC has 7 members (TRPC1-7) and is the most characterized subfamily. TRPC is activated by DAG from receptor-induced PLC activation, or stimulation of translocation to the plasma membrane, or by depletion of ER Ca^{2+} [88, 89]. It is

involved in different cellular processes such as keratinocyte Ca^{2+} homeostasis, myoblast differentiation and cardiac hypertrophy [90-92].

TRPV is composed of 6 members (TRPV1-6). It is activated by vanilloid, vanilloid-like compounds and heat [93]. The most well-known member is TRPV1 (also known as capsaicin-activated/capsaicin receptor). TRPV1 activation prevents adipogenesis and obesity by increasing energy expenditure [94, 95]. TRPV4 inhibits adipogenesis in TRPV4 knockout mice or wild-type mice treated with a TRPV4 antagonist by improving insulin sensitivity and reducing obesity and adipose inflammation [96].

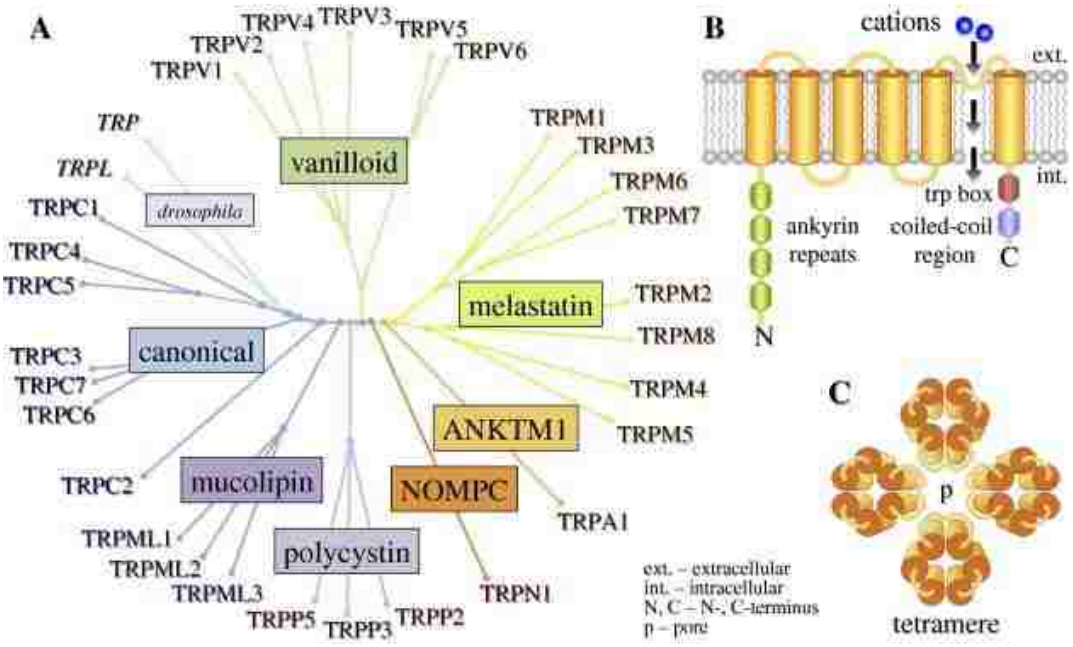

Figure 1.2 TRP family of ion channels (Reprinted with permission from Elsevier Ltd. Authors: Piper Nelson, Andreas Beck and Henrique Cheng. Vet. J. 2011; 187:153-164.)

TRPA includes three *Drosophila*, two *Caenorhabditis elegans* and one mammalian member known as TRPA1. TRPA1 is expressed in chemosensory C-fibers and activated by polygodial, acrolein and crotonaldehyde. They are

involved in inflammatory pain signaling during asthma and chronic obstructive pulmonary disease [87, 97]. TRPA1 knockout or wild-type mice treated with TRPA1 antagonists show reduced pain and inflammation [98].

TRPN is found in *Caenorhabditis elegans, Drosophila* and zebrafish. It is the primary transduction channel in *Drosophila* mechanosensory cilia in both external and chordotonal sensory neurons [99]. TRPML is composed of 3 members (TRPML1-3). They are expressed in intracellular vesicles of the endolysosome system [100, 101]. TRPP is a mechanosensor channel, existing in kidneys and ovaries where it responds to fluid movement in kidney and follicle maturation and differentiation in ovaries [87].

The TRPM subfamily includes 8 members (TRPM1-8). TRPM1 was named after it was found as a tumor suppressor gene in melanoma cells [102]. Mutation of TRPM1 is observed in patients with autosomal-recessive complete congenital stationary night blindness [103]. TRPM2 has a Nudix enzyme domain in the C-terminal that is activated by heat, β-NAD^+, ADP-ribose and hydrogen peroxide, but is suppressed by intracellular ATP [104-107]. It increases Ca^{2+} oscillations and cell proliferation in hBMSCs but has no effect on osteogenesis and adipogenesis [108]. TRPM3 exists in the brain and kidneys where its activity is increased by sphingosine derivatives and hypotonic solution and is involved in Ca^{2+} homeostasis [109, 110]. Among all TRPM channels, only TRPM4 and TRPM5 channels are Ca^{2+} impermeable. In spite of conducting Na^+, they have a profound effect on intracellular Ca^{2+} signals because the depolarization resulting from channel opening controls the activation of Ca^{2+} channels in the plasma membrane. TRPM5, which

shares 50% sequence homology with TRPM4, is found in the intestines, taste receptors, brain, and pancreatic β cells [111, 112]. TRPM2 and TRPM5 control Ca^{2+} signals and insulin secretion from pancreatic β cells [113-116]. TRPM6 and TRPM7 are also 'chanzymes' with alpha-kinase domain in the C-terminal region and facilitates Ca^{2+} and Mg^{2+} influx. TRPM6 is expressed in intestinal epithelia and kidney tubule cells and is important for Mg^{2+} homeostasis [117]. Mutation of TRPM6 induces hypomagnesemia with secondary hypocalcemia and patients with this defect have abnormal renal Mg^{2+} excretion [118]. TRPM6 knockout mice have lower survival rates, neural tube defects, and infertility [119]. TRPM7 is essential for MSC and ESC survival, proliferation as well as osteoblast differentiation and osteogenesis [120-122]. It is important for proliferation and adipogenesis of preadipocytes, as channel suppression inhibits these processes [123]. TRPM8 is predominantly expressed in dorsal root ganglia and neurons from trigeminal ganglia and is activated by cold and cooling agents such as menthol and icilin [124, 125]. Brown adipose tissue (BAT) express TRPM8, and when activated, it will enhance uncoupling protein 1 production for thermogenesis and prevention of obesity [126].

1.3.2 TRPM4

TRPM4 is a Ca^{2+}-activated non selective cation (CAN) channel [127]. They form tetramers to make a functional unit. Its selectivity filter is linked to six amino acids between the 5^{th} and 6^{th} transmembrane helices. Mutations of Glu^{981}, Asp^{982} and Asp^{984} to Ala shifts the voltage dependency to a more positive potential and replacement of Gln^{977} with Glu enables Ca^{2+} permeability [128]. Its structure

includes ATP, calmodulin and protein kinase C (PKC) binding sites [129]. Two divalent cation binding sites and negatively charged amino acids in the C-terminus help preserve the normal Ca^{2+} sensitivity [130]. TRPM4 is ubiquitously expressed throughout the body [102, 127, 131-136].

TRPM4's activity is enhanced by decavanadate and BTP2 [137, 138]. TRPM4's desensitization is delayed by Mg^{2+}-ATP, calmodulin, PIP_2 or phosphorylation via PKC [129, 139, 140]. The channel is also activated by high temperature [141]. Hydrogen peroxide inhibits TRPM4 desensitization [142]. Intracellular nucleotides (ATP, ADP, and AMP), spermine, glibenclamide, flufenamic acid and 9-phenanthrol inhibit TRPM4 [143, 144]. 9-phenanthrol is the most specific TRPM4 inhibitor since it does not block TRPM5 or TRPM7 [145].

TRPM4 was first characterized as a Ca^{2+}-activated nonselective cation channel with three typical features such as Ca^{2+} activation, voltage dependency and monovalent cation conductance [127]. In excitable cells, TRPM4 depolarizes the cell membrane and facilitates VDCC opening while the opposite effect occurs in non-excitable cells as it decreases the driving force for Ca^{2+} entry via SOCs [127, 146]. In T lymphocytes, it decreases Ca^{2+} signals by inhibiting SOCs and IL-2 production [147]. TRPM4 expression is lower in T helper type 1 compared to T helper type 2 cells; inhibition of the channel increases Ca^{2+} signals, NFATc1 nuclear localization, and IL-2 production but decreases motility in T helper type 2 [148]. Mast cells from TRPM4 knockout mice exhibit enhanced Ca^{2+} entry and proinflammatory mediators such as leukotriene C_4, D_4, E_4 [149, 150]. TRPM4 is also important for dendritic cell migration because TRPM4 knockout impairs this

process [151]. It is essential for umbilical cord endothelial cell migration [152]. TRPM4 also facilitates cell proliferation in Hela cells, a cervical cancer-derived cell line [132]. In excitable cells, TRPM4 stimulates myogenic vasoconstriction of cerebral artery myocytes as channel inhibition reduces myogenic tone and impairs autoregulation [153, 154]. TRPM4 is upregulated in vascular endothelium after hypoxia/ischemia *in vitro* and *in vivo* and channel inhibition enhances angiogenesis, and capillary integrity [155]. Spontaneously hypertensive rats have higher TRPM4 expression in ventricular cardiomyocytes compared to normotensive rat [156]. It contributes to the action potential in atrial and ventricular cardiomyocytes [157, 158]. TRPM4 prevents bradycardia because channel blockers decrease the action potential rate in the sinus node [159]. Our lab characterized functional TRPM4 channels in pancreatic α and β cells where it facilitates VDCC opening to increase Ca^{2+} signals and glucagon and insulin secretion [146, 160]. TRPM4 is up-regulated after spinal cord injury and subarachnoid hemorrhage [161-164]. TRPM4 knockout mice are hypertensive due to increased catecholamine secretion from adrenal chromaffin cells [131]. Hypoxia opens L-type VDCCs and increases intracellular Ca^{2+} concentration and TRPM4 activity to generate inspiratory bursts, synaptic drive currents in pre-Bötzinger complex [165]. The channel contributes to the pathogenesis of inflammation and neuronal injury in autoimmune encephalomyelitis and multiple sclerosis [134]. It plays a role in producing the slow inward cation current in cerebral Purkinje cells because TRPM4 knockout reduces current amplitude compared to wild-type mice [135]. TRPM4 may regulate K^+ transport during endolymph formation in strial marginal cells and

in inner hair cells in mouse cochlea [136]. TRPM4 missense mutation is observed in South African Afrikaner pedigree with progressive familial heart block type 1 [166]. Another TRPM4 mutation is observed in patients with Brugada syndrome [167].

1.4 AVP AND Ca^{2+} SIGNALING

1.4.1 Structure

The structure of AVP varies among species (Table 1.1). It is a nine amino acid peptide with one disulfide bond between the 1st and 6th position and Arg in the 8th position in most species.

1.4.2 Biosynthesis, storage and release

AVP is synthesized in magnocellular neurons of the supraoptic and paraventricular nuclei as a large precursor molecule. Moreover, the synthesis is directed by three exons separated by two introns: exon 1 (residues 1 through 21) for the signal peptide AVP and N-terminal end of the neurophysin; exon 2 for the middle portion of neurophysin II (residues 22 through 88); exon 3 for the C-terminal end of neurophysin II (residues 89 through 107) and a 39-residue glycopeptide called copeptin (Figure 1.3). After synthesis, the preprovasopressin is cleaved into the signal peptide and pro-vasopressin and stored into secretory vesicles in the Golgi apparatus, followed by splitting into AVP and neurophysin II [168, 169]. Neurophysin II is important for targeting, packaging and storing before it is released into the blood [170]. Under nerve impulses, the vesicles are transported down the axon via exocytosis; subsequently, AVP and neurophysin separate after leaving the nerve terminals [171]. In addition, AVP is synthesized in

other tissues such as sympathetic ganglia, heart, ovaries, adrenal gland, testis, thymus and pancreas [172-178].

Table 1.1 Structure of AVP in different species (Modified from [179].)

S — S Cys-Tyr-Phe-Gln-Asn-Cys-Pro-Arg-Gly-NH_2	Arginine vasopressin (AVP)	Most mammals
S — S Cys-Tyr-Phe-Gln-Asn-Cys-Pro-Lys-Gly-NH_2	Lysine vasopressin (LVP)	Pigs, hippos, warthogs, some marsupials
S — S Cys-Phe-Phe-Gln-Asn-Cys-Pro-Arg-Gly-NH_2	Phenypressin	Some marsupials
S — S Cys-Tyr-Ile-Gln-Asn-Cys-Pro-Arg-Gly-NH_2	Vasotocin	Non-mammals
S — S Cys-Phe-Ile-Arg-Asn-Cys-Pro-Lys-Gly-NH_2	Lys-conopressin	Great pond nail (*Lymnaea stagnalis*)
S — S Cys-Ile-Ile-Arg-Asn-Cys-Pro-Arg-Gly-NH_2	Arg-conopressin	Striated cone (*Conus striatus*)
S — S Cys-Phe-Val-Arg-Asn-Cys-Pro-Thr-Gly-NH_2	Annetocin	Red worm (*Eisenia foetida*)
S — S Cys-Leu-Ile-Arg-Asn-Cys-Pro-Arg-Gly-NH_2	Inotocin	Migratory locust (*Locusta migratoria*)

1.4.3 Receptors and mechanisms of action

AVP exerts its effect in the body by binding to three types of receptors: V1a, V1b and V2. AVP receptors are G-protein-coupled with seven transmembrane domain [180]. V1a receptors are the most prevalent in the body ranging from smooth muscle, mesangial cells, and lymphocytes to astrocytes [181-184]. The V1a receptors in humans and rats are 418 and 394 amino acids, respectively [185, 186]. V1b receptors are present mainly in the anterior pituitary, adrenal medulla, and pancreatic α and β cells [187-190] . Human and rat V1b receptors encode 424 and

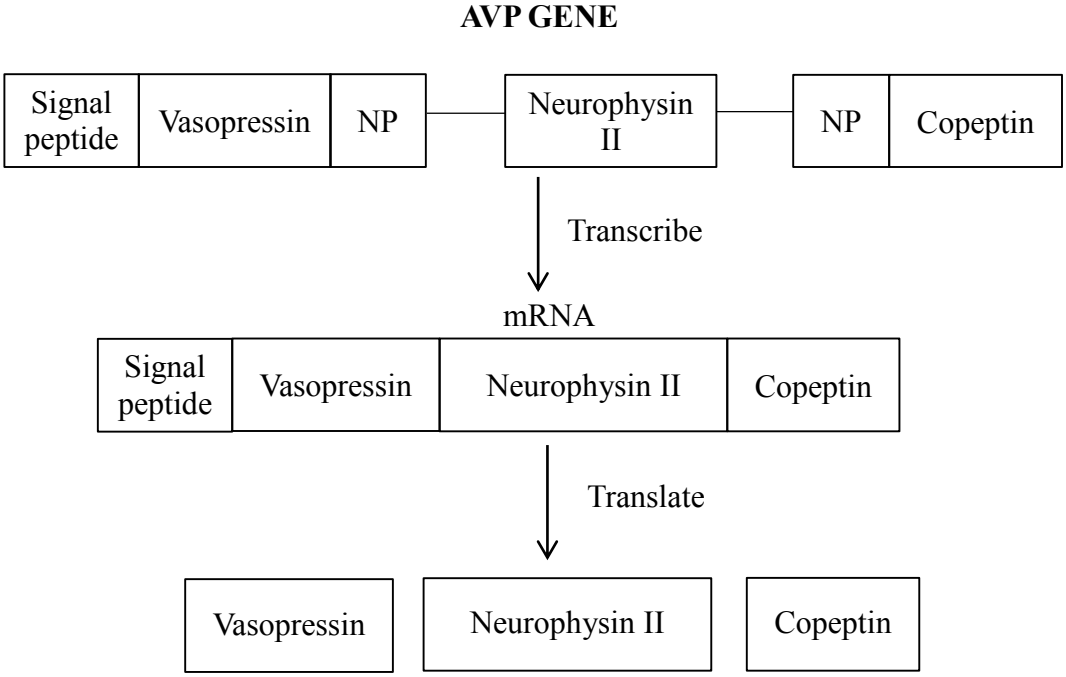

Figure 1.3 AVP synthesis (Modified from [179].)

425 amino acids, respectively and share 81% identity [187, 191]. Human V1b has 45% and 39% homology with the V1a and V2 receptors [187]. The V2 receptor is found in the renal distal and principal cells of the collecting ducts [192, 193]. It is also found in endothelial cells and skeletal muscle of the lungs [194]. This receptor in humans and rats contains 371 and 370 amino acids with over 80% homology [192, 193, 195]. The signaling cascade via V1 receptors is by the Gq-protein-PLC-IP_3 pathway that increases intracellular Ca^{2+} for a number of cellular processes [196, 197]. V1a receptors are linked to behavior and aggression [197]. On the other hand, the V1b receptor has a critical role in behavior and episodic memory [198]. V1a and V1b receptors are associated with food and alcohol intake, circadian rhythm, and thermoregulation [197]. V2 receptors are coupled to Gs proteins that activate the cAMP-PKA pathway and induce translocation of aquaporin-2 channels

for water reabsorption in the kidneys [192, 199]. Because of its effect in the kidneys, AVP is also called as antidiuretic hormone. The factors affecting AVP secretion are listed in Table 1.2.

Table 1.2 Factors regulating AVP secretion (Modified from [179].)

Stimulation	Inhibition
Major factors	
Hyperosmolality Hypovolemia Hypotension	Hypoosmolality Hypervolemia
Additional factors	
Cerebrospinal fluid sodium increase Nausea, vomiting Stressor, lactation Hyperthermia Ageing	Hypothermia α-adrenergic agonists γ-aminobutyric acid Alcohol Cortisol Iodothyronines Atrial natriuretic peptide
Drugs: Nicotine, Opiates, Barbiturates, Sulfonylureas, Antineoplastic agents, Neurosteroids	Apelin AVP

1.4.4 Agonists, blockers and their importance in research and clinical application

AVP agonists and antagonists are used for treating many diseases. Desmopressin, an AVP analog is used to treat diabetes insipidus [200]. V1a antagonists are used in the treatment of ocular hypertension, congestive heart failure, myocardial infarction, and preterm labor. V1b antagonists improve anxiety and depression. V2 antagonists are used in hyponatremia, polycystic kidney diseases and cirrhotic ascites [201, 202].

1.5 STATEMENT OF PROBLEMS AND SPECIFIC AIMS

In the United States, the direct expenses of osteoporotic fractures are estimated to be around $18 billion each year [203]. In addition, the total cost related

to adolescent obesity is estimated to be $254 billion [204]. Therefore, understanding the mechanisms controlling osteogenesis and adipogenesis from stem cells is important for bone healing and obesity prevention. However, there is limited information regarding the effects of Ca^{2+} signaling on stem cell differentiation. Calcium oscillations stimulate transcription factors and gene expression [205]. They are important for the G_1/S phase of the cell cycle and originate from IP_3-mediated Ca^{2+} release from the ER in ESCs and BMSCs [83, 85]. In addition, they are observed during stem cell differentiation but cease at the end of this process [84, 206]. Physical manipulation of Ca^{2+} oscillations increases osteogenesis in hBMSCs [207]. As a result, the overall goal of this dissertation is to investigate the effect of TRPM4 and AVP on Ca^{2+} signaling for controlling stem cell differentiation. Currently, there are no reports of TRPM4 in any type of stem cell. Therefore, we hypothesize that TRPM4 is a critical regulator of Ca^{2+} signaling and stem cell differentiation. Our first aim is determine the role of TRPM4 in rDFSCs (Chapter 2) and hASCs (Chapter 3). Furthermore, AVP induces myogenesis and T cell differentiation via V1 receptors; however, there is no information in hASC differentiation [182, 208]. Our lab found that AVP increases intracellular Ca^{2+} concentration in hASCs. Consequently, we hypothesize that hASCs have AVP receptors which are involved in Ca^{2+} signaling and adipogenic differentiation. Our second aim is to characterize the mechanism by which AVP increases intracellular Ca^{2+} and its role in adipogenesis in hASCs (Chapter 4).

1.6 REFERENCES

1 Lanza, R. and Atala, A. (2013) Essentials of Stem Cell Biology. Elsevier Science.

2 Phillips, M. I., Tang, Y.-L. and Cheng, H. (2012) Human Stem Cell Therapy. In Molecular and Cellular Therapeutics. 187-207, John Wiley & Sons, Ltd.

3 Master, Z., McLeod, M. and Mendez, I. (2007) Benefits, risks and ethical considerations in translation of stem cell research to clinical applications in Parkinson's disease. J. Med. Ethics. **33**, 169-173.

4 Okita, K., Ichisaka, T. and Yamanaka, S. (2007) Generation of germline-competent induced pluripotent stem cells. Nature. **448**, 313-317.

5 Yu, J., Vodyanik, M. A., Smuga-Otto, K., Antosiewicz-Bourget, J., Frane, J. L., Tian, S., Nie, J., Jonsdottir, G. A., Ruotti, V., Stewart, R., Slukvin, II and Thomson, J. A. (2007) Induced pluripotent stem cell lines derived from human somatic cells. Science. **318**, 1917-1920.

6 Hu, K. (2014) All roads lead to induced pluripotent stem cells: the technologies of iPSC generation. Stem cells and development. **23**, 1285-1300.

7 Okano, H., Nakamura, M., Yoshida, K., Okada, Y., Tsuji, O., Nori, S., Ikeda, E., Yamanaka, S. and Miura, K. (2013) Steps toward safe cell therapy using induced pluripotent stem cells. Circ. Res. **112**, 523-533.

8 Riggs, J. W., Barrilleaux, B. L., Varlakhanova, N., Bush, K. M., Chan, V. and Knoepfler, P. S. (2013) Induced pluripotency and oncogenic transformation are related processes. Stem Cells Dev. **22**, 37-50.

9 Amabile, G. and Meissner, A. (2009) Induced pluripotent stem cells: current progress and potential for regenerative medicine. Trends Mol. Med. **15**, 59-68.

10 Lobo, N. A., Shimono, Y., Qian, D. and Clarke, M. F. (2007) The biology of cancer stem cells. Annu. Rev. Cell Dev. Biol. **23**, 675-699.

11 Huang, G. T., Gronthos, S. and Shi, S. (2009) Mesenchymal stem cells derived from dental tissues vs. those from other sources: their biology and role in regenerative medicine. J. Dent. Res. **88**, 792-806.

12 Honda, M. J., Imaizumi, M., Tsuchiya, S. and Morsczeck, C. (2010) Dental follicle stem cells and tissue engineering. J. Oral Sci. **52**, 541-552.

13 Gimble, J. M., Katz, A. J. and Bunnell, B. A. (2007) Adipose-derived stem cells for regenerative medicine. Circ. Res. **100**, 1249-1260.

14 Yu, G., Floyd, Z. E., Wu, X., Hebert, T., Halvorsen, Y. D., Buehrer, B. M. and Gimble, J. M. (2011) Adipogenic differentiation of adipose-derived stem cells. Methods Mol. Biol. **702**, 193-200.

15 Skancke, J. (2009) Stem Cell Research. Greenhaven Press.

16 Handa, K., Saito, M., Yamauchi, M., Kiyono, T., Sato, S., Teranaka, T. and Sampath Narayanan, A. (2002) Cementum matrix formation in vivo by cultured dental follicle cells. Bone. **31**, 606-611.

17 Handa, K., Saito, M., Tsunoda, A., Yamauchi, M., Hattori, S., Sato, S., Toyoda, M., Teranaka, T. and Narayanan, A. S. (2002) Progenitor cells from dental follicle are able to form cementum matrix in vivo. Connect. Tissue Res. **43**, 406-408.

18 Morsczeck, C., Gotz, W., Schierholz, J., Zeilhofer, F., Kuhn, U., Mohl, C., Sippel, C. and Hoffmann, K. H. (2005) Isolation of precursor cells (PCs) from human dental follicle of wisdom teeth. Matrix Biol. **24**, 155-165.

19 Morsczeck, C., Moehl, C., Gotz, W., Heredia, A., Schaffer, T. E., Eckstein, N., Sippel, C. and Hoffmann, K. H. (2005) In vitro differentiation of human dental follicle cells with dexamethasone and insulin. Cell Biol. Int. **29**, 567-575.

20 Shoi, K., Aoki, K., Ohya, K., Takagi, Y. and Shimokawa, H. (2014) Characterization of pulp and follicle stem cells from impacted supernumerary maxillary incisors. Pediatr. Dent. **36**, 79-84.

21 Dai, Y., He, H., Wise, G. E. and Yao, S. (2011) Hypoxia promotes growth of stem cells in dental follicle cell populations. Journal of biomedical science and engineering. **4**, 454-461.

22 Morsczeck, C., Frerich, B. and Driemel, O. (2009) Dental stem cell patents. Recent patents on DNA & gene sequences. **3**, 39-43.

23 Tamaki, Y., Nakahara, T., Ishikawa, H. and Sato, S. (2013) In vitro analysis of mesenchymal stem cells derived from human teeth and bone marrow. Odontology. **101**, 121-132.

24 Tomic, S., Djokic, J., Vasilijic, S., Vucevic, D., Todorovic, V., Supic, G. and Colic, M. (2011) Immunomodulatory properties of mesenchymal stem cells derived from dental pulp and dental follicle are susceptible to activation by toll-like receptor agonists. Stem cells and development. **20**, 695-708.

25 Haddouti, E. M., Skroch, M., Zippel, N., Müller, C., Birova, B., Pansky, A., Kleinfeld, C., Winter, M. and Tobiasch, E. (2009) Human dental follicle precursor cells of wisdom teeth: isolation and differentiation towards osteoblasts for implants with and without scaffolds. Materialwissenschaft und Werkstofftechnik. **40**, 732-737.

26 Park, B. W., Jang, S. J., Byun, J. H., Kang, Y. H., Choi, M. J., Park, W. U., Lee, W. J. and Rho, G. J. (2014) Cryopreservation of human dental follicle tissue for use as a resource of autologous mesenchymal stem cells. J. Tissue Eng. Regen. Med.

27 Yao, S., He, H., Gutierrez, D. L., Rad, M. R., Liu, D., Li, C., Flanagan, M. and Wise, G. E. (2013) Expression of bone morphogenetic protein-6 in dental follicle stem cells and its effect on osteogenic differentiation. Cells Tissues Organs. **198**, 438-447.

28 Rezai Rad, M., Wise, G. E., Brooks, H., Flanagan, M. B. and Yao, S. (2013) Activation of proliferation and differentiation of dental follicle stem cells (DFSCs) by heat stress. Cell Prolif. **46**, 58-66.

29 Beck, H. C., Gosau, M., Kristensen, L. P. and Morsczeck, C. (2014) A site-specific phosphorylation of the focal adhesion kinase controls the formation of spheroid cell clusters. Neurochem. Res. **39**, 1199-1205.

30 Kemoun, P., Laurencin-Dalicieux, S., Rue, J., Farges, J. C., Gennero, I., Conte-Auriol, F., Briand-Mesange, F., Gadelorge, M., Arzate, H., Narayanan, A. S., Brunel, G. and Salles, J. P. (2007) Human dental follicle cells acquire cementoblast features under stimulation by BMP-2/-7 and enamel matrix derivatives (EMD) in vitro. Cell Tissue Res. **329**, 283-294.

31 Li, C., Yang, X., He, Y., Ye, G., Li, X., Zhang, X., Zhou, L. and Deng, F. (2012) Bone morphogenetic protein-9 induces osteogenic differentiation of rat dental follicle stem cells in P38 and ERK1/2 MAPK dependent manner. Int. J. Med. Sci. **9**, 862-871.

32 Chen, X., Zhang, T., Shi, J., Xu, P., Gu, Z., Sandham, A., Yang, L. and Ye, Q. (2013) Notch1 signaling regulates the proliferation and self-renewal of human dental follicle cells by modulating the G1/S phase transition and telomerase activity. PLoS One. **8**, e69967.

33 Viale-Bouroncle, S., Gosau, M. and Morsczeck, C. (2014) NOTCH1 signaling regulates the BMP2/DLX-3 directed osteogenic differentiation of dental follicle cells. Biochem. Biophys. Res. Commun. **443**, 500-504.

34 Aonuma, H., Ogura, N., Takahashi, K., Fujimoto, Y., Iwai, S., Hashimoto, H., Ito, K., Kamino, Y. and Kondoh, T. (2012) Characteristics and osteogenic differentiation of stem/progenitor cells in the human dental follicle analyzed by gene expression profiling. Cell Tissue Res. **350**, 317-331.

35 Felthaus, O., Viale-Bouroncle, S., Driemel, O., Reichert, T. E., Schmalz, G. and Morsczeck, C. (2012) Transcription factors TP53 and SP1 and the osteogenic differentiation of dental stem cells. Differentiation. **83**, 10-16.

36 Press, T., Viale-Bouroncle, S., Felthaus, O., Gosau, M. and Morsczeck, C. (2014) EGR1 supports the osteogenic differentiation of dental stem cells. Int. Endod. J.

37 Zippel, N., Limbach, C. A., Ratajski, N., Urban, C., Luparello, C., Pansky, A., Kassack, M. U. and Tobiasch, E. (2012) Purinergic receptors influence the differentiation of human mesenchymal stem cells. Stem Cells Dev. **21**, 884-900.

38 Zuk, P. A., Zhu, M., Ashjian, P., De Ugarte, D. A., Huang, J. I., Mizuno, H., Alfonso, Z. C., Fraser, J. K., Benhaim, P. and Hedrick, M. H. (2002) Human adipose tissue is a source of multipotent stem cells. Mol. Biol. Cell. **13**, 4279-4295.

39 Bourin, P., Bunnell, B. A., Casteilla, L., Dominici, M., Katz, A. J., March, K. L., Redl, H., Rubin, J. P., Yoshimura, K. and Gimble, J. M. (2013) Stromal cells from the adipose tissue-derived stromal vascular fraction and culture expanded adipose tissue-derived stromal/stem cells: a joint statement of the International Federation for Adipose Therapeutics and Science (IFATS) and the International Society for Cellular Therapy (ISCT). Cytotherapy. **15**, 641-648.

40 McIntosh, K., Zvonic, S., Garrett, S., Mitchell, J. B., Floyd, Z. E., Hammill, L., Kloster, A., Di Halvorsen, Y., Ting, J. P., Storms, R. W., Goh, B., Kilroy, G., Wu, X. and Gimble, J. M. (2006) The immunogenicity of human adipose-derived cells: temporal changes in vitro. Stem Cells. **24**, 1246-1253.

41 Peng, W., Gao, T., Yang, Z. L., Zhang, S. C., Ren, M. L., Wang, Z. G. and Zhang, B. (2012) Adipose-derived stem cells induced dendritic cells undergo tolerance and inhibit Th1 polarization. Cell. Immunol. **278**, 152-157.

42 Izadpanah, R., Kaushal, D., Kriedt, C., Tsien, F., Patel, B., Dufour, J. and Bunnell, B. A. (2008) Long-term in vitro expansion alters the biology of adult mesenchymal stem cells. Cancer Res. **68**, 4229-4238.

43 Sen, A., Lea-Currie, Y. R., Sujkowska, D., Franklin, D. M., Wilkison, W. O., Halvorsen, Y. D. and Gimble, J. M. (2001) Adipogenic potential of human adipose derived stromal cells from multiple donors is heterogeneous. J. Cell. Biochem. **81**, 312-319.

44 Sauer, H., Sharifpanah, F., Hatry, M., Steffen, P., Bartsch, C., Heller, R., Padmasekar, M., Howaldt, H. P., Bein, G. and Wartenberg, M. (2011) NOS inhibition synchronizes calcium oscillations in human adipose tissue-derived mesenchymal stem cells by increasing gap-junctional coupling. J. Cell. Physiol. **226**, 1642-1650.

45 Liu, Q., Cen, L., Zhou, H., Yin, S., Liu, G., Liu, W., Cao, Y. and Cui, L. (2009) The role of the extracellular signal-related kinase signaling pathway in osteogenic differentiation of human adipose-derived stem cells and in adipogenic transition initiated by dexamethasone. Tissue engineering. Part A. **15**, 3487-3497.

46 Jaiswal, R. K., Jaiswal, N., Bruder, S. P., Mbalaviele, G., Marshak, D. R. and Pittenger, M. F. (2000) Adult human mesenchymal stem cell differentiation to the osteogenic or adipogenic lineage is regulated by mitogen-activated protein kinase. J. Biol. Chem. **275**, 9645-9652.

47 Cho, H. H., Kim, Y. J., Kim, S. J., Kim, J. H., Bae, Y. C., Ba, B. and Jung, J. S. (2006) Endogenous Wnt signaling promotes proliferation and suppresses osteogenic differentiation in human adipose derived stromal cells. Tissue Eng. **12**, 111-121.

48 Osathanon, T., Subbalekha, K., Sastravaha, P. and Pavasant, P. (2012) Notch signalling inhibits the adipogenic differentiation of single-cell-derived mesenchymal stem cell clones isolated from human adipose tissue. Cell Biol. Int. **36**, 1161-1170.

49 Fontaine, C., Cousin, W., Plaisant, M., Dani, C. and Peraldi, P. (2008) Hedgehog signaling alters adipocyte maturation of human mesenchymal stem cells. Stem Cells. **26**, 1037-1046.

50 James, A. W., Pang, S., Askarinam, A., Corselli, M., Zara, J. N., Goyal, R., Chang, L., Pan, A., Shen, J., Yuan, W., Stoker, D., Zhang, X., Adams, J. S., Ting, K. and Soo, C. (2012) Additive effects of sonic hedgehog and Nell-1 signaling in osteogenic versus adipogenic differentiation of human adipose-derived stromal cells. Stem Cells Dev. **21**, 2170-2178.

51 Hebert, T. L., Wu, X., Yu, G., Goh, B. C., Halvorsen, Y. D., Wang, Z., Moro, C. and Gimble, J. M. (2009) Culture effects of epidermal growth factor (EGF) and basic fibroblast growth factor (bFGF) on cryopreserved human adipose-derived stromal/stem cell proliferation and adipogenesis. J. Tissue Eng. Regen. Med. **3**, 553-561.

52 Huang, S., Wang, S., Bian, C., Yang, Z., Zhou, H., Zeng, Y., Li, H., Han, Q. and Zhao, R. C. (2012) Upregulation of miR-22 promotes osteogenic differentiation and inhibits adipogenic differentiation of human adipose tissue-derived mesenchymal stem cells by repressing HDAC6 protein expression. Stem Cells Dev. **21**, 2531-2540.

53 Li, H., Li, T., Wang, S., Wei, J., Fan, J., Li, J., Han, Q., Liao, L., Shao, C. and Zhao, R. C. (2013) miR-17-5p and miR-106a are involved in the balance between osteogenic and adipogenic differentiation of adipose-derived mesenchymal stem cells. Stem cell research. **10**, 313-324.

54 Kim, J. H., Kim, S. H., Song, S. Y., Kim, W. S., Song, S. U., Yi, T., Jeon, M. S., Chung, H. M., Xia, Y. and Sung, J. H. (2014) Hypoxia induces adipocyte differentiation of adipose-derived stem cells by triggering reactive oxygen species generation. Cell Biol. Int. **38**, 32-40.

55 Cervelli, V., Scioli, M. G., Gentile, P., Doldo, E., Bonanno, E., Spagnoli, L. G. and Orlandi, A. (2012) Platelet-rich plasma greatly potentiates insulin-induced adipogenic differentiation of human adipose-derived stem cells through a serine/threonine kinase Akt-dependent mechanism and promotes clinical fat graft maintenance. Stem cells translational medicine. **1**, 206-220.

56 Berridge, M. J., Lipp, P. and Bootman, M. D. (2000) The versatility and universality of calcium signalling. Nat. Rev. Mol. Cell Biol. **1**, 11-21

57 Dolphin, A. C. (2006) A short history of voltage-gated calcium channels. Br. J. Pharmacol. **147 Suppl 1**, S56-62.

58 Saegusa, H. and Tanabe, T. (2014) N-type voltage-dependent Ca2+ channel in non-excitable microglial cells in mice is involved in the pathophysiology of neuropathic pain. Biochem. Biophys. Res. Commun. **450**, 142-147.

59 Badou, A., Jha, M. K., Matza, D. and Flavell, R. A. (2013) Emerging roles of L-type voltage-gated and other calcium channels in T lymphocytes. Front. Immunol. **4**, 243.

60 Beauvais, F., Burtin, C. and Benveniste, J. (1995) Voltage-dependent ion channels on human basophils: do they exist? Immunol. Lett. **46**, 81-83.

61 Heubach, J. F., Graf, E. M., Leutheuser, J., Bock, M., Balana, B., Zahanich, I., Christ, T., Boxberger, S., Wettwer, E. and Ravens, U. (2004) Electrophysiological properties of human mesenchymal stem cells. J. Physiol. **554**, 659-672.

62 Kawano, S., Shoji, S., Ichinose, S., Yamagata, K., Tagami, M. and Hiraoka, M. (2002) Characterization of Ca(2+) signaling pathways in human mesenchymal stem cells. Cell Calcium. **32**, 165-174.

63 Bai, X., Ma, J., Pan, Z., Song, Y. H., Freyberg, S., Yan, Y., Vykoukal, D. and Alt, E. (2007) Electrophysiological properties of human adipose tissue-derived stem cells. Am. J. Physiol. Cell Physiol. **293**, C1539-1550.

64 Ge, J., Ju, Y., Xue, Z., Feng, Y., Huang, X., Liu, H. and Zhao, S. (2013) Distal C terminus of CaV1.2 channels plays a crucial role in the neural differentiation of dental pulp stem cells. PLoS One. **8**, e81332.

65 Putney, J. W., Jr. (1986) A model for receptor-regulated calcium entry. Cell Calcium. **7**, 1-12.

66 Smyth, J. T., Hwang, S. Y., Tomita, T., DeHaven, W. I., Mercer, J. C. and Putney, J. W. (2010) Activation and regulation of store-operated calcium entry. J. Cell. Mol. Med. **14**, 2337-2349.

67 Neher, E. (1992) Cell physiology. Controls on calcium influx. Nature. **355**, 298-299.

68 Hoth, M. and Penner, R. (1992) Depletion of intracellular calcium stores activates a calcium current in mast cells. Nature. **355**, 353-356.

69 Vig, M., Beck, A., Billingsley, J. M., Lis, A., Parvez, S., Peinelt, C., Koomoa, D. L., Soboloff, J., Gill, D. L., Fleig, A., Kinet, J. P. and Penner, R. (2006) CRACM1 multimers form the ion-selective pore of the CRAC channel. Curr. Biol. **16**, 2073-2079.

70 Feske, S., Gwack, Y., Prakriya, M., Srikanth, S., Puppel, S. H., Tanasa, B., Hogan, P. G., Lewis, R. S., Daly, M. and Rao, A. (2006) A mutation in Orai1 causes immune deficiency by abrogating CRAC channel function. Nature. **441**, 179-185.

71 Prakriya, M., Feske, S., Gwack, Y., Srikanth, S., Rao, A. and Hogan, P. G. (2006) Orai1 is an essential pore subunit of the CRAC channel. Nature. **443**, 230-233.

72 DeHaven, W. I., Smyth, J. T., Boyles, R. R. and Putney, J. W., Jr. (2007) Calcium inhibition and calcium potentiation of Orai1, Orai2, and Orai3 calcium release-activated calcium channels. J Biol Chem. **282**, 17548-17556.

73 Lis, A., Peinelt, C., Beck, A., Parvez, S., Monteilh-Zoller, M., Fleig, A. and Penner, R. (2007) CRACM1, CRACM2, and CRACM3 are store-operated Ca2+ channels with distinct functional properties. Curr. Biol. **17**, 794-800.

74 Peinelt, C., Vig, M., Koomoa, D. L., Beck, A., Nadler, M. J., Koblan-Huberson, M., Lis, A., Fleig, A., Penner, R. and Kinet, J. P. (2006) Amplification of CRAC current by STIM1 and CRACM1 (Orai1). Nat. Cell Biol. **8**, 771-773.

75 Jones, B. F., Boyles, R. R., Hwang, S. Y., Bird, G. S. and Putney, J. W. (2008) Calcium influx mechanisms underlying calcium oscillations in rat hepatocytes. Hepatology. **48**, 1273-1281.

76 Beck, A., Fleig, A., Penner, R. and Peinelt, C. (2014) Regulation of endogenous and heterologous Ca(2+) release-activated Ca(2+) currents by pH. Cell Calcium. **56**, 235-243.

77 Hokin, M. R. and Hokin, L. E. (1953) Enzyme secretion and the incorporation of P32 into phospholipides of pancreas slices. J. Biol. Chem. **203**, 967-977.

78 Michell, R. H. and Allan, D. (1975) Inositol cyclis phosphate as a product of phosphatidylinositol breakdown by phospholipase C (Bacillus cereus). FEBS Lett. **53**, 302-304.

79 Islam, M. S. (2012) Calcium Signaling. Springer Netherlands.

80 Streb, H., Bayerdorffer, E., Haase, W., Irvine, R. F. and Schulz, I. (1984) Effect of inositol-1,4,5-trisphosphate on isolated subcellular fractions of rat pancreas. J. Membr. Biol. **81**, 241-253.

81 Streb, H., Irvine, R. F., Berridge, M. J. and Schulz, I. (1983) Release of Ca2+ from a nonmitochondrial intracellular store in pancreatic acinar cells by inositol-1,4,5-trisphosphate. Nature. **306**, 67-69.

82 Tan, G., Shim, W., Gu, Y., Qian, L., Chung, Y. Y., Lim, S. Y., Yong, P., Sim, E. and Wong, P. (2010) Differential effect of myocardial matrix and integrins on cardiac differentiation of human mesenchymal stem cells. Differentiation. **79**, 260-271.

83 Kapur, N., Mignery, G. A. and Banach, K. (2007) Cell cycle-dependent calcium oscillations in mouse embryonic stem cells. Am. J. Physiol. Cell Physiol. **292**, C1510-1518.

84 Kawano, S., Otsu, K., Kuruma, A., Shoji, S., Yanagida, E., Muto, Y., Yoshikawa, F., Hirayama, Y., Mikoshiba, K. and Furuichi, T. (2006) ATP autocrine/paracrine signaling induces calcium oscillations and NFAT activation in human mesenchymal stem cells. Cell Calcium. **39**, 313-324.

85 Resende, R. R., Adhikari, A., da Costa, J. L., Lorencon, E., Ladeira, M. S., Guatimosim, S., Kihara, A. H. and Ladeira, L. O. (2010) Influence of spontaneous calcium events on cell-cycle progression in embryonal carcinoma and adult stem cells. Biochim. Biophys. Acta. **1803**, 246-260.

86 Hu, R., He, M. L., Hu, H., Yuan, B. X., Zang, W. J., Lau, C. P., Tse, H. F. and Li, G. R. (2009) Characterization of calcium signaling pathways in human preadipocytes. J. Cell. Physiol. **220**, 765-770.

87 Nelson, P. L., Beck, A. and Cheng, H. (2011) Transient receptor proteins illuminated: current views on TRPs and disease. Vet. J. **187**, 153-164.

88 Wang, Y., Deng, X., Hewavitharana, T., Soboloff, J. and Gill, D. L. (2008) Stim, ORAI and TRPC channels in the control of calcium entry signals in smooth muscle. Clin. Exp. Pharmacol. Physiol. **35**, 1127-1133.

89 Putney, J. W., Jr. (2007) Frontiers in Neuroscience. Multiple Mechanisms of TRPC Activation. In TRP Ion Channel Function in Sensory Transduction and Cellular Signaling Cascades (Liedtke, W. B. and Heller, S., eds.), CRC Press Taylor & Francis Group, LLC, Boca Raton (FL).

90 Beck, B., Lehen'kyi, V., Roudbaraki, M., Flourakis, M., Charveron, M., Bordat, P., Polakowska, R., Prevarskaya, N. and Skryma, R. (2008) TRPC channels determine human keratinocyte differentiation: new insight into basal cell carcinoma. Cell Calcium. **43**, 492-505.

91 Nakayama, H., Wilkin, B. J., Bodi, I. and Molkentin, J. D. (2006) Calcineurin-dependent cardiomyopathy is activated by TRPC in the adult mouse heart. FASEB J. **20**, 1660-1670.

92 Louis, M., Zanou, N., Van Schoor, M. and Gailly, P. (2008) TRPC1 regulates skeletal myoblast migration and differentiation. J. Cell Sci. **121**, 3951-3959.

93 Brauchi, S., Orta, G., Salazar, M., Rosenmann, E. and Latorre, R. (2006) A hot-sensing cold receptor: C-terminal domain determines thermosensation in transient receptor potential channels. J. Neurosci. **26**, 4835-4840.

94 Iwasaki, Y., Tamura, Y., Inayoshi, K., Narukawa, M., Kobata, K., Chiba, H., Muraki, E., Tsunoda, N. and Watanabe, T. (2011) TRPV1 agonist monoacylglycerol increases UCP1 content in brown adipose tissue and suppresses accumulation of visceral fat in mice fed a high-fat and high-sucrose diet. Biosci. Biotechnol. Biochem. **75**, 904-909.

95 Zhang, L. L., Yan Liu, D., Ma, L. Q., Luo, Z. D., Cao, T. B., Zhong, J., Yan, Z. C., Wang, L. J., Zhao, Z. G., Zhu, S. J., Schrader, M., Thilo, F., Zhu, Z. M. and Tepel, M. (2007) Activation of transient receptor potential vanilloid type-1 channel prevents adipogenesis and obesity. Circ. Res. **100**, 1063-1070.

96 Ye, L., Kleiner, S., Wu, J., Sah, R., Gupta, R. K., Banks, A. S., Cohen, P., Khandekar, M. J., Bostrom, P., Mepani, R. J., Laznik, D., Kamenecka, T. M., Song, X., Liedtke, W., Mootha, V. K., Puigserver, P., Griffin, P. R., Clapham, D. E. and Spiegelman, B. M. (2012) TRPV4 is a regulator of adipose oxidative metabolism, inflammation, and energy homeostasis. Cell. **151**, 96-110.

97 Escalera, J., von Hehn, C. A., Bessac, B. F., Sivula, M. and Jordt, S. E. (2008) TRPA1 mediates the noxious effects of natural sesquiterpene deterrents. J. Biol. Chem. **283**, 24136-24144.

98 Bessac, B. F. and Jordt, S. E. (2010) Sensory detection and responses to toxic gases: mechanisms, health effects, and countermeasures. Proceedings of the American Thoracic Society. **7**, 269-277.

99 Lee, J., Moon, S., Cha, Y. and Chung, Y. D. (2010) Drosophila TRPN(=NOMPC) channel localizes to the distal end of mechanosensory cilia. PLoS One. **5**, e11012.

100 Feng, X., Huang, Y., Lu, Y., Xiong, J., Wong, C. O., Yang, P., Xia, J., Chen, D., Du, G., Venkatachalam, K., Xia, X. and Zhu, M. X. (2014) Drosophila TRPML forms PI(3,5)P2-activated cation channels in both endolysosomes and plasma membrane. J. Biol. Chem. **289**, 4262-4272.

101 Nilius, B. and Szallasi, A. (2014) Transient receptor potential channels as drug targets: from the science of basic research to the art of medicine. Pharmacol. Rev. **66**, 676-814.

102 Xu, X. Z., Moebius, F., Gill, D. L. and Montell, C. (2001) Regulation of melastatin, a TRP-related protein, through interaction with a cytoplasmic isoform. Proc. Natl. Acad. Sci. U. S. A. **98**, 10692-10697.

103 Audo, I., Kohl, S., Leroy, B. P., Munier, F. L., Guillonneau, X., Mohand-Said, S., Bujakowska, K., Nandrot, E. F., Lorenz, B., Preising, M., Kellner, U., Renner, A. B., Bernd, A., Antonio, A., Moskova-Doumanova, V., Lancelot, M. E., Poloschek, C. M., Drumare, I., Defoort-Dhellemmes, S., Wissinger, B., Leveillard, T., Hamel, C. P., Schorderet, D. F., De Baere, E., Berger, W., Jacobson, S. G., Zrenner, E., Sahel, J. A., Bhattacharya, S. S. and Zeitz, C. (2009) TRPM1 is mutated in patients with autosomal-recessive complete congenital stationary night blindness. Am. J. Hum. Genet. **85**, 720-729.

104 Hara, Y., Wakamori, M., Ishii, M., Maeno, E., Nishida, M., Yoshida, T., Yamada, H., Shimizu, S., Mori, E., Kudoh, J., Shimizu, N., Kurose, H., Okada, Y., Imoto, K. and Mori, Y. (2002) LTRPC2 Ca2+-permeable channel activated by changes in redox status confers susceptibility to cell death. Mol. Cell. **9**, 163-173.

105 Perraud, A. L., Fleig, A., Dunn, C. A., Bagley, L. A., Launay, P., Schmitz, C., Stokes, A. J., Zhu, Q., Bessman, M. J., Penner, R., Kinet, J. P. and Scharenberg, A. M. (2001) ADP-ribose gating of the calcium-permeable LTRPC2 channel revealed by Nudix motif homology. Nature. **411**, 595-599.

106 Sano, Y., Inamura, K., Miyake, A., Mochizuki, S., Yokoi, H., Matsushime, H. and Furuichi, K. (2001) Immunocyte Ca2+ influx system mediated by LTRPC2. Science. **293**, 1327-1330.

107 Nilius, B., Droogmans, G. and Wondergem, R. (2003) Transient receptor potential channels in endothelium: solving the calcium entry puzzle? Endothelium. **10**, 5-15.

108 Tao, R., Sun, H. Y., Lau, C. P., Tse, H. F., Lee, H. C. and Li, G. R. (2011) Cyclic ADP ribose is a novel regulator of intracellular Ca2+ oscillations in human bone marrow mesenchymal stem cells. J. Cell. Mol. Med. **15**, 2684-2696.

109 Grimm, C., Kraft, R., Sauerbruch, S., Schultz, G. and Harteneck, C. (2003) Molecular and functional characterization of the melastatin-related cation channel TRPM3. J. Biol. Chem. **278**, 21493-21501.

110 Grimm, C., Kraft, R., Schultz, G. and Harteneck, C. (2005) Activation of the melastatin-related cation channel TRPM3 by D-erythro-sphingosine [corrected]. Mol. Pharmacol. **67**, 798-805.

111 Prawitt, D., Monteilh-Zoller, M. K., Brixel, L., Spangenberg, C., Zabel, B., Fleig, A. and Penner, R. (2003) TRPM5 is a transient Ca2+-activated cation channel responding to rapid changes in [Ca2+]i. Proc. Natl. Acad. Sci. U. S. A. **100**, 15166-15171.

112 Zhang, Y., Hoon, M. A., Chandrashekar, J., Mueller, K. L., Cook, B., Wu, D., Zuker, C. S. and Ryba, N. J. (2003) Coding of sweet, bitter, and umami tastes: different receptor cells sharing similar signaling pathways. Cell. **112**, 293-301.

113 Togashi, K., Hara, Y., Tominaga, T., Higashi, T., Konishi, Y., Mori, Y. and Tominaga, M. (2006) TRPM2 activation by cyclic ADP-ribose at body temperature is involved in insulin secretion. EMBO J. **25**, 1804-1815.

114 Wagner, T. F., Loch, S., Lambert, S., Straub, I., Mannebach, S., Mathar, I., Dufer, M., Lis, A., Flockerzi, V., Philipp, S. E. and Oberwinkler, J. (2008) Transient receptor potential M3 channels are ionotropic steroid receptors in pancreatic beta cells. Nat. Cell Biol. **10**, 1421-1430.

115 Cheng, H., Beck, A., Launay, P., Gross, S. A., Stokes, A. J., Kinet, J. P., Fleig, A. and Penner, R. (2007) TRPM4 controls insulin secretion in pancreatic beta-cells. Cell Calcium. **41**, 51-61.

116 Colsoul, B., Schraenen, A., Lemaire, K., Quintens, R., Van Lommel, L., Segal, A., Owsianik, G., Talavera, K., Voets, T., Margolskee, R. F., Kokrashvili, Z., Gilon, P., Nilius, B., Schuit, F. C. and Vennekens, R. (2010) Loss of high-frequency glucose-induced Ca2+ oscillations in pancreatic islets correlates with impaired glucose tolerance in Trpm5-/- mice. Proc. Natl. Acad. Sci. U. S. A. **107**, 5208-5213.

117 Schlingmann, K. P., Weber, S., Peters, M., Niemann Nejsum, L., Vitzthum, H., Klingel, K., Kratz, M., Haddad, E., Ristoff, E., Dinour, D., Syrrou, M., Nielsen, S., Sassen, M., Waldegger, S., Seyberth, H. W. and Konrad, M. (2002) Hypomagnesemia with secondary hypocalcemia is caused by mutations in TRPM6, a new member of the TRPM gene family. Nat. Genet. **31**, 166-170.

118 Walder, R. Y., Landau, D., Meyer, P., Shalev, H., Tsolia, M., Borochowitz, Z., Boettger, M. B., Beck, G. E., Englehardt, R. K., Carmi, R. and Sheffield, V. C. (2002) Mutation of TRPM6 causes familial hypomagnesemia with secondary hypocalcemia. Nat. Genet. **31**, 171-174.

119 Walder, R. Y., Yang, B., Stokes, J. B., Kirby, P. A., Cao, X., Shi, P., Searby, C. C., Husted, R. F. and Sheffield, V. C. (2009) Mice defective in Trpm6 show embryonic mortality and neural tube defects. Hum. Mol. Genet. **18**, 4367-4375.

120 Cheng, H., Feng, J. M., Figueiredo, M. L., Zhang, H., Nelson, P. L., Marigo, V. and Beck, A. (2010) Transient receptor potential melastatin type 7 channel is critical for the survival of bone marrow derived mesenchymal stem cells. Stem cells and development. **19**, 1393-1403.

121 Jin, J., Wu, L. J., Jun, J., Cheng, X., Xu, H., Andrews, N. C. and Clapham, D. E. (2012) The channel kinase, TRPM7, is required for early embryonic development. Proc. Natl. Acad. Sci. U. S. A. **109**, E225-233.

122 Abed, E., Martineau, C. and Moreau, R. (2011) Role of melastatin transient receptor potential 7 channels in the osteoblastic differentiation of murine MC3T3 cells. Calcif. Tissue Int. **88**, 246-253.

123 Chen, K. H., Xu, X. H., Liu, Y., Hu, Y., Jin, M. W. and Li, G. R. (2014) TRPM7 channels regulate proliferation and adipogenesis in 3T3-L1 preadipocytes. J. Cell. Physiol. **229**, 60-67.

124 Peier, A. M., Moqrich, A., Hergarden, A. C., Reeve, A. J., Andersson, D. A., Story, G. M., Earley, T. J., Dragoni, I., McIntyre, P., Bevan, S. and Patapoutian, A. (2002) A TRP channel that senses cold stimuli and menthol. Cell. **108**, 705-715.

125 Andersson, D. A., Chase, H. W. and Bevan, S. (2004) TRPM8 activation by menthol, icilin, and cold is differentially modulated by intracellular pH. J. Neurosci. **24**, 5364-5369.

126 Ma, S., Yu, H., Zhao, Z., Luo, Z., Chen, J., Ni, Y., Jin, R., Ma, L., Wang, P., Zhu, Z., Li, L., Zhong, J., Liu, D., Nilius, B. and Zhu, Z. (2012) Activation of the cold-sensing TRPM8 channel triggers UCP1-dependent thermogenesis and prevents obesity. J. Mol. Cell. Biol. **4**, 88-96.

127 Launay, P., Fleig, A., Perraud, A. L., Scharenberg, A. M., Penner, R. and Kinet, J. P. (2002) TRPM4 is a Ca2+-activated nonselective cation channel mediating cell membrane depolarization. Cell. **109**, 397-407.

128 Nilius, B., Prenen, J., Janssens, A., Owsianik, G., Wang, C., Zhu, M. X. and Voets, T. (2005) The selectivity filter of the cation channel TRPM4. J. Biol. Chem. **280**, 22899-22906.

129 Nilius, B., Prenen, J., Tang, J., Wang, C., Owsianik, G., Janssens, A., Voets, T. and Zhu, M. X. (2005) Regulation of the Ca2+ sensitivity of the nonselective cation channel TRPM4. J. Biol. Chem. **280**, 6423-6433.

130 Yamaguchi, S., Tanimoto, A., Otsuguro, K. I., Hibino, H. and Ito, S. (2014) Negatively-charged Amino Acids near and in Transient Receptor Potential (TRP) Domain of TRPM4 Channel Are One Determinant of Its Ca2+ Sensitivity. J. Biol. Chem. **289**, 35265-35282.

131 Mathar, I., Vennekens, R., Meissner, M., Kees, F., Van der Mieren, G., Camacho Londono, J. E., Uhl, S., Voets, T., Hummel, B., van den Bergh, A., Herijgers, P., Nilius, B., Flockerzi, V., Schweda, F. and Freichel, M. (2010) Increased catecholamine secretion contributes to hypertension in TRPM4-deficient mice. J. Clin. Invest. **120**, 3267-3279.

132 Armisen, R., Marcelain, K., Simon, F., Tapia, J. C., Toro, J., Quest, A. F. and Stutzin, A. (2011) TRPM4 enhances cell proliferation through up-regulation of the beta-catenin signaling pathway. J. Cell. Physiol. **226**, 103-109.

133 Crowder, E. A., Saha, M. S., Pace, R. W., Zhang, H., Prestwich, G. D. and Del Negro, C. A. (2007) Phosphatidylinositol 4,5-bisphosphate regulates inspiratory burst activity in the neonatal mouse preBotzinger complex. J. Physiol. **582**, 1047-1058.

134 Schattling, B., Steinbach, K., Thies, E., Kruse, M., Menigoz, A., Ufer, F., Flockerzi, V., Bruck, W., Pongs, O., Vennekens, R., Kneussel, M., Freichel, M., Merkler, D. and Friese, M. A. (2012) TRPM4 cation channel mediates axonal and neuronal degeneration in experimental autoimmune encephalomyelitis and multiple sclerosis. Nat. Med. **18**, 1805-1811.

135 Kim, Y. S., Kang, E., Makino, Y., Park, S., Shin, J. H., Song, H., Launay, P. and Linden, D. J. (2013) Characterizing the conductance underlying depolarization-induced slow current in cerebellar Purkinje cells. J. Neurophysiol. **109**, 1174-1181.

136 Sakuraba, M., Murata, J., Teruyama, R., Kamiya, K., Yamaguchi, J., Okano, H., Uchiyama, Y. and Ikeda, K. (2014) Spatiotemporal expression of TRPM4 in the mouse cochlea. J. Neurosci. Res. **92**, 1409-1418.

137 Takezawa, R., Cheng, H., Beck, A., Ishikawa, J., Launay, P., Kubota, H., Kinet, J. P., Fleig, A., Yamada, T. and Penner, R. (2006) A pyrazole derivative potently inhibits lymphocyte Ca2+ influx and cytokine production by facilitating transient receptor potential melastatin 4 channel activity. Mol. Pharmacol. **69**, 1413-1420.

138 Nilius, B., Prenen, J., Janssens, A., Voets, T. and Droogmans, G. (2004) Decavanadate modulates gating of TRPM4 cation channels. J. Physiol. **560**, 753-765.

139 Zhang, Z., Okawa, H., Wang, Y. and Liman, E. R. (2005) Phosphatidylinositol 4,5-bisphosphate rescues TRPM4 channels from desensitization. J. Biol. Chem. **280**, 39185-39192.

140 Nilius, B., Mahieu, F., Prenen, J., Janssens, A., Owsianik, G., Vennekens, R. and Voets, T. (2006) The Ca2+-activated cation channel TRPM4 is regulated by phosphatidylinositol 4,5-biphosphate. EMBO J. **25**, 467-478.

141 Talavera, K., Yasumatsu, K., Voets, T., Droogmans, G., Shigemura, N., Ninomiya, Y., Margolskee, R. F. and Nilius, B. (2005) Heat activation of TRPM5 underlies thermal sensitivity of sweet taste. Nature. **438**, 1022-1025.

142 Simon, F., Leiva-Salcedo, E., Armisen, R., Riveros, A., Cerda, O., Varela, D., Eguiguren, A. L., Olivero, P. and Stutzin, A. (2010) Hydrogen peroxide removes TRPM4 current desensitization conferring increased vulnerability to necrotic cell death. J. Biol. Chem. **285**, 37150-37158.

143 Nilius, B., Prenen, J., Voets, T. and Droogmans, G. (2004) Intracellular nucleotides and polyamines inhibit the Ca2+-activated cation channel TRPM4b. Pflugers Arch. **448**, 70-75.

144 Grand, T., Demion, M., Norez, C., Mettey, Y., Launay, P., Becq, F., Bois, P. and Guinamard, R. (2008) 9-phenanthrol inhibits human TRPM4 but not TRPM5 cationic channels. Br. J. Pharmacol. **153**, 1697-1705.

145 Guinamard, R., Hof, T. and Del Negro, C. A. (2014) The TRPM4 channel inhibitor 9-phenanthrol. Br. J. Pharmacol. **171**, 1600-1613.

146 Nelson, P. L., Zolochevska, O., Figueiredo, M. L., Soliman, A., Hsu, W. H., Feng, J. M., Zhang, H. and Cheng, H. (2011) Regulation of Ca(2+)-entry in pancreatic alpha-cell line by transient receptor potential melastatin 4 plays a vital role in glucagon release. Mol. Cell. Endocrinol. **335**, 126-134.

147 Launay, P., Cheng, H., Srivatsan, S., Penner, R., Fleig, A. and Kinet, J. P. (2004) TRPM4 regulates calcium oscillations after T cell activation. Science. **306**, 1374-1377.

148 Weber, K. S., Hildner, K., Murphy, K. M. and Allen, P. M. (2010) Trpm4 differentially regulates Th1 and Th2 function by altering calcium signaling and NFAT localization. J. Immunol. **185**, 2836-2846.

149 Vennekens, R., Olausson, J., Meissner, M., Bloch, W., Mathar, I., Philipp, S. E., Schmitz, F., Weissgerber, P., Nilius, B., Flockerzi, V. and Freichel, M. (2007) Increased IgE-dependent mast cell activation and anaphylactic responses in mice lacking the calcium-activated nonselective cation channel TRPM4. Nat. Immunol. **8**, 312-320.

150 Shimizu, T., Owsianik, G., Freichel, M., Flockerzi, V., Nilius, B. and Vennekens, R. (2009) TRPM4 regulates migration of mast cells in mice. Cell Calcium. **45**, 226-232.

151 Barbet, G., Demion, M., Moura, I. C., Serafini, N., Leger, T., Vrtovsnik, F., Monteiro, R. C., Guinamard, R., Kinet, J. P. and Launay, P. (2008) The calcium-activated nonselective cation channel TRPM4 is essential for the migration but not the maturation of dendritic cells. Nat. Immunol. **9**, 1148-1156.

152 Sarmiento, D., Montorfano, I., Cerda, O., Caceres, M., Becerra, A., Cabello-Verrugio, C., Elorza, A. A., Riedel, C., Tapia, P., Velasquez, L. A., Varela, D. and Simon, F. (2014) Increases in reactive oxygen species enhance vascular endothelial cell migration through a mechanism dependent on the transient receptor potential melastatin 4 ion channel. Microvasc. Res. **98**, 187-196.

153 Earley, S., Waldron, B. J. and Brayden, J. E. (2004) Critical role for transient receptor potential channel TRPM4 in myogenic constriction of cerebral arteries. Circ. Res. **95**, 922-929.

154 Reading, S. A. and Brayden, J. E. (2007) Central role of TRPM4 channels in cerebral blood flow regulation. Stroke. **38**, 2322-2328.

155 Loh, K. P., Ng, G., Yu, C. Y., Fhu, C. K., Yu, D., Vennekens, R., Nilius, B., Soong, T. W. and Liao, P. (2013) TRPM4 inhibition promotes angiogenesis after ischemic stroke. Pflugers Arch. **466**, 563-576.

156 Guinamard, R., Demion, M., Magaud, C., Potreau, D. and Bois, P. (2006) Functional expression of the TRPM4 cationic current in ventricular cardiomyocytes from spontaneously hypertensive rats. Hypertension. **48**, 587-594.

157 Simard, C., Hof, T., Keddache, Z., Launay, P. and Guinamard, R. (2013) The TRPM4 non-selective cation channel contributes to the mammalian atrial action potential. J. Mol. Cell. Cardiol. **59**, 11-19.

158 Mathar, I., Kecskes, M., Van Der Mieren, G., Jacobs, G., Uhl, S., Camacho Londono, J. E., Flockerzi, V., Voets, T., Freichel, M., Nilius, B., Herijgers, P. and Vennekens, R. (2013) Increased ss-Adrenergic Inotropy in Ventricular Myocardium from Trpm4-/- Mice. Circ. Res. **114**, 283-94.

159 Hof, T., Simard, C., Rouet, R., Salle, L. and Guinamard, R. (2013) Implication of the TRPM4 nonselective cation channel in mammalian sinus rhythm. Heart Rhythm. **10**, 1683-1689.

160 Marigo, V., Courville, K., Hsu, W. H., Feng, J. M. and Cheng, H. (2009) TRPM4 impacts on Ca2+ signals during agonist-induced insulin secretion in pancreatic beta-cells. Mol. Cell. Endocrinol. **299**, 194-203.

161 Gerzanich, V., Woo, S. K., Vennekens, R., Tsymbalyuk, O., Ivanova, S., Ivanov, A., Geng, Z., Chen, Z., Nilius, B., Flockerzi, V., Freichel, M. and Simard, J. M. (2009) De novo expression of Trpm4 initiates secondary hemorrhage in spinal cord injury. Nat. Med. **15**, 185-191.

162 Simard, J. M., Woo, S. K., Aarabi, B. and Gerzanich, V. (2013) The Sur1-Trpm4 Channel in Spinal Cord Injury. Journal of spine. **Suppl 4:** 002.

163 Woo, S. K., Kwon, M. S., Ivanov, A., Gerzanich, V. and Simard, J. M. (2013) The sulfonylurea receptor 1 (Sur1)-transient receptor potential melastatin 4 (Trpm4) channel. J. Biol. Chem. **288**, 3655-3667.

164 Tosun, C., Kurland, D. B., Mehta, R., Castellani, R. J., Dejong, J. L., Kwon, M. S., Woo, S. K., Gerzanich, V. and Simard, J. M. (2013) Inhibition of the sur1-trpm4 channel reduces neuroinflammation and cognitive impairment in subarachnoid hemorrhage. Stroke. **44**, 3522-3528.

165 Mironov, S. L. (2013) Calmodulin and calmodulin kinase II mediate emergent bursting activity in the brainstem respiratory network (preBotzinger complex). J. Physiol. **591**, 1613-1630.

166 Kruse, M., Schulze-Bahr, E., Corfield, V., Beckmann, A., Stallmeyer, B., Kurtbay, G., Ohmert, I., Schulze-Bahr, E., Brink, P. and Pongs, O. (2009) Impaired endocytosis of the ion channel TRPM4 is associated with human progressive familial heart block type I. J. Clin. Invest. **119**, 2737-2744.

167 Liu, H., Chatel, S., Simard, C., Syam, N., Salle, L., Probst, V., Morel, J., Millat, G., Lopez, M., Abriel, H., Schott, J. J., Guinamard, R. and Bouvagnet, P. (2013) Molecular genetics and functional anomalies in a series of 248 Brugada cases with 11 mutations in the TRPM4 channel. PLoS One. **8**, e54131.

168 Malven, P. V. (1993) Mammalian Neuroendocrinology. Taylor & Francis.

169 Cross, B. A. and Leng, G. (1983) The Neurohypophysis, Structure, Function, and Control: Proceedings of the 3rd International Conference on the Neurohypophysis, Held at Babraham, Cambridge (U.K.), on September 14-16th, 1982. Elsevier.

170 Ginsburg, M. and Ireland, M. (1966) The role of neurophysin in the transport and release of neurohypophysical hormones. J. Endocrinol. **35**, 289-298.

171 Hall, J. E. (2010) Guyton and Hall Textbook of Medical Physiology: Enhanced E-book. Elsevier Health Sciences.

172 Hanley, M. R., Benton, H. P., Lightman, S. L., Todd, K., Bone, E. A., Fretten, P., Palmer, S., Kirk, C. J. and Michell, R. H. (1984) A vasopressin-like peptide in the mammalian sympathetic nervous system. Nature. **309**, 258-261.

173 Hupf, H., Grimm, D., Riegger, G. A. and Schunkert, H. (1999) Evidence for a vasopressin system in the rat heart. Circ. Res. **84**, 365-370.

174 Ang, V. T. and Jenkins, J. S. (1984) Neurohypophysial hormones in the adrenal medulla. J. Clin. Endocrinol. Metab. **58**, 688-691.

175 Kasson, B. G., Meidan, R. and Hsueh, A. J. (1985) Identification and characterization of arginine vasopressin-like substances in the rat testis. J. Biol. Chem. **260**, 5302-5307.

176 Markwick, A. J., Lolait, S. J. and Funder, J. W. (1986) Immunoreactive arginine vasopressin in the rat thymus. Endocrinology. **119**, 1690-1696.

177 Schaeffer, J. M., Liu, J., Hsueh, A. J. and Yen, S. S. (1984) Presence of oxytocin and arginine vasopressin in human ovary, oviduct, and follicular fluid. J. Clin. Endocrinol. Metab. **59**, 970-973.

178 Yibchok-anun, S., Abu-Basha, E. A., Yao, C. Y., Panichkriangkrai, W. and Hsu, W. H. (2004) The role of arginine vasopressin in diabetes-associated increase in glucagon secretion. Regul. Pept. **122**, 157-162.

179 Laycock, J. F. (2010) Perspectives on Vasopressin. Imperial College Press.

180 de Keyzer, Y., Auzan, C., Lenne, F., Beldjord, C., Thibonnier, M., Bertagna, X. and Clauser, E. (1994) Cloning and characterization of the human V3 pituitary vasopressin receptor. FEBS Lett. **356**, 215-220.

181 Tahara, A., Tsukada, J., Tomura, Y., Suzuki, T., Yatsu, T. and Shibasaki, M. (2008) Effect of vasopressin on type IV collagen production in human mesangial cells. Regul. Pept. **147**, 60-66.

182 Jessop, D. S., Murphy, D. and Larsen, P. J. (1995) Thymic vasopressin (AVP) transgene expression in rats: a model for the study of thymic AVP hyper-expression in T cell differentiation. J. Neuroimmunol. **62**, 85-90.

183 Serradeil-Le Gal, C., Herbert, J. M., Delisee, C., Schaeffer, P., Raufaste, D., Garcia, C., Dol, F., Marty, E., Maffrand, J. P. and Le Fur, G. (1995) Effect of SR-49059, a vasopressin V1a antagonist, on human vascular smooth muscle cells. Am. J. Physiol. **268**, H404-410.

184 Syed, N., Martens, C. A. and Hsu, W. H. (2007) Arginine vasopressin increases glutamate release and intracellular Ca2+ concentration in hippocampal and cortical astrocytes through two distinct receptors. J. Neurochem. **103**, 229-237.

185 Morel, A., O'Carroll, A. M., Brownstein, M. J. and Lolait, S. J. (1992) Molecular cloning and expression of a rat V1a arginine vasopressin receptor. Nature. **356**, 523-526.

186 Thibonnier, M., Auzan, C., Madhun, Z., Wilkins, P., Berti-Mattera, L. and Clauser, E. (1994) Molecular cloning, sequencing, and functional expression of a cDNA encoding the human V1a vasopressin receptor. J. Biol. Chem. **269**, 3304-3310.

187 Sugimoto, T., Saito, M., Mochizuki, S., Watanabe, Y., Hashimoto, S. and Kawashima, H. (1994) Molecular cloning and functional expression of a cDNA encoding the human V1b vasopressin receptor. J. Biol. Chem. **269**, 27088-27092.

188 Grazzini, E., Lodboerer, A. M., Perez-Martin, A., Joubert, D. and Guillon, G. (1996) Molecular and functional characterization of V1b vasopressin receptor in rat adrenal medulla. Endocrinology. **137**, 3906-3914.

189 Lee, B., Yang, C., Chen, T. H., al-Azawi, N. and Hsu, W. H. (1995) Effect of AVP and oxytocin on insulin release: involvement of V1b receptors. Am. J. Physiol. **269**, E1095-1100.

190 Yibchok-Anun, S., Cheng, H., Heine, P. A. and Hsu, W. H. (1999) Characterization of receptors mediating AVP- and OT-induced glucagon release from the rat pancreas. Am. J. Physiol. **277**, E56-62.

191 Saito, M., Sugimoto, T., Tahara, A. and Kawashima, H. (1995) Molecular cloning and characterization of rat V1b vasopressin receptor: evidence for its expression in extra-pituitary tissues. Biochem. Biophys. Res. Commun. **212**, 751-757.

192 Birnbaumer, M., Seibold, A., Gilbert, S., Ishido, M., Barberis, C., Antaramian, A., Brabet, P. and Rosenthal, W. (1992) Molecular cloning of the receptor for human antidiuretic hormone. Nature. **357**, 333-335.

193 Lolait, S. J., O'Carroll, A. M., McBride, O. W., Konig, M., Morel, A. and Brownstein, M. J. (1992) Cloning and characterization of a vasopressin V2 receptor and possible link to nephrogenic diabetes insipidus. Nature. **357**, 336-339.

194 Kaufmann, J. E., Iezzi, M. and Vischer, U. M. (2003) Desmopressin (DDAVP) induces NO production in human endothelial cells via V2 receptor- and cAMP-mediated signaling. J. Thromb. Haemost. **1**, 821-828.

195 Richter, D. and Gross, P. (1993) Vasopressin. John Libbey Eurotext.

196 Thibonnier, M. (1992) Signal transduction of V1-vascular vasopressin receptors. Regul. Pept. **38**, 1-11.

197 Koshimizu, T. A., Nakamura, K., Egashira, N., Hiroyama, M., Nonoguchi, H. and Tanoue, A. (2012) Vasopressin V1a and V1b receptors: from molecules to physiological systems. Physiol. Rev. **92**, 1813-1864.

198 DeVito, L. M., Konigsberg, R., Lykken, C., Sauvage, M., Young, W. S., 3rd and Eichenbaum, H. (2009) Vasopressin 1b receptor knock-out impairs memory for temporal order. J. Neurosci. **29**, 2676-2683.

199 Kaufmann, J. E., Oksche, A., Wollheim, C. B., Gunther, G., Rosenthal, W. and Vischer, U. M. (2000) Vasopressin-induced von Willebrand factor secretion from endothelial cells involves V2 receptors and cAMP. J. Clin. Invest. **106**, 107-116.

200 Oiso, Y., Robertson, G. L., Norgaard, J. P. and Juul, K. V. (2013) Clinical review: Treatment of neurohypophyseal diabetes insipidus. J. Clin. Endocrinol. Metab. **98**, 3958-3967.

201 Lemmens-Gruber, R. and Kamyar, M. (2006) Vasopressin antagonists. Cell. Mol. Life Sci. **63**, 1766-1779.

202 Manning, M., Stoev, S., Chini, B., Durroux, T., Mouillac, B. and Guillon, G. (2008) Peptide and non-peptide agonists and antagonists for the vasopressin and oxytocin V1a, V1b, V2 and OT receptors: research tools and potential therapeutic agents. Prog. Brain Res. **170**, 473-512.

203 Compston, J. (2010) Osteoporosis: social and economic impact. Radiol. Clin. North Am. **48**, 477-482.

204 Lightwood, J., Bibbins-Domingo, K., Coxson, P., Wang, Y. C., Williams, L. and Goldman, L. (2009) Forecasting the future economic burden of current adolescent overweight: an estimate of the coronary heart disease policy model. Am. J. Public Health. **99**, 2230-2237.

205 Dolmetsch, R. E., Xu, K. and Lewis, R. S. (1998) Calcium oscillations increase the efficiency and specificity of gene expression. Nature. **392**, 933-936.

206 Kawano, S., Otsu, K., Shoji, S., Yamagata, K. and Hiraoka, M. (2003) Ca(2+) oscillations regulated by Na(+)-Ca(2+) exchanger and plasma membrane Ca(2+) pump induce fluctuations of membrane currents and potentials in human mesenchymal stem cells. Cell Calcium. **34**, 145-156.

207 Sun, S., Liu, Y., Lipsky, S. and Cho, M. (2007) Physical manipulation of calcium oscillations facilitates osteodifferentiation of human mesenchymal stem cells. FASEB J. **21**, 1472-1480.

208 Gutkowska, J., Miszkurka, M., Danalache, B., Gassanov, N., Wang, D. and Jankowski, M. (2007) Functional arginine vasopressin system in early heart maturation. Am. J. Physiol. Heart Circ. Physiol. **293**, H2262-2270.

CHAPTER 2: TRANSIENT RECEPTOR POTENTIAL MELASTATIN 4 CHANNEL CONTROLS CALCIUM SIGNALS AND DENTAL FOLLICLE STEM CELL DIFFERENTIATION*

2.1 INTRODUCTION

Stem cell therapy offers a promising approach in providing an advanced and reliable therapeutic strategy for tissue regeneration and disease treatment. However, fundamental processes controlling the fate of stem cells are not well understood. Dental follicle stem cells (DFSCs) are derived from the neural crest and give origin to the periodontal ligament (PDL) [1, 2]. These cells are multipotent and can differentiate into various cell types including osteoblasts, adipocytes, and neurons [3]. In addition, they can be easily obtained from extracted third molars that are usually discarded as medical waste. Therefore, DFSCs represent an alternative source of stem cells for tissue regeneration. The transient receptor potential (TRP) proteins are a family of ion channels initially identified in the *Drosophila melanogaster* visual system [4]. Despite intensive research, information regarding their function in stem cells remains largely unknown. The melastatin subfamily of TRP channels is composed of eight members (transient receptor potential melastatin [TRPM1–8]), with TRPM4 and TRPM5 being the only non-calcium conducting channels [5, 6]. Both are permeable mainly to Na^+, resulting in depolarization upon channel activation. The ability of TRPM4 to depolarize cells transforms the normal intracellular Ca^{2+} oscillations into sustained

---

* Reprinted with permission from John Wiley and Sons Inc. Authors: Piper Nelson, Tran Doan Ngoc Tran, Hanjie Zhang, Olga Zolochevska, Marxa Figueiredo, Ji-Ming Feng, Dina L. Gutierrez, Rui Xiao, Shaomian Yao, Arthur Penn, Li-Jun Yang and Henrique Cheng. Stem Cells. 2013;31:167–177.

Ca^{2+} increases in T lymphocytes [7]. This is due to a decrease in the driving force for Ca^{2+} entry via store-operated Ca^{2+} channels (SOCs), the main pathway for Ca^{2+} entry in nonexcitable cells, such as DFSCs of mesenchymal origin [3]. Of the TRPMs, only the TRPM7 has been reported in stem cells. It is essential for bone marrow-derived mesenchymal stem cell (MSC) proliferation and survival and is required for early embryonic development [8, 9].

Oscillations in the intracellular Ca^{2+} concentration ($[Ca^{2+}]_i$) are commonly observed during stem cell differentiation, and there is evidence that they may control the differentiation process. Physical manipulation of Ca^{2+} signals with noninvasive electrical stimulation enhances Ca^{2+} entry and osteodifferentiation of human MSCs (hMSCs; [10]). That study suggests that increased Ca^{2+} entry is a result of activation of G protein-coupled receptors and the opening of Ca^{2+} channels. In addition, activation of gene transcription by nuclear factor of activated T-cells (NFAT) in immune cells appears to be controlled by the shape and frequency of the Ca^{2+} signals [7, 11]. Interestingly, both Ca^{2+} signals and NFAT-activated gene transcription disappear at the completion of adipogenesis in hMSCs [12]. Similar observations have been made during the terminal stages of osteoblast differentiation [10], implying that Ca^{2+} signals may be important for directing and terminating the process. Furthermore, oscillations in the $[Ca^{2+}]_i$ control the transition from the G_1 phase to the S phase of the cell cycle to preserve embryonic stem cell (ESC) pluripotency [13]. Therefore, the question of how Ca^{2+} signals control stem cell differentiation is fundamentally important.

The TRPM4 channel is a widely expressed protein present in both electrically excitable and nonexcitable cells. Patch-clamp recordings revealed that it is a Ca^{2+}-activated nonselective cation (CAN) channel, inhibited by nucleotides and polyamines [5, 14]. Although not permeable to Ca^{2+}, TRPM4 has a significant impact on Ca^{2+} signals because it provides a mechanism that allows cells to depolarize in a Ca^{2+}-dependent manner. In nonexcitable cells such as undifferentiated stem cells, TRPM4-mediated depolarization decreases the driving force for Ca^{2+} entry through SOCs, whereas in excitable cells (e.g., neuron, endocrine, or cardiac muscle), TRPM4 has the opposite effect by providing the depolarization necessary for the opening of voltage-dependent Ca^{2+} channels. Previous studies identified SOCs in hMSCs and mESCs [15, 16]. In fact, molecular suppression of TRPM4 increases both Ca^{2+} entry via SOCs and interleukin 2 (IL-2) production in nonexcitable T lymphocytes [7]. Studies in excitable cells revealed a significant reduction in insulin secretion during glucose stimulation in pancreatic β-cells after TRPM4 knockdown [17]; this reduction results from a decrease in the magnitude of the Ca^{2+} signals [18]. A similar observation was made in glucagon secreting α-cells [19]. In addition to the effects in immune and islet cells, the control of Ca^{2+} signals by TRPM4 is critical for myogenic constriction of cerebral arteries, migration of dendritic cells, and cardiac function [20–22]. Given the importance of Ca^{2+} signals for stem cell differentiation, it is possible that ion channels such as TRPM4 could be involved in their regulatory mechanism.

In this study, we investigated the role of TRPM4 in differentiation of rat DFSC, a MSC from the first molar tooth. We examined TRPM4 gene expression

by reverse transcriptase polymerase chain reaction (RT-PCR) and tested whether currents with the characteristics of those known for this channel could be detected using the patch-clamp technique. To gain insight into TRPM4 function, we generated stable knockdown cells via short hairpin RNA (shRNA). These cells were then used in cell proliferation, Ca^{2+} imaging analysis, and differentiation experiments. Finally, we performed whole genome microarray analysis to examine potential genes regulated by TRPM4 during DFSC differentiation.

2.2 MATERIALS AND METHODS

2.2.1 Reagents

All reagents were purchased from Sigma-Aldrich (St. Louis, MO, http://www.sigmaaldrich.com), except for fura-2 acetoxymethyl ester (Fura-2AM), which was from Molecular Probes (Eugene, OR, http://probes.invitrogen.com).

2.2.2 Cell culture

DFSCs of the first mandibular molar were harvested from Sprague–Dawley rat pups 5–7 days postnatal and cultured according to published methods [23]. Cells were grown in α-minimum essential medium (MEM) supplemented with 20% FBS and aerated with 5% CO_2 and 95% air at 37°C. Experiments were performed with cells from passages 2 through 8. MC3T3-E1 preosteoblast cells were grown in α-MEM supplemented with 10% fetal bovine serum (FBS) and cultured as described for DFSCs. Human adipocyte stem cells (hACSs) were maintained in Dulbecco's modified Eagles medium (DMEM)/Ham's F-12 medium (Sigma-Aldrich) with 10% FBS and aerated with 5% CO_2 at 37°C. All experiments were performed with cells from passages 6 through 8.

2.2.3 Induction and detection of cell differentiation

2.2.3.1 Osteogenesis

Cells were induced with osteogenic medium, consisting of DMEM-LG supplemented with 10% FBS, 10 nM dexamethasone, 0.1 mM ascorbic-acid-2-phosphate, and 10 mM β-glycerophosphate. The medium was changed every 4 days during osteogenesis. After a 14-day period, the medium was aspirated, and the cultures were washed twice with phosphate buffered saline (PBS), fixed with 10% formaldehyde, washed again with distilled water, and incubated with 1% Alizarin Red S (ARS) in dH_2O. After incubation, the staining solution was removed, and the cultures were washed with distilled water to remove excess dye. Stained monolayers were visualized by phase contrast microscopy with an inverted microscope (Zeiss, Thornwood, NY, http://microscopy.zeiss.com).

2.2.3.2 Adipogenesis

Cells were induced with adipogenic medium containing DMEM-LG supplemented with 10% FBS, 50 μg/ml ascorbic acid, 0.1 μM dexamethazone, and 50 μg/ml indomethacin. Adipogenesis was determined by oil red O (ORO) staining. Briefly, cells were washed with PBS, fixed with 10% formalin for 10 minutes, washed twice with dH_2O, and incubated with 60% isopropanol for 5 minutes. Cells were then stained with ORO solution for 5 minutes and washed again to remove excess dye. The presence of lipid droplets was visualized by phase contrast microscopy with an inverted microscope.

2.2.4 RT-PCR

RNA was extracted from DFSCs, hASCs, MC3T3-E1 cells, and bone tissue

using the RNAqueous-4PCR kit according to manufacturer's instructions (Ambion, Austin, TX, http://www.ambion.com). The RNA was purified with DNase 1 treatment. Reverse transcription was performed with MMLV-Reverse Transcriptase. PCR was performed with Ambion's RETROscript kit and rat primers with the sequences listed (forward/reverse [5′–3′]): TTGGCATACTGGGAGACG CA/GGCCCAAGATCGTCATCGT (TRPM4; 301 bp); CAAGTGTGACATGGT GGCCATCTT/GCTCAGGTGGCTGAGCAGGAT (TRPM5; 600 bp); GCAAAT GACTCCACTCTC/GATTCTCTCTTCACTCCCAG (TRPM7; 422 bp). Rat glyceraldehyde-3-phosphate dehydrogenase (GAPDH) (420 bp) and ultrapure water were used as positive and negative controls, respectively. The human primers (forward/reverse [5′–3′]) were: AGCATGGTGCCGGAGAA/GGTGTCTCTATT CCGGACCACA (TRPM4; 600 bp); CAGAACATCACCTCACACCAG/GGTT CTCGCTCTTCTGGTTC (TRPM5; 640 bp); TGAAACGAGTGAGTTCTCTTG CTG/CACAGGTGTAAATGGAATGCTC (TRPM7; 309 bp); AACAGCGACAC CCACTCCTC/GGAGGGGAGATTCAGTGTGGT (GAPDH; 258 bp).

2.2.5 Electrophysiology

Cells were maintained in standard modified Ringer's solution of the following composition (in mM): NaCl 140, KCl 2.8, $CaCl_2$ 1, $MgCl_2$ 2, glucose 4, HEPES-NaOH 10, pH 7.2 adjusted with NaOH. The standard internal solution contained (in mM): Cs-glutamate 120, NaCl 8, $MgCl_2$ 1, Cs-BAPTA 10, HEPES-CsOH 10, pH 7.2 adjusted with CsOH. The internal solution's buffered Ca^{2+} concentration was adjusted as necessary with $CaCl_2$ (calculated with WebMaxC http://www.stanford.edu/~cpatton webmaxcS.htm/). The Na^+-free

modified Ringer's solution contained (in mM): choline-Cl 140, KCl 2.8, $CaCl_2$ 1, $MgCl_2$ 2, glucose 4, HEPES-CsOH 10, pH 7.2 adjusted with CsOH. The osmolarity of the solutions were approximately 300 mOsm/L. TRPM4 currents were recorded in the tight-seal whole-cell configuration mode at 21°C–25°C. High-resolution current recordings were acquired by a computer-based patch-clamp amplifier system (EPC-10, HEKA, Lambrecht, Germany, http://www.heka.com). Patch pipettes had resistances of 4–7 MΩ and were coated in Sigmacote silicon solution (Sigma-Aldrich). Immediately following establishment of the whole-cell configuration, voltage ramps of 50 millisecond duration spanning the voltage range of −100 to +100 mV at a rate of 0.5 Hz over a period of 300–600 seconds. All voltages were corrected for a liquid junction potential of 10 mV between external and internal solutions, calculated with Igor PPT Liquid Junction Potential software (Wavemetrics, Portland, OR, http://www.wavemetrics.com).

2.2.6 Generation of TRPM4 knockdown cells

Lentivirus plasmids were obtained from Sigma-Aldrich in a pLKO.1 backbone and contained either nonspecific control (SHC002) or TRPM4-specific shRNA (SHDNA-NM_175130, TRCN0000068684 and TRCN0000068686) under the control of the U6 promoter, plus the puromycin resistance and green fluorescent protein (GFP) reporter genes. Cells were selected in 1 μg/mL puromycin for 1 week, and transduction efficiency was determined by FACScan flow cytometry (BD Biosciences, Franklin Lakes, NJ, http://www.bdbiosciences.com) to sort GFP^+ cells. Stably transduced cells were used for functional experiments.

2.2.7 Cell proliferation assay

An (3-(4,5-dimethylthiazol-2-yl)-2,5-diphenyltetrazolium bromide (MTT) assay was used to compare the proliferation rates between control and TRPM4 knockdown cells. One week following lentiviral transduction 10^4 cells per well were seeded into three 96-well plates and cultured in normal growth medium for 3 days. Cells were then placed in osteogenic or adipogenic medium and analyzed by an MTT-based assay kit (Bioassay Systems, Hayward, CA, http://www.bioassaysys.com) at 48, 72, and 96 hours. MTT solution was added to each well and incubated at 37°C for 4 hours. Then, solubilization buffer was added to dissolve the insoluble formazan product. The absorbance at 550 nm was measured with an Ultramark Microplate Imaging System (BioRad, Hercules, CA, http://www.bio-rad.com). Cell proliferation was expressed as the absorbance of the cells minus the background.

2.2.8 Calcium imaging analysis

Cells were loaded with 5 μM Fura-2AM for 30 minutes at 37°C. A Ca^{2+}-imaging buffer containing (in mM) NaCl 136, KCl 4.8, $CaCl_2$ 1.2, $MgSO_4$ 1.2, HEPES 10, glucose 4, and 0.1% BSA at a pH of 7.3 was used for Fura-2AM loading and perfusion throughout imaging experiments. Calcium measurements were obtained with a dual excitation fluorometric imaging system (TILL-Photonics, Gräfelfingen, Germany, http://www.till-photonics.com) controlled by TILLvisION software. Fura-2AM-loaded cells were excited by wavelengths of 340 nm and 380 nm. Fluorescence emissions were sampled at a frequency of 1 Hz and computed

into relative ratio units of the fluorescence intensity of the different wavelengths (F_{340}/F_{380}).

2.2.9 Alkaline phosphatase activity

Quantification of alkaline phosphatase (ALP) enzyme activity at different time points during osteogenesis was made with an ALP assay kit (BioChain, Newark, CA) according to the manufacturer's instructions. Differentiation experiments were performed in quadruplicate in a 24-well plate (four wells per time point) and repeated three times. The cells were washed in PBS and lysed with 0.5 ml 0.2% Triton X-100 in distilled water prior to ALP activity determination. Samples were assayed in duplicate in a 96-well plate and analyzed at 405 nm with a microcount plate reader BS10000 (PerkinElmer, Waltham, MA, http://www.perkinelmer.com).

2.2.10 Microarray analysis

Raw/normalized intensity values and the log-ratios of all possible pairwise comparisons were preprocessed by the microarray manufacturer (PhalanxBio Inc., Belmont, CA, http://www.phalanxbiotech.com). The genes that were associated with osteogenesis or adipogenesis and affected by TRPM4 knockdown were selected based on the following two criteria: first, genes displaying at least twofold upregulation/downregulation during cell differentiation in either cell population (minimum absolute fold-change ≥2 between control cells prior to differentiation [C0] and after 14 days [C14] and between TRPM4 knockdown cells prior to differentiation [KD0] and after 14 days [KD14]). Second, fold change differences in genes exhibiting differential upregulation/downregulation between control and

knockdown cell populations during cell differentiation (i.e., differences that exist between fold-change values found in control and knockdown cells).

Following gene selection, we identified the biological functions that are most significantly associated ($p < .05$) with selected gene sets via Ingenuity Pathway Analysis (IPA 9.0, Ingenuity Systems, Redwood City, CA, http://www.ingenuity.com). A right-tailed Fisher's exact test was used to calculate a *p*-value, determining the probability that each biological function assigned to that gene set is due to chance alone. Gene networks were created with Ingenuity pathway designer.

2.2.11 Data analysis

Patch-clamp recordings are shown as means + SEM and were plotted with Igor Pro 5 software program (Wavemetrics). The optical density (OD) values from control and TRPM4 knockdown groups in the MTT and ALP assays are shown as means + SEM and were compared by a two-tailed, unpaired Student's *t*-test for each time point. Statistical significance was established at $p<.05$.

2.3 RESULTS

2.3.1 DFSCs express TRPM4 and differentiate into osteoblasts and adipocytes

First, we used RT-PCR analysis to determine whether DFSCs expressed the TRPM4 gene. We identified TRPM4 expression with the predicted molecular size (301 bp) but not the TRPM5 (600 bp), a closely related channel with similar function (Figure 2.1,A). We also confirmed TRPM4 expression in murine preosteoblast MC3T3-E1 cells and rat mandible and tibia bones. Both cells and bone tissues expressed the TRPM7 (422 bp), which is required for cell proliferation

and viability [8, 24]. In order to investigate whether stem cells of human origin expressed TRPM4, we performed RT-PCR with RNA extracted from hASCs. We identified similar gene expression pattern as the one observed with DFSCs (Figure 2.1,A). To demonstrate the multipotency of DFSCs, we tested their differentiation capability into osteoblasts and adipocytes determined by ARS and ORO staining at the end of 14 days (Figure 2.1,B). These stem cells were capable of differentiation into the respective cell types as indicated by extracellular matrix mineralization and lipid droplet accumulation. The adipogenic potential of hASCs is shown in Figure 2.1,B.

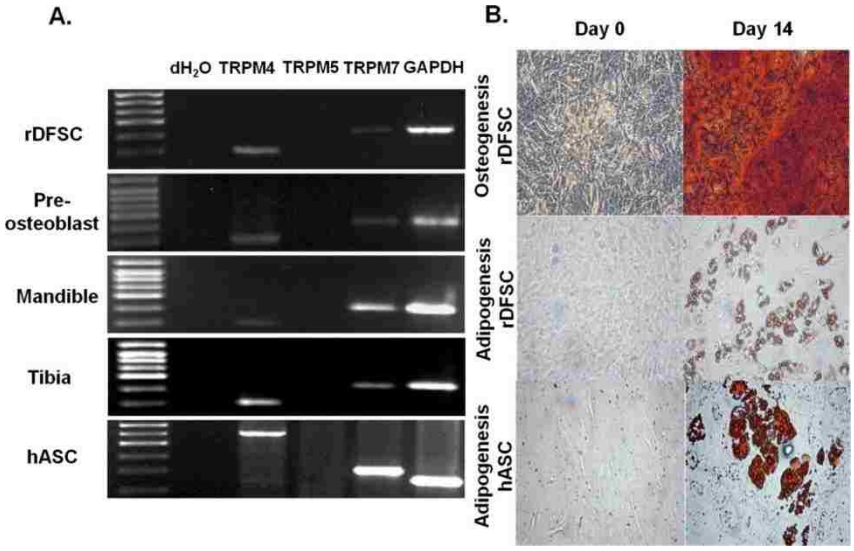

Figure 2.1 TRPM4 gene expression and multipotency of dental follicle stem cells. (A): Total RNA isolated from rat DFSCs, mandible, and tibia bones, mouse preosteoblast MC3T3-E1 cells, hASCs and reverse-transcribed into cDNA. Reverse transcriptase polymerase chain reaction was performed with specific TRPM4 and TRPM5 primers. TRPM7 and GAPDH primers served as positive controls. (B): The multipotency of DFSCs was confirmed after 14 days in osteogenic (upper panel) and adipogenic (lower panel) differentiation medium with Alizarin Red S and oil red O staining. The adipogenic potential of hASCs is also shown. Note the presence of mineralization in the extracellular matrix as well as lipid droplet accumulation at ×32 magnification. Abbreviations: GAPDH, glyceraldehyde 3-phosphate dehydrogenase; hASC, human adipocyte stem cells; rDFSC, rat dental follicle stem cells; TRPM4, transient receptor potential melastatin 4.

2.3.2 DFSCs have functional TRPM4 channels

Next, we performed electrophysiological recordings to investigate the biophysical properties of TRPM4, which is activated by increases in $[Ca^{2+}]_i$ [5]. We performed whole-cell patch-clamp recordings during perfusion of DFSCs with buffered Ca^{2+} concentrations ranging from 0.1 to 3 μM at 0 mV holding potential (Figure 2.2,A). These experiments resulted in a concentration-dependent activation of TRPM4 currents with an EC_{50} of 0.94 μM and Hill coefficient of 7.79 (Figure 2.2,C, 2.2,D). The current–voltage relationships (*I*/*V*) that are the signature of an ion channel are typical of those reported for TRPM4 (Figure 2.2,B). Perfusion of hASCs with increasing buffered Ca^{2+} concentrations (0.1–3 μM) also resulted in a concentration-dependent activation of currents and *I*/*V* similar to those described for channel (Figure 2.2,E, 2.2,F). In addition to Ca^{2+} activation, TRPM4 is voltage-dependent, where negative potentials inhibit and positive potentials increase its open probability [5, 25]. We tested the effect of −60 mV, 0 mV, and +60 mV holding potentials on TRPM4 currents with 1 μM buffered Ca^{2+}. Patch-clamp recordings at negative potentials suppressed and at positive potentials increased the current amplitude compared to 0 mV (Figure 2.3,A). The effect of voltage on TRPM4 is shown by the *I*/*V* from representative cells (Figure 2.3,B). The opening of TRPM4 results in Na^+ entry into cells and depolarization. Hence, we examined channel conductivity by replacing NaCl in the extracellular solution with choline chloride. Under this condition, inward currents were completely abolished compared to cells maintained in NaCl solution during experiments with 1 μM buffered Ca^{2+} and +60 mV holding potential (Figure 2.3,C). The replacement of

Na^+ caused a noticeable shift in the reversal potential due to hyperpolarization (Figure 2.3,D; black arrow).

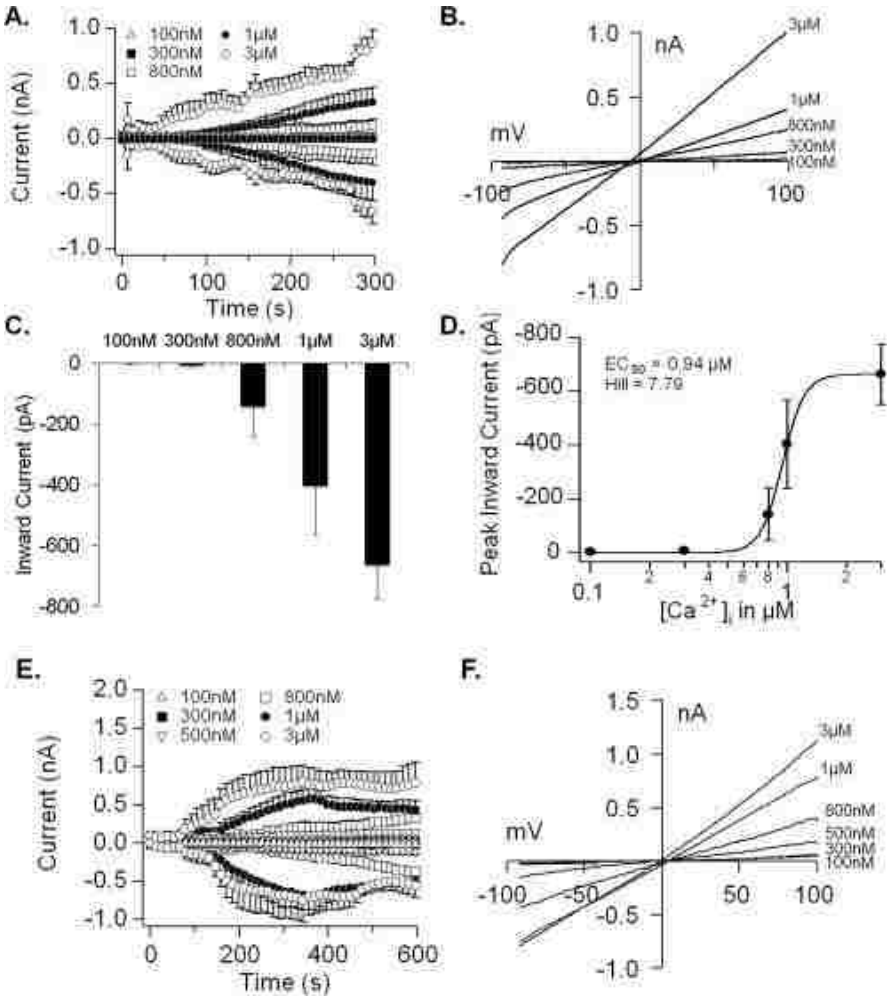

Figure 2.2 Calcium-dependent activation of transient receptor potential melastatin 4 (TRPM4) currents in dental follicle stem cells. (A): Average inward and outward currents during perfusion with increasing buffered Ca^{2+}concentrations. Traces represent the mean + SEM (n = 5–8 cells per concentration) recorded at 0 mV holding potential. (B): Current–voltage relationship (I/V) under experimental conditions described in (A) taken from representative cells at 300 second for each Ca^{2+} concentration. (C): Average inward currents (mean + SEM) from cells represented in panel (A). (D): A dose-response analysis revealed an EC_{50} of 0.94 µM and Hill coefficient of 7.79. (E): Average inward and outward currents during perfusion of human adipocyte stem cells with increasing buffered Ca^{2+} concentrations. Traces represent the mean + SEM (n = 3–6 cells per concentration) recorded at 0 mV holding potential. (F): Current–voltage relationship (I/V) under experimental conditions described in (E) taken from representative cells at 600 second for each Ca^{2+} concentration.

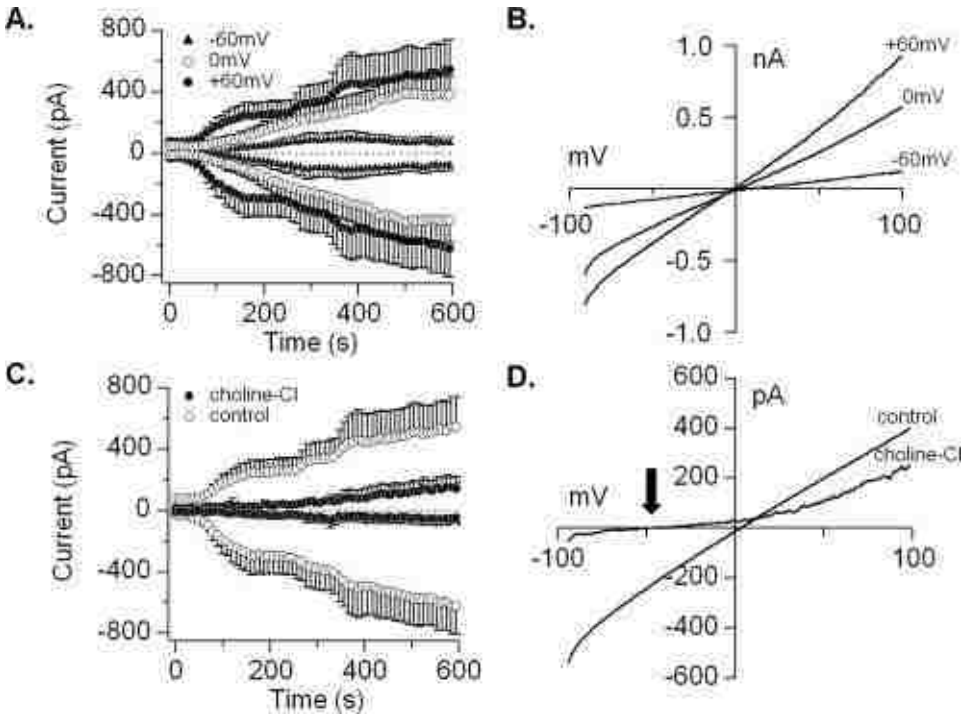

Figure 2.3 Voltage dependency and ionic conductivity of transient receptor potential melastatin 4 (TRPM4) in dental follicle stem cells (DFSCs). (A): Average inward and outward currents in response to 1 μM Ca^{2+} at +60 mV, 0 mV, and −60 mV holding potentials. Traces are mean + SEM (n = 5–6 cells per holding potential). (B): Current–voltage relationship (I/V) under experimental conditions described above at 600 s from representative cells. (C): Average inward and outward currents from DFSCs maintained in NaCl solution compared to cells kept in extracellular buffer with choline-Cl replacing NaCl. Traces are mean + SEM (n = 6–12 cells). (D): Current–voltage relationship (I/V) taken at 600 second from a representative cell. Note the shift in reversal potential (arrow) and hyperpolarization caused by the lack of Na^{+} entry with choline-Cl substitution.

2.3.3 Molecular suppression of TRPM4 inhibits channel activity and cell proliferation

To investigate the functional significance of TRPM4 in DFSCs, we used shRNA and a lentiviral vector to generate stable TRPM4 knockdown cells. We confirmed the effectiveness of the shRNA by performing patch-clamp recordings with 1 μM buffered Ca^{2+} and 0 mV holding potential (HP) to activate the channel.

TRPM4 currents were significantly reduced in knockdown cells compared to control shRNA (Figure 2.4,A) and confirmed by the *I*/*V* (Figure 2.4,B). In stem cells, a decrease in cell proliferation is required prior to differentiation [26, 27]. Therefore, we used the MTT assay to examine whether cell proliferation was impacted by TRPM4 during osteogenesis and adipogenesis. Inhibition of TRPM4 significantly decreased cell proliferation compared to control shRNA cells during a 96-hour period when placed in osteogenic medium (Figure 2.4,C). Under adipogenic conditions, there was a reduction in cell proliferation only during the initial 48 hours with TRPM4 knockdown (Figure 2.4,D). Based on these results, we reasoned that if cell proliferation decreased during osteogenesis, there was a possibility that TRPM4 suppression would facilitate osteoblast but not adipocyte differentiation.

2.3.4 TRPM4 inhibits osteogenesis but facilitates adipogenesis

In order to test TRPM4's function on DFSC differentiation, we cultured cells in osteogenic and adipogenic media over 21 days and performed ARS and ORO staining on days 0, 7, 14, and 21. Inhibition of TRPM4 with two different sets of shRNAs (I and II) enhanced mineralization of DFSCs under osteogenic conditions compared to control shRNA cells, as determined by ARS staining (Figure 2.5,A). Furthermore, DFSCs cultured under adipogenic conditions failed to differentiate into adipocytes, as indicated by the absence of ORO staining (Figure 2.5,B). These results suggest that TRPM4 inhibits osteogenesis but is required for or at least facilitates adipogenesis.

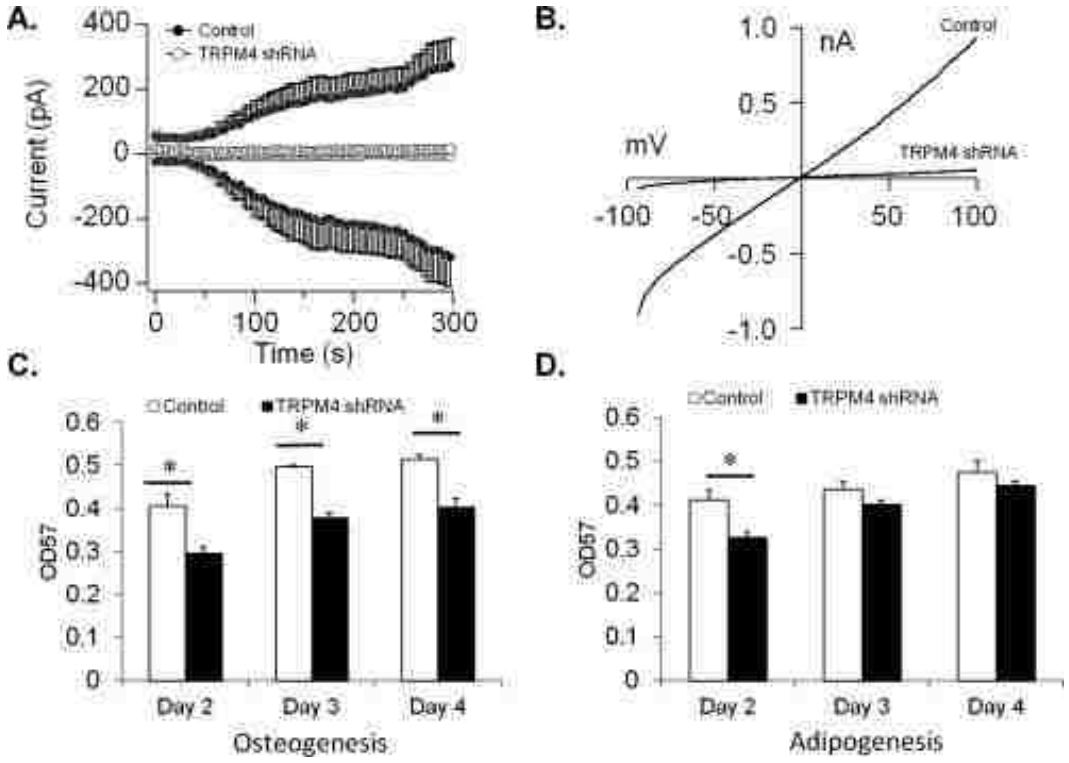

Figure 2.4 TRPM4 knockdown and its impact on cell proliferation. (A): Average inward and outward currents from control shRNA (n = 9) and TRPM4 shRNA cells (n = 6) recorded at +60 mV holding potential and 1 μM buffered Ca^{2+}. A noticeable reduction in current amplitude is seen with TRPM4 knockdown. Traces represent mean + SEM. (B): Current–voltage relationship (I/V) obtained from representative cells at 300 s. (C, D): The effect of TRPM4 knockdown on cell proliferation was examined by MTT assay. A significant decrease in cell proliferation was observed in TRPM4 shRNA cells compared to control shRNA at all time points under osteogenic but not adipogenic conditions. Data are shown as mean + S.E.M. (n = 6 wells/time point); *, $p < .05$. Abbreviations: MTT, (3-(4,5-Dimethylthiazol-2-yl)-2,5-diphenyltetrazolium bromide; TRPM4, transient receptor potential melastatin 4; shRNA, short hairpin RNA.

2.3.5 TRPM4 controls Ca^{2+} signals and ALP enzyme activity

Calcium oscillations are linked to stem cell differentiation, and TRPM4 is key regulator of Ca^{2+} signaling in different cell types [7, 18, 19, 12]. Therefore, we performed real-time Ca^{2+} imaging analysis to determine its impact on Ca^{2+} signals

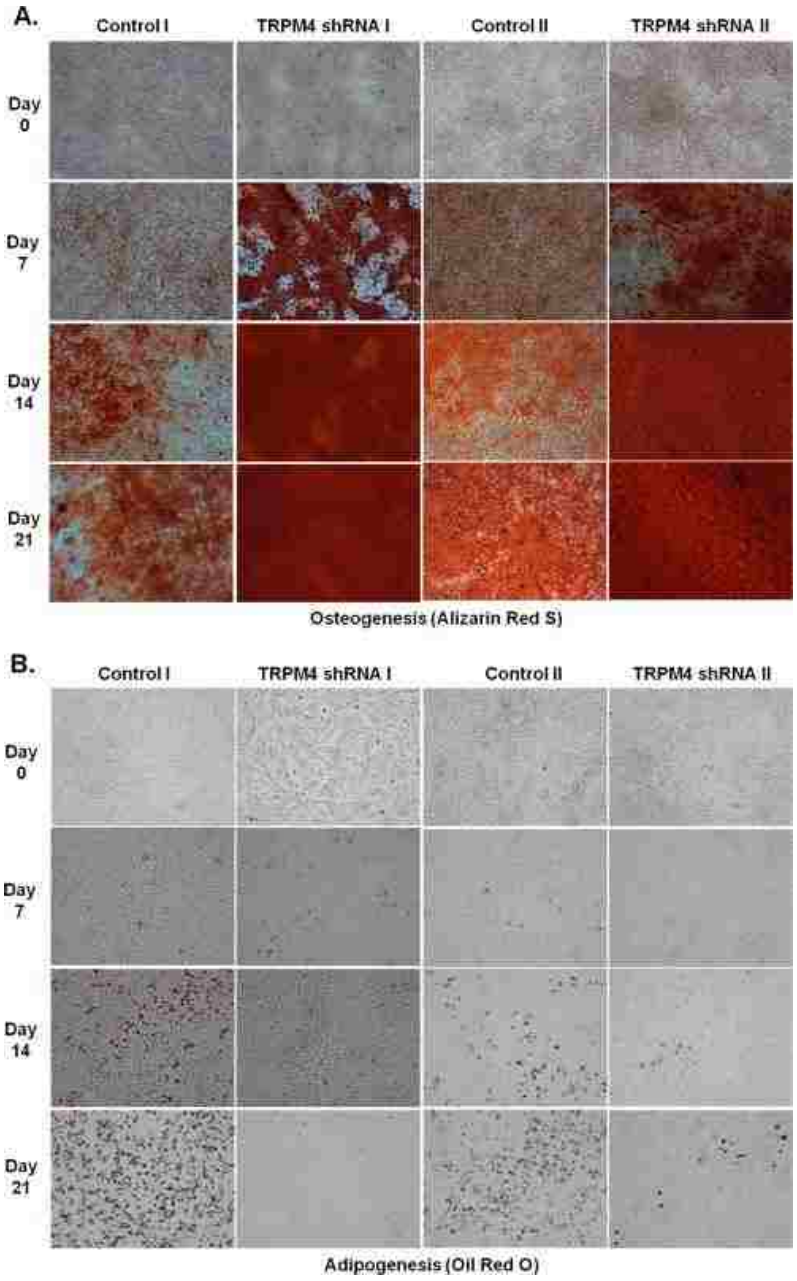

Figure 2.5 Molecular suppression of TRPM4 enhances osteogenesis but inhibits adipogenesis. (A): Extracellular matrix mineralization shown by Alizarin Red S staining during a 21-day period in control shRNA and TRPM4 shRNA cells. (B): Lipid droplet accumulation during a 21-day period in control shRNA and TRPM4 shRNA cells after Oil Red O staining. Suppression of TRPM4 enhanced mineralization during osteogenesis but inhibited lipid droplet accumulation during adipogenesis. Images are representative of three different experiments (×10 magnification). Abbreviations: TRPM4, transient receptor potential melastatin 4; shRNA, short hairpin RNA.

generated by ATP, which influence stem cell differentiation [28, 29]. Stimulation of control shRNA cells with 100 μM ATP resulted in the typical increase in $[Ca^{2+}]_i$ characterized by a first phase due to Ca^{2+} release from the ER, followed by a secondary phase due to Ca^{2+} influx via SOCs (Figure 2.6,A). TRPM4 knockdown transformed the biphasic Ca^{2+} pattern into a gradual and sustained increase (Figure 2.6,B). The average responses of cells from three different cell passages are shown in Figure 2.6,C. The proliferation and osteogenic differentiation assays combined with the Ca^{2+} signaling data prompted us to investigate whether enhanced osteoblast differentiation and mineralization in knockdown cells were associated with an increase in ALP enzyme activity. This enzyme is one of the hallmarks for osteogenesis [30]. We found that there was also a significant increase in ALP enzyme activity on days 14 and 21 of osteoblast differentiation compared to control shRNA cells (Figure 2.6,D).

2.3.6 Genes regulated by TRPM4 during osteogenic and adipogenic differentiation

Finally, we used whole genome microarray analysis to investigate potential genes controlled by TRPM4 during 14 days of differentiation. Based on the approach described for microarray analysis, we first examined genes involved in osteogenesis because of the enhancement of mineralization and osteoblast formation with TRPM4 knockdown. We identified four genes involved in bone mineralization (nuclear factor erythroid-derived 2 [NFE2], asporin [ASPN], matrix extracellular phosphoglycoprotein [MEPE], and matrix γ-carboxyglutamate protein [MGP]). All four genes were upregulated (MEPE 11-fold; MGP 8.6-fold; NFE2 1.9-fold) compared to control shRNA cells, while ASPN gene expression was 37.4-

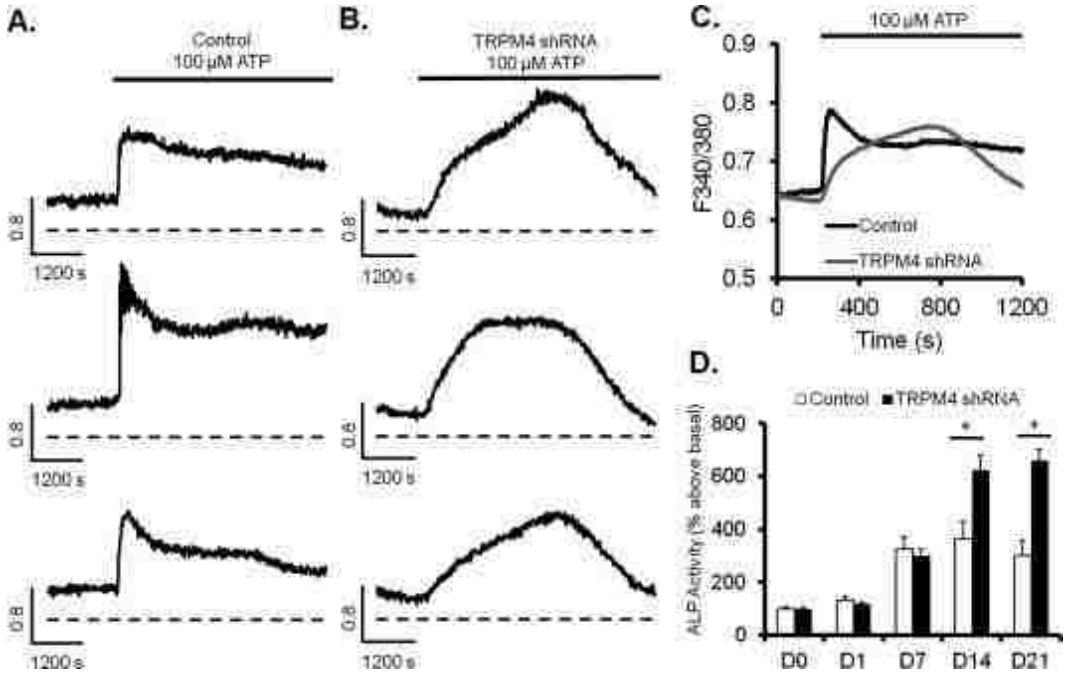

Figure 2.6 TRPM4 regulates Ca^{2+} signals and increases ALP enzyme activity. (A): Calcium signals from single control shRNA cells in response to 100 µM ATP. (B): Same experiment as in (A), except with TRPM4 shRNA cells. (C): Average Ca^{2+} signals from control shRNA (n = 47 cells) and TRPM4 knockdown (n = 64 cells) from three different experiments. (D): ALP enzyme activity during a 21-day period under osteogenic differentiation conditions. Results are presented as mean + SEM from three different experiments (n = 4 wells per time point); *, p < .05. Abbreviations: ALP, alkaline phosphatase; TRPM4, transient receptor potential melastatin 4; shRNA, short hairpin RNA.

fold higher in controls than knockdown cells (Figure 2.7,A). We also identified four genes involved in osteoblast differentiation (Cbp/p300-interacting transactivator 1 [CITED1], cyclin-dependent kinase 6 [CDK6], c-fos induced growth factor [FIGF], and IL 6 receptor [IL6R]). Both CITED1 and CDK6 genes were downregulated 1.5- and 0.9-fold in controls compared to TRPM4 shRNA cells, whereas FIGF and IL6 were upregulated twofold and 0.7-fold, respectively (Figure 2.7,A). In addition, we found the bone development gene, Lumican (LUM), upregulated 12.6-fold with TRPM4 suppression. Furthermore, our results indicated that TRPM4 knockdown inhibited adipogenesis. We identified eight genes: Lipin 1 (LPIN1), tribbles

homolog 3 (TRIB3), WNT inhibitory factor 1 (WIF1), secreted frizzled-related protein 1 (SFRP1), matrix metallopeptidase 3 (MMP3), selenium binding protein 1 (SELENBP1), aldehyde dehydrogenase 6 family member A1 (ALDH6A1), and regulator of G-protein signaling 2 (RGS2) involved in this process (Figure 2.7,B). Of the eight, the TRIB3 was the only gene downregulated, with a 24.7-fold reduction in knockdown compared to control cells. From the upregulated genes, SFRP1 (10.8-fold) and RGS2 (onefold) expression were higher in control cells. TRPM4 suppression increased LPIN1 (3.7-fold), WIF1 (1.3-fold), MMP3 (22.9-fold), SELENBP1 (3.2-fold), and ALDH6A1 (1.4-fold) over control cells. The genes involved in brown fat differentiation are shown in the diagram (Figure 2.7,B).

2.4 DISCUSSION

The study describes for the first time the expression and functions of TRPM4 in stem cells. Using rat DFSCs, we identified TRPM4 gene expression and currents typical for the channel, which were Ca^{2+}-dependent, voltage sensitive, and conducted mainly Na^{+}. Perfusion of cells with increasing Ca^{2+} concentrations resulted in the activation of TRPM4 with an EC_{50} of 0.94 μM and Hill coefficient of 7.79. This is consistent with previous findings in pancreatic α and β cells [19]; thus it appears that in DFSCs, TRPM4 is more sensitive to changes in $[Ca^{2+}]_i$. The TRPM4 channel also exhibited a strong voltage dependency with currents suppressed at negative and facilitated at positive holding potentials [5, 25]. These currents were mainly due to Na^{+} entry into cells, as prior to performing functional studies. Under both conditions, we were able to identify mineralization and lipid droplet accumulation after 14 days.

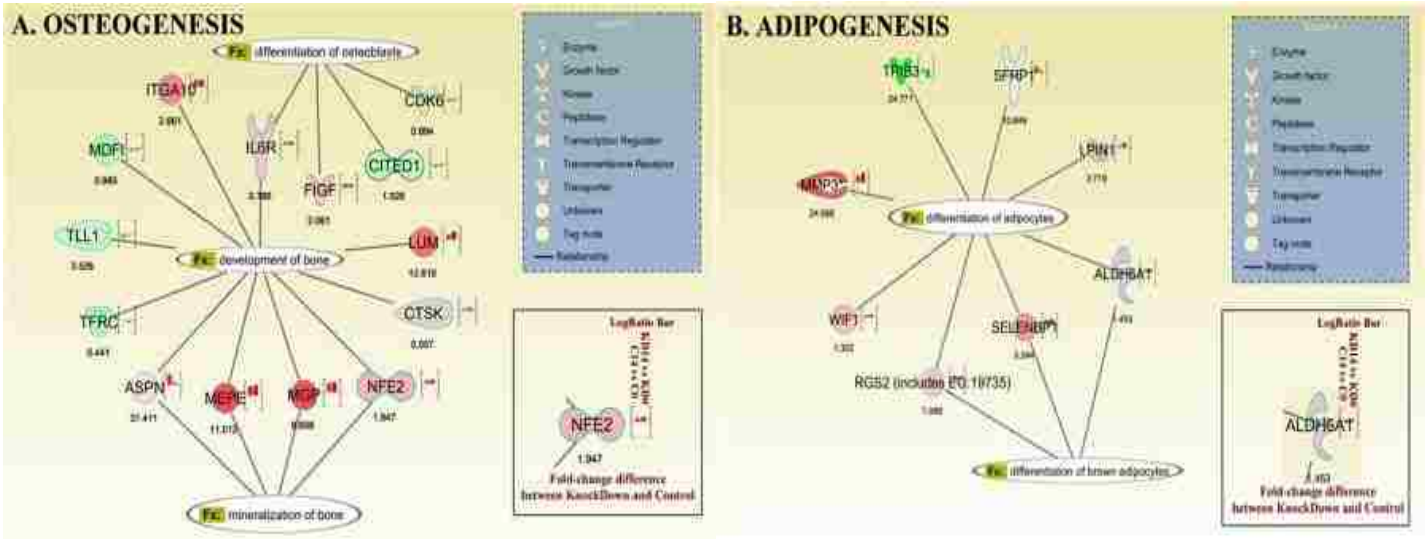

Figure 2.7 Whole genome microarray analysis of osteogenic and adipogenic genes impacted by transient receptor potential melastatin 4 (TRPM4). **(A):** Gene expression related to osteoblast differentiation, bone development and mineralization in TRPM4 shRNA cells after 14 days in osteogenic conditions. **(B):** Gene expression related to adipocyte differentiation from TRPM4 shRNA cells after 14 days in adipogenic conditions. RNA was extracted from control shRNA [C] and TRPM4 knockdown cells [KD] prior to differentiation induction [C0 and KD0] and after 2 weeks of differentiation [C14 and KD14]. The values under each gene represent the difference in fold change between C14 and KD14 groups. Red/green color indicates upregulation/downregulation during differentiation in control (left bars) and knockdown cells (right bars). The biological functions shown in the diagrams have $p < .05$. Abbreviations: ALDH6A1, aldehyde dehydrogenase 6 family member A1; ASPN, asporin; CDK6, cyclin-dependent kinase 6; CITED1, Cbp/p300-interacting transactivator 1; CTSK, cathepsin K; FIGF, c-fos induced growth factor; IL6R, interleukin 6 receptor; ITGA10, integrin alpha-10; LUM, Lumican; LPIN1, Lipin 1; MDFI, myoD family inhibitor; MGP, matrix γ-carboxyglutamate protein; MEPE, matrix extracellular phosphoglycoprotein; MMP3, matrix metallopeptidase 3; NFE2, Nuclear factor erythroid-derived 2; RGS2, regulator of G-protein signaling 2; SFRP1, secreted frizzled-related protein 1; SELENBP1, selenium binding protein 1; TRIB3, tribbles homolog 3; TFRC, transferrin receptor protein 1; TLL1, tolloid-like 1; WIF1, WNT inhibitory factor 1; shRNA, short hairpin RNA.

To investigate the role of TRPM4 in DFSC differentiation, we generated stable knockdown cells with shRNA and a lentiviral vector. We selected this approach because of concern over loss of knockdown effect with transient transfection during differentiation. Inhibition of TRPM4 was confirmed with elevated Ca^{2+} concentration and+60 mV holding potential that resulted in a significant reduction in current amplitude. In DFSCs, inhibition of TRPM4 did not cause cell death, which is similar to findings in knockout mice [31, 32], suggesting that TRPM4 is not lethal. With the availability of the knockdown cells, we examined TRPM4's impact on proliferation and differentiation. A decrease in stem cell proliferation is a prerequisite for osteogenesis and adipogenesis [26, 27]. The fact that TRPM4 suppression decreased DFSCs proliferation during the initial 96 hours of osteogenesis, but not of adipogenesis, indicated a possible enhancement of osteoblast differentiation. This hypothesis was supported by the increased mineralization and ALP enzyme activity; however, under adipogenic conditions, DFSCs failed to differentiate into adipocytes. These findings suggest that TRPM4 functions as an inhibitor of osteogenesis, while it is required and/or facilitates adipogenesis.

Calcium oscillations are often present during stem cell differentiation and are linked to the differentiation process by activating specific transcription factors [12, 13]. To provide insights into the mechanism controlling DFSC differentiation, we investigated their Ca^{2+} signaling pattern of DFSCs during agonist stimulation. Inhibition of TRPM4 transformed the normal ATP-induced biphasic Ca^{2+} pattern, characterized by a sharp increase (ER release–first phase) followed by influx

(Ca^{2+} entry via SOCs–secondary phase) and then a gradual increase followed by a sharp decrease. This was unexpected and different from observations in T lymphocytes, which also use SOCs as the main Ca^{2+} entry pathway. TRPM4 suppression in immune cells results in a sustained secondary phase without impacting the first phase and increases IL-2 production via the calcineurin-NFAT pathway [7, 11]. It is possible that in DFSCs there could be direct interaction between TRPM4 and the ER to control the rate of Ca^{2+} release and refill. Such relationship between ER proteins (e.g., stromal interaction molecule 1) and ion channels (e.g., SOCs) are essential for Ca^{2+} signaling in nonexcitable cells [33, 34]. Another possibility is that of TRPM4 multimerization with SOCs to control the rate of Ca^{2+} influx. Several TRP members are capable of homomultimerization and heteromultimerization [35–38]. However, the gradual increase in $[Ca^{2+}]_i$ with TRPM4 suppression suggests a regulatory mechanism between TRPM4 and the ER. Further studies will be required to elucidate the mechanism underlying the control of Ca^{2+} signals by TRPM4 in DFSCs.

Functional studies in different cell types provide a direct link between TRPM4, Ca^{2+} signaling, and cellular responses. Together, they control dendritic cell migration and cytokine production in T lymphocytes [7, 11, 21]. They also regulate insulin and glucagon secretion from pancreatic islet cells and myogenic constriction in cerebral arteries [18–20]. Because gene transcription is one of the downstream events regulated by TRPM4, we performed whole genome microarray analysis to identify potential genes responsible for the enhancement of osteogenesis and inhibition of adipogenesis. We identified four genes involved in osteoblast

differentiation (CITED1, CDK6, FIGF, IL6R) and four in bone mineralization (NFE2, ASPN, MEPE, MGP). Comparison between osteogenic differentiation genes from control and knockdown cells revealed a maximum of twofold differences, whereas for bone mineralization, the MEPE and MGP genes were upregulated 11- and 8.6-fold with TRPM4 suppression. These findings are consistent with studies in human dental pulp and murine preosteoblast cells, where MEPE expression enhances osteoblast differentiation and mineralization via the BMP-2 signaling pathway [39, 40]. Although the role of MGP in dental tissue is unclear, studies in knockout mice show increased mineralization of pulmonary and renal arteries via the BMP-4 pathway [41]. This is contrary to our observation in DFSCs. Perhaps the differences in signaling pathway and tissues affected by MGP expression could account for this disparity. In fact, the BMP-2 pathway is reported to control DFSC differentiation into osteoblasts [42]. Furthermore, TRPM4 knockdown inhibited ASPN expression 39.4-fold over control cells. This is relevant to DFSCs because this gene is predominantly expressed in the PDL and in dental follicle cells that give rise to the ligament [43]. Since ASPN expression inhibits differentiation and mineralization of the PDL [43], its suppression by TRPM4 knockdown may have contributed to the enhanced osteogenesis. Interestingly, we found the LUM gene upregulated 12.6-fold over control cells. Its roles in collagen formation, epithelial cell migration, and tissue repair suggest a possible role for TRPM4 on bone development [44, 45].

When TRPM4 knockdown cells were placed in adipogenic medium, they failed to differentiate into adipocytes. Of the genes related to this process, the TRB3

was downregulated 24.7-fold compared to control cells. This finding is consistent with reports in type 2 diabetic rats, where silencing of the TRB3 decreases adipocyte formation [46]. Two other notable genes, SFRP1 and MMP3, were upregulated in both groups. TRPM4 knockdown inhibited SFRP1 expression 10.8-fold compared to control cells, and SFRP1 is reported to be a regulator of the Wnt/β-catenin pathway. Its expression enhances adipocyte differentiation in humans and mice [47]. The analysis also revealed a 22.9-fold increase in MMP3 expression compared to control cells. The knockout of this gene also enhances adipogenesis during mammary gland involution in mice, along with adipocyte hypertrophy [48]. The effects of TRPM4 knockdown on the TRB3, SFRP1, and MMP3 genes are expected to inhibit adipocyte differentiation based on their roles during adipogenesis.

Conclusion

TRPM4 is a CAN channel present in DFSCs. These stem cells not only express the TRPM4 gene but also have currents typical for the channel. Functional experiments suggested that TRPM4 acts as an inhibitor of osteogenesis, since channel suppression increased mineralization and ALP enzyme activity. However, it appears to be required and/or facilitates adipogenesis due to the absence of adipocyte differentiation in TRPM4 knockdown cells. The effect of TRPM4 on osteogenesis and adipogenesis seems to be linked to the Ca^{2+} signals, which could be a key factor controlling expression of certain genes.

2.5 REFERENCES

1 Chai, Y., Jiang, X., Ito, Y., Bringas, P., Jr., Han, J., Rowitch, D. H., Soriano, P., McMahon, A. P. and Sucov, H. M. (2000) Fate of the mammalian cranial neural crest during tooth and mandibular morphogenesis. Development. **127**, 1671-1679.

2 Cho, M. I. and Garant, P. R. (2000) Development and general structure of the periodontium. Periodontol. 2000. **24**, 9-27.

3 Honda, M. J., Imaizumi, M., Tsuchiya, S. and Morsczeck, C. (2010) Dental follicle stem cells and tissue engineering. J. Oral Sci. **52**, 541-552.

4 Nelson, P. L., Beck, A. and Cheng, H. (2011) Transient receptor proteins illuminated: current views on TRPs and disease. Vet. J. **187**, 153-164.

5 Launay, P., Fleig, A., Perraud, A. L., Scharenberg, A. M., Penner, R. and Kinet, J. P. (2002) TRPM4 is a Ca2+-activated nonselective cation channel mediating cell membrane depolarization. Cell. **109**, 397-407.

6 Ullrich, N. D., Voets, T., Prenen, J., Vennekens, R., Talavera, K., Droogmans, G. and Nilius, B. (2005) Comparison of functional properties of the Ca2+-activated cation channels TRPM4 and TRPM5 from mice. Cell Calcium. **37**, 267-278.

7 Launay, P., Cheng, H., Srivatsan, S., Penner, R., Fleig, A. and Kinet, J. P. (2004) TRPM4 regulates calcium oscillations after T cell activation. Science. **306**, 1374-1377.

8 Cheng, H., Feng, J. M., Figueiredo, M. L., Zhang, H., Nelson, P. L., Marigo, V. and Beck, A. (2010) Transient receptor potential melastatin type 7 channel is critical for the survival of bone marrow derived mesenchymal stem cells. Stem Cells Dev. **19**, 1393-1403.

9 Jin, J., Wu, L. J., Jun, J., Cheng, X., Xu, H., Andrews, N. C. and Clapham, D. E. (2012) The channel kinase, TRPM7, is required for early embryonic development. Proc. Natl. Acad. Sci. U. S. A. **109**, E225-233.

10 Sun, S., Liu, Y., Lipsky, S. and Cho, M. (2007) Physical manipulation of calcium oscillations facilitates osteodifferentiation of human mesenchymal stem cells. FASEB J. **21**, 1472-1480.

11 Weber, K. S., Hildner, K., Murphy, K. M. and Allen, P. M. (2010) Trpm4 differentially regulates Th1 and Th2 function by altering calcium signaling and NFAT localization. J. Immunol. **185**, 2836-2846.

12 Kawano, S., Otsu, K., Kuruma, A., Shoji, S., Yanagida, E., Muto, Y., Yoshikawa, F., Hirayama, Y., Mikoshiba, K. and Furuichi, T. (2006) ATP autocrine/paracrine signaling induces calcium oscillations and NFAT activation in human mesenchymal stem cells. Cell Calcium. **39**, 313-324.

13 Kapur, N., Mignery, G. A. and Banach, K. (2007) Cell cycle-dependent calcium oscillations in mouse embryonic stem cells. Am. J. Physiol. Cell Physiol. **292**, C1510-1518.

14 Nilius, B., Prenen, J., Voets, T. and Droogmans, G. (2004) Intracellular nucleotides and polyamines inhibit the Ca2+-activated cation channel TRPM4b. Pflugers Arch. **448**, 70-75.

15 Kawano, S., Shoji, S., Ichinose, S., Yamagata, K., Tagami, M. and Hiraoka, M. (2002) Characterization of Ca(2+) signaling pathways in human mesenchymal stem cells. Cell Calcium. **32**, 165-174.

16 Yanagida, E., Shoji, S., Hirayama, Y., Yoshikawa, F., Otsu, K., Uematsu, H., Hiraoka, M., Furuichi, T. and Kawano, S. (2004) Functional expression of Ca2+ signaling pathways in mouse embryonic stem cells. Cell Calcium. **36**, 135-146.

17 Cheng, H., Beck, A., Launay, P., Gross, S. A., Stokes, A. J., Kinet, J. P., Fleig, A. and Penner, R. (2007) TRPM4 controls insulin secretion in pancreatic beta-cells. Cell Calcium. **41**, 51-61.

18 Marigo, V., Courville, K., Hsu, W. H., Feng, J. M. and Cheng, H. (2009) TRPM4 impacts on Ca2+ signals during agonist-induced insulin secretion in pancreatic beta-cells. Mol. Cell. Endocrinol. **299**, 194-203.

19 Nelson, P. L., Zolochevska, O., Figueiredo, M. L., Soliman, A., Hsu, W. H., Feng, J. M., Zhang, H. and Cheng, H. (2011) Regulation of Ca(2+)-entry in pancreatic alpha-cell line by transient receptor potential melastatin 4 plays a vital role in glucagon release. Mol. Cell. Endocrinol. **335**, 126-134.

20 Earley, S., Straub, S. V. and Brayden, J. E. (2007) Protein kinase C regulates vascular myogenic tone through activation of TRPM4. Am. J. Physiol. Heart Circ. Physiol. **292**, H2613-2622.

21 Barbet, G., Demion, M., Moura, I. C., Serafini, N., Leger, T., Vrtovsnik, F., Monteiro, R. C., Guinamard, R., Kinet, J. P. and Launay, P. (2008) The calcium-activated nonselective cation channel TRPM4 is essential for the migration but not the maturation of dendritic cells. Nat. Immunol. **9**, 1148-1156.

22 Guinamard, R., Demion, M., Magaud, C., Potreau, D. and Bois, P. (2006) Functional expression of the TRPM4 cationic current in ventricular cardiomyocytes from spontaneously hypertensive rats. Hypertension. **48**, 587-594.

23 Yao, S., Pan, F., Prpic, V. and Wise, G. E. (2008) Differentiation of stem cells in the dental follicle. J. Dent. Res. **87**, 767-771.

24 Schmitz, C., Perraud, A. L., Johnson, C. O., Inabe, K., Smith, M. K., Penner, R., Kurosaki, T., Fleig, A. and Scharenberg, A. M. (2003) Regulation of vertebrate cellular Mg2+ homeostasis by TRPM7. Cell. **114**, 191-200.

25 Nilius, B., Prenen, J., Droogmans, G., Voets, T., Vennekens, R., Freichel, M., Wissenbach, U. and Flockerzi, V. (2003) Voltage dependence of the Ca2+-activated cation channel TRPM4. J. Biol. Chem. **278**, 30813-30820.

26 Reichert, M. and Eick, D. (1999) Analysis of cell cycle arrest in adipocyte differentiation. Oncogene. **18**, 459-466.

27 Owen, T. A., Aronow, M., Shalhoub, V., Barone, L. M., Wilming, L., Tassinari, M. S., Kennedy, M. B., Pockwinse, S., Lian, J. B. and Stein, G. S. (1990) Progressive development of the rat osteoblast phenotype in vitro: reciprocal relationships in expression of genes associated with osteoblast proliferation and differentiation during formation of the bone extracellular matrix. J. Cell. Physiol. **143**, 420-430.

28 Zippel, N., Limbach, C. A., Ratajski, N., Urban, C., Luparello, C., Pansky, A., Kassack, M. U. and Tobiasch, E. (2012) Purinergic receptors influence the differentiation of human mesenchymal stem cells. Stem Cells Dev. **21**, 884-900.

29 Coppi, E., Pugliese, A. M., Urbani, S., Melani, A., Cerbai, E., Mazzanti, B., Bosi, A., Saccardi, R. and Pedata, F. (2007) ATP modulates cell proliferation and elicits two different electrophysiological responses in human mesenchymal stem cells. Stem Cells. **25**, 1840-1849.

30 Morsczeck, C. (2006) Gene expression of runx2, Osterix, c-fos, DLX-3, DLX-5, and MSX-2 in dental follicle cells during osteogenic differentiation in vitro. Calcif. Tissue Int. **78**, 98-102.

31 Mathar, I., Vennekens, R., Meissner, M., Kees, F., Van der Mieren, G., Camacho Londono, J. E., Uhl, S., Voets, T., Hummel, B., van den Bergh, A., Herijgers, P., Nilius, B., Flockerzi, V., Schweda, F. and Freichel, M. (2010) Increased catecholamine secretion contributes to hypertension in TRPM4-deficient mice. J. Clin. Invest. **120**, 3267-3279.

32 Gerzanich, V., Woo, S. K., Vennekens, R., Tsymbalyuk, O., Ivanova, S., Ivanov, A., Geng, Z., Chen, Z., Nilius, B., Flockerzi, V., Freichel, M. and Simard, J. M. (2009) De novo expression of Trpm4 initiates secondary hemorrhage in spinal cord injury. Nat. Med. **15**, 185-191.

33 Huang, G. N., Zeng, W., Kim, J. Y., Yuan, J. P., Han, L., Muallem, S. and Worley, P. F. (2006) STIM1 carboxyl-terminus activates native SOC, I(crac) and TRPC1 channels. Nat. Cell Biol. **8**, 1003-1010.

34 Peinelt, C., Vig, M., Koomoa, D. L., Beck, A., Nadler, M. J., Koblan-Huberson, M., Lis, A., Fleig, A., Penner, R. and Kinet, J. P. (2006) Amplification of CRAC current by STIM1 and CRACM1 (Orai1). Nat. Cell Biol. **8**, 771-773.

35 Poteser, M., Graziani, A., Rosker, C., Eder, P., Derler, I., Kahr, H., Zhu, M. X., Romanin, C. and Groschner, K. (2006) TRPC3 and TRPC4 associate to form a redox-sensitive cation channel. Evidence for expression of native TRPC3-TRPC4 heteromeric channels in endothelial cells. J. Biol. Chem. **281**, 13588-13595.

36 Rosker, C., Graziani, A., Lukas, M., Eder, P., Zhu, M. X., Romanin, C. and Groschner, K. (2004) Ca(2+) signaling by TRPC3 involves Na(+) entry and local coupling to the Na(+)/Ca(2+) exchanger. J. Biol. Chem. **279**, 13696-13704.

37 Hellwig, N., Albrecht, N., Harteneck, C., Schultz, G. and Schaefer, M. (2005) Homo- and heteromeric assembly of TRPV channel subunits. J. Cell Sci. **118**, 917-928.

38 Murakami, M., Xu, F., Miyoshi, I., Sato, E., Ono, K. and Iijima, T. (2003) Identification and characterization of the murine TRPM4 channel. Biochem. Biophys. Res. Commun. **307**, 522-528.

39 Cho, Y. D., Kim, W. J., Yoon, W. J., Woo, K. M., Baek, J. H., Lee, G., Kim, G. S. and Ryoo, H. M. (2012) Wnt3a stimulates Mepe, matrix extracellular phosphoglycoprotein, expression directly by the activation of the canonical Wnt signaling pathway and indirectly through the stimulation of autocrine Bmp-2 expression. J. Cell. Physiol. **227**, 2287-2296.

40 Wei, X., Ling, J., Wu, L., Liu, L. and Xiao, Y. (2007) Expression of mineralization markers in dental pulp cells. J. Endod. **33**, 703-708.

41 Yao, Y., Jumabay, M., Wang, A. and Bostrom, K. I. (2011) Matrix Gla protein deficiency causes arteriovenous malformations in mice. J. Clin. Invest. **121**, 2993-3004.

42 Silverio, K. G., Davidson, K. C., James, R. G., Adams, A. M., Foster, B. L., Nociti, F. H., Jr., Somerman, M. J. and Moon, R. T. (2012) Wnt/beta-catenin pathway regulates bone morphogenetic protein (BMP2)-mediated differentiation of dental follicle cells. J. Periodontal Res. **47**, 309-319.

43 Yamada, S., Tomoeda, M., Ozawa, Y., Yoneda, S., Terashima, Y., Ikezawa, K., Ikegawa, S., Saito, M., Toyosawa, S. and Murakami, S. (2007) PLAP-1/asporin, a novel negative regulator of periodontal ligament mineralization. J. Biol. Chem. **282**, 23070-23080.

44 Ishiwata, T., Yamamoto, T., Kawahara, K., Kawamoto, Y., Matsuda, Y., Ishiwata, S. and Naito, Z. (2010) Enhanced expression of lumican inhibited the attachment and growth of human embryonic kidney 293 cells. Exp. Mol. Pathol. **88**, 363-370.

45 Kiga, N., Tojyo, I., Matsumoto, T., Hiraishi, Y., Shinohara, Y., Makino, S. and Fujita, S. (2011) Expression of lumican and fibromodulin following interleukin-1 beta stimulation of disc cells of the human temporomandibular joint. Eur. J. Histochem. **55**, e11.

46 Ti, Y., Xie, G. L., Wang, Z. H., Bi, X. L., Ding, W. Y., Wang, J., Jiang, G. H., Bu, P. L., Zhang, Y., Zhong, M. and Zhang, W. (2011) TRB3 gene silencing alleviates diabetic cardiomyopathy in a type 2 diabetic rat model. Diabetes. **60**, 2963-2974.

47 Lagathu, C., Christodoulides, C., Tan, C. Y., Virtue, S., Laudes, M., Campbell, M., Ishikawa, K., Ortega, F., Tinahones, F. J., Fernandez-Real, J. M., Oresic, M., Sethi, J. K. and Vidal-Puig, A. (2010) Secreted frizzled-related protein 1 regulates adipose tissue expansion and is dysregulated in severe obesity. Int. J. Obes. (Lond.). **34**, 1695-1705.

48 Maquoi, E., Demeulemeester, D., Voros, G., Collen, D. and Lijnen, H. R. (2003) Enhanced nutritionally induced adipose tissue development in mice with stromelysin-1 gene inactivation. Thromb. Haemost. **89**, 696-704.

CHAPTER 3: HISTAMINE-INDUCED Ca^{2+} SIGNALLING IS MEDIATED BY TRPM4 CHANNELS IN HUMAN ADIPOSE-DERIVED STEM CELLS*

3.1 INTRODUCTION

Transient receptor potential channels (TRPs) are a family of proteins originally identified in the *Drosophila melanogaster* visual system and have important roles in cellular function. All TRPs include six transmembrane segments with the pore region between segments 5 and 6 and intracellular N- and C-termini. They are divided into the following six subfamilies: TRPC (canonical), TRPV (vanilloid), TRPM (melastatin), TRPP (polycystin), TRPML (mucolipin) and TRPA (ankyrin) [1]. TRPM4 belongs to the melastatin subfamily, and TRPM4 and TRPM5 are the only Ca^{2+}-activated channels [2, 3]. Although not permeable to Ca^{2+}, TRPM4 is proposed to facilitate voltage-dependent Ca^{2+} channel (VDCC) activation in excitable cells and to decrease the driving force for Ca^{2+} influx via store-operated Ca^{2+} channels (SOCs) in non-excitable cells by depolarization [2, 4, 5]. Recently, we have reported that molecular inhibition of TRPM4 inhibits adipogenesis in rat dental follicle stem cells (rDFSCs), which suggests that the channel is required for adipocyte differentiation [6]. This regulatory mechanism is mediated via Ca^{2+} signalling and the expression of specific adipogenic genes. In rDFSCs, inhibition of TRPM4 transforms the primary and secondary phases of the Ca^{2+} signals into a gradual and sustained increase that is similar to the one observed

---

* This research was originally published in Biochemical Journal. Authors: Tran Doan Ngoc Tran, Olga Zolochevska, Marxa L. Figueiredo, Hai Wang, Li-Jun Yang, Jeffrey M. Gimble, Shaomian Yao and Henrique Cheng. Histamine-induced Ca^{2+} signalling is mediated by TRPM4 channels in human adipose-derived stem cells. Biochemical Journal. 2014; 463: 123-134 © the Biochemical Society.

in non-excitable cells (e.g. immune cells) that utilizes SOCs as the main pathway for Ca^{2+} influx [7, 8]. The opposite phenomenon occurs in excitable cells (e.g. pancreatic α- and β-cells and dendrite), where TRPM4 suppression decreases the magnitude of the Ca^{2+} signals due to a reduction in VDCC channel activity [5, 9, 10].

Ionized Ca^{2+} is a well-known second messenger controlling basically every cellular process. Elevations in $[Ca^{2+}]_i$ are observed frequently in response to hormone and growth factor stimulation as well as spontaneous increases. These Ca^{2+} signals are often due to influx from the extracellular space and release from intracellular stores. In stem cells, SOCs were first reported by Kawano et al. [53]. It was shown that Ca^{2+} influx contributes to the signals that co-ordinate cell proliferation and differentiation. In addition, Ca^{2+} oscillations are important for specificity and effectiveness of gene expression, for example nuclear factor of activated T-cells (NFAT) transcription activity [11]. This is supported by the fact that NFAT translocation into the nucleus is needed for stem cell differentiation, but halts at the terminal stages of adipogenesis and osteogenesis [12, 13]. An increase in Ca^{2+} influx in mesenchymal stem cells accelerates osteogenic differentiation via the mitogen-activated protein kinase (MAPK) pathway [13]. Ca^{2+} signalling is also required for embryonic and mesenchymal stem cell cycle progression through G_1/S-phase by inducing expression of c-*myc*, a key gene for self-renewal and pluripotency [14–16]. Furthermore, increases in $[Ca^{2+}]_i$ up-regulate peroxisome-proliferator-activated receptor γ (PPARγ) gene expression, a critical transcription factor for adipocyte differentiation [17].

Ion channels are important regulators of cell proliferation and differentiation due to their ability to conduct Ca^{2+} directly into cells or indirectly by controlling the opening and closure of Ca^{2+} channels. In the first report of TRPM4 in stem cells, we have determined that the channel is required for adipocyte differentiation in rDFSCs by controlling Ca^{2+} signals and adipocyte-specific genes [6]. There are no reports of TRPM4 in any other type of stem cell. However, members of the TRP family such as the TRPM7 are required for bone marrow stem cell proliferation and viability [18]. The channel is also important for early embryonic development [19]. TRPM2 enhances mesenchymal stem cell proliferation [20]. Among non-TRPs, the delayed rectifier K^+ and Ca^{2+}-activated K^+ channels are required for mesenchymal stem cell proliferation [21–23]. In human adipose-derived stem cells (hASCs), the delayed rectifier K^+, Ca^{2+}-activated K^+, transient outward K^+ and tetrodotoxin (TTX)-sensitive transient inward Na^+ channels are present, although their roles in differentiation remain unknown [24]. Despite the lack of information on TRPs during hASC differentiation, some control the functioning of pre-adipocyte and adipocyte cells. TRPC1 and TRPC5 are responsible for constitutive Ca^{2+} influx in differentiated 3T3-L1 cells and adipose tissues [25]. Expression of TRPV1 diminishes during adipogenesis in obese humans and mice [26], and channel activation results in Ca^{2+} influx and uncoupling of protein 1-dependent thermogenesis [27]. Nevertheless, TRPV1-null mice fail to become obese on a high-fat diet because of increased thermogenic activity [28]. Recently, TRPM8 was shown to stimulate uncoupling protein 1-dependent thermogenesis and prevent obesity in mice [29]. Because of TRPM4's

ability to control Ca^{2+} signalling in other cell types and its requirement for adipogenesis in rDFSCs, we have examined its impact on Ca^{2+} signals and adipocyte differentiation in hASCs, which is a more suitable stem cell type for adipogenic studies [30].

3.2 MATERIALS AND METHODS

3.2.1 Reagents

All reagents were purchased from Sigma–Aldrich, except for fura 2 acetoxymethyl ester (fura 2/AM), which was from Molecular Probes, and D-calcium pantothenate, which was from Acros Organics.

3.2.2 Cell culture

hASCs were isolated from lipoaspirates of abdomen and breast adipose tissues according to [31]. The multi-potency of this stem cell type has been confirmed by different laboratories [32–36]. Tissues were donated by one consenting Caucasian female and one consenting Caucasian male, aged 34 and 55 years respectively, body mass index (BMI) from 28.2 to 33.78, under a protocol reviewed and approved by the Pennington Biomedical Institutional Review Board (#PBRC23040) and maintained in Dulbecco's modified Eagle's medium (DMEM)/Ham's F-12 medium with 10% FBS (Atlanta Biologicals) and aerated with 5% CO_2 at 37°C. All experiments were performed with cells from passages 3 to 8.

3.2.3 Induction and detection of adipogenesis

Cells reaching between 80% and 90% confluence were induced with differentiation medium containing DMEM/Ham's F-12 supplemented with 3%

FBS, 0.25 mM 3-isobutyl-1-methylxanthine (IBMX), 33 μM biotin, 17 μM D-calcium pantothenate and 100 nM human insulin for 3 days. Adipocyte medium having the same composition as differentiation medium except for IBMX and rosiglitazone (5 μM) was changed every 3 days from day 3 to day 21 [37]. Adipogenesis was determined by Oil Red O staining. Briefly, cells were washed with PBS, fixed with 10% formalin for 10 min, washed twice with distilled water and incubated with 60% propan-2-ol for 5 min. Cells were then stained with Oil Red O solution for 5 min and washed again to remove excess dye. The presence of lipid droplets was visualized by phase-contrast microscopy using an inverted microscope (Zeiss). Adipocyte cell count was performed with Image-Pro® Analyzer 7.0 (Media Cybernetics).

3.2.4 RT-PCR

Total RNA was extracted from hASCs using the RNAqueous-4PCR® kit according to the manufacturer's instructions (Ambion). The RNA was purified using DNase I treatment. Reverse transcription (RT) and PCR were performed using the RETROscript® kit (Ambion). Total RNA was extracted from abdominal adipose tissue from three females, ages 40–60 years, BMI from 27 to 30, according to an approved protocol by Institutional Review Board of the University of Florida using TRIzol® reagent (Invitrogen). Briefly, 300 mg of human adipose tissue was placed in a mortar pre-chilled with liquid nitrogen. A pestle was used to homogenize the deep frozen tissue with the presence of liquid nitrogen throughout the process. To the sample, 1 ml of TRIzol® was added, and the mixture was transferred to a 1.5 ml Eppendorf tube. After 5 min of incubation at room

temperature, 100 µl of chloroform was added to the mixture, vortex-mixed vigorously for 15 s and kept at room temperature for another 10 min. The mixture was phase-separated by centrifugation at 12000 ***g*** for 15 min at 4°C. Following centrifugation, the mixture was kept at 4°C for 30 min to let the fat solidify. After careful removal of the upper layer of fat, the middle aqueous phase was transferred into a new tube. To precipitate the RNA, 500 µl of propan-2-ol was added. After 10 min of incubation at room temperature, precipitated RNA was pelleted by centrifugation at 12000 ***g*** for 10 min at 4°C. The pellet was then washed with 75% ethanol. After briefly air-drying the RNA pellet, 50 µl of RNase-free water was added to dissolve the RNA and the concentration was determined by measuring the A_{260}/A_{280} ratio. Transcriptor first- strand cDNA synthesis kit was purchased from Roche. Random primer and 4 µg of total RNA were used to generate cDNA. The primers used are listed in Table 3.1.

Table 3.1 List of primers of ion channel genes for RT-PCR

Gene	Forward primer (5'-3')	Reverse primer (5'-3')	Size (bp)
TRPM4 (for hASCs)	AGCATGGTGCCGGAGAA	GGTGTCTCTATTCCGGACCACA	600
TRPM4 (for human adipose tissue)	CCTCTTTGGCGAGTGCTATC	CAAAAGAAGGCGAGAACCAG	222
TRPM5	CAGAACATCACCTCACACCAG	GGTTCTCGCTCTTCTGGTTC	640
TRPM6	CCAGAGCCAGGAGAAAACAG	AAAGGGGAACTCTCCTCCAA	419
TRPM7	TGAAACGAGTGAGTTCTCTTGCTG	CACAGGTGTAAATGGAATGCTC	309
Cav1.1	AACGCCAAGAGGAGTATTATG	ATGGCTGTTGCTATGGTTGC	425
Cav1.2	CTGGACAAGAACCAGCGACAGTGCG	ATCACGATCAGGAGGGCCACATAGGG	562

(Table 3.1 continued)

Gene	Forward primer (5'-3')	Reverse primer (5'-3')	Size (bp)
Cav1.3	TATGTGGCCCTCCTCATAGC	CTCAGGGTCACAGAGCTTCC	219
Cav1.4	GGACCATGGCCCCATCTATAATTACCG	CCTGAAGAGCCACCTTGCCGAAC	764
GAPDH	AACAGCGACACCCACTCCTC	GGAGGGGAGATTCAGTGTGGT	258

GAPDH, glyceraldehyde-3-phosphate dehydrogenase.

3.2.5 Quantitative RT–PCR

From each sample, 2 μg of total RNA was reverse-transcribed into 20 μl of cDNA. Each PCR was prepared by mixing 2 μl of the cDNA with 2× SYBR Green PCR master mix (Life Technologies) and gene-specific primers (Table 3.2). The PCR was carried out with ABI 7300 real-time PCR system (Life Technologies) to obtain the C_T value. Relative gene expression (RGE) was calculated by the ΔC_T method using β-actin as the endogenous control for normalization and Cyclophilin B as the reference control with an RGE of 1.

Table 3.2 List of primers of adipogenic marker genes for quantitative RT-PCR

Gene	Forward primer (5'-3')	Reverse primer (5'-3')	Size (bp)
C/EBPα	CGGTGGACAAGAACAGCAAC	CGGAATCTCCTAGTCCTGGC	365
C/EBPβ	CACAGCGACGACTGCAAGATCC	CTTGAACAAGTTCCGCAGGGTG	188
PPARγ2	GCTGTTATGGGTGAAACTCTG	ATAAGGTGGAGATGCAGGTTC	325
aP2	TGGTTGATTTTCCATCCCAT	TACTGGGCCAGGAATTTGAT	150
Adiponectin	GGCCGTGATGGCAGAGAT	TTTCACCGATGTCTCCCTTAGG	88
Cyclophilin B	GGAGATGGCACAGGAGGAAA	CGTAGTGCTTCAGTTTGAAGTTCTCA	72

3.2.6 Western blot analysis

hASCs from two different lines were grown to confluency and collected into protein lysis buffer with the addition of protease inhibitor cocktail. Protein concentration was determined by the Bradford method. BSA protein standard was purchased from Bio-Rad Laboratories. Then, 50 μg of protein was separated by SDS/8% PAGE. Proteins were transferred on to a nitrocellulose membrane and subjected to sequential Western blotting analysis with anti-TRPM4 (1:300) antibody (Alomone Labs) overnight at 4°C and visualized by ECL Prime Western Blotting Detection Reagent (GE Healthcare Life Sciences) followed by anti-$Ca_v1.2$ (1:300) antibody (Alomone Labs) without stripping off the membrane.

3.2.7 Generation of stable TRPM4 knockdown cells

hASCs were transduced with lentivirus plasmids (Sigma–Aldrich) in a pLKO.1 backbone containing either non-specific control (SHC002) or shRNAs specific for human TRPM4 (TRCN0000044924 and TRCN0000044926) under the control of the U6 promoter, with the puromycin-resistance gene and a *GFP* gene. Cells were selected in puromycin and used for electrophysiology, Ca^{2+} imaging analysis and adipogenic differentiation experiments.

3.2.8 Electrophysiology

Cells were maintained in standard modified Ringer's solution of the following composition: 140 mM NaCl, 2.8 mM KCl, 1 mM $CaCl_2$, 2 mM $MgCl_2$, 4 mM glucose and 10 mM Hepes/NaOH (pH 7.2). Replacement of extracellular Na^+ was accomplished by 140 mM *N*-methyl-D-glucamine (NMDG). The internal solution contained 120 mM caesium glutamate, 8 mM NaCl, 1 mM $MgCl_2$, 10 mM

caesium 1,2-bis-(*o*-aminophenoxy) ethane-*N*,*N*,*N*',*N*'-tetra-acetic acid (BAPTA), 10 mM Hepes/CsOH (pH 7.2). The internal solution's buffered Ca^{2+} concentration was adjusted as necessary with $CaCl_2$. The osmolarity of the solutions was ~300 mOsm/l. TRPM4 currents were recorded in the tight-seal whole-cell configuration mode at 21–25°C. High-resolution current recordings were acquired by a computer-based patch-clamp amplifier system (EPC-10, HEKA). Patch pipettes had resistances between 4 and 7 mΩ and were coated with Sigmacote silicon solution (Sigma–Aldrich). Immediately following establishment of the whole-cell configuration, voltage ramps of 50-ms duration spanning the voltage range of −100 to +100 mV were delivered from a holding potential of 0 mV at a rate of 0.5 Hz over a period of 300 s. All voltages were corrected for a liquid junction potential of 10 mV between external and internal solutions and calculated using Igor PPT Liquid Junction Potential software (Wavemetrics).

3.2.9 Calcium imaging analysis

Cells were loaded with 2 μM fura 2/AM for 30 min at 37°C. The imaging buffer containing 136 mM NaCl, 4.8 mM KCl, 1.2 mM $CaCl_2$, 1.2 mM $MgSO_4$, 10 mM Hepes, 4 mM glucose and 0.1% BSA (pH 7.3) was used for fura 2/AM loading and perfusion throughout the experiments. Calcium measurements were obtained using a dual-excitation fluorimetric imaging system (TILL-Photonics) controlled by TILLvisION software. Fura 2/AM loaded cells in a perfusion chamber were excited at 340- and 380-nm wavelengths. Fluorescence emissions were sampled at a frequency of 1 Hz and computed into relative ratio units of the

fluorescence intensity of the difference of wavelengths (F_{340}/F_{380}). Data were expressed as averages from several cells from three separate experiments.

3.2.10 Data analysis

Patch-clamp recordings, peak Ca^{2+} signals and adipocyte counts are shown as means±S.E.M. and were analysed using a two-tailed and unpaired Student's *t* test (GraphPad Software). Statistical significance was established at $P<0.05$.

3.3 RESULTS

3.3.1 TRPM4 expression in hASCs and human adipose tissue

Using RT–PCR, we have detected TRPM4 transcripts in hASCs and human adipose tissue, but not TRPM5, a related channel with similar function. In addition, we have identified *TRPM6* and *TRPM7* gene expression in stem cells and differentiated adipocytes (Figure 3.1,A). The presence of TRPM4 protein in hASCs was confirmed in two different cell lines by Western blot analysis (Figure 3.1,B).

3.3.2 Biophysical characterization of TRPM4 in hASCs

Since hASCs expressed the *TRPM4* gene, we have performed patch-clamp recordings in the whole-cell configuration mode to determine whether the channel was functionally active. On the basis of the Ca^{2+}-activated property of TRPM4, we have perfused a single hASC with intracellular buffered Ca^{2+} concentration ranging from 0.1 to 3 μM. As a result, currents with the characteristics of those previously described [2, 7] developed in a concentration-dependent manner with peak amplitude at 3 μM (Figures 3.1,C and 3.1,D). The current–voltage (*I–V*) relationship taken from representative cells at 300 s into the recording for each Ca^{2+}

concentration is shown in Figure 3.1,E. The calculated EC_{50} was 0.9 µM and the Hill coefficient was 9.09 (Figure 3.1,F). Another property of TRPM4 is the voltage-

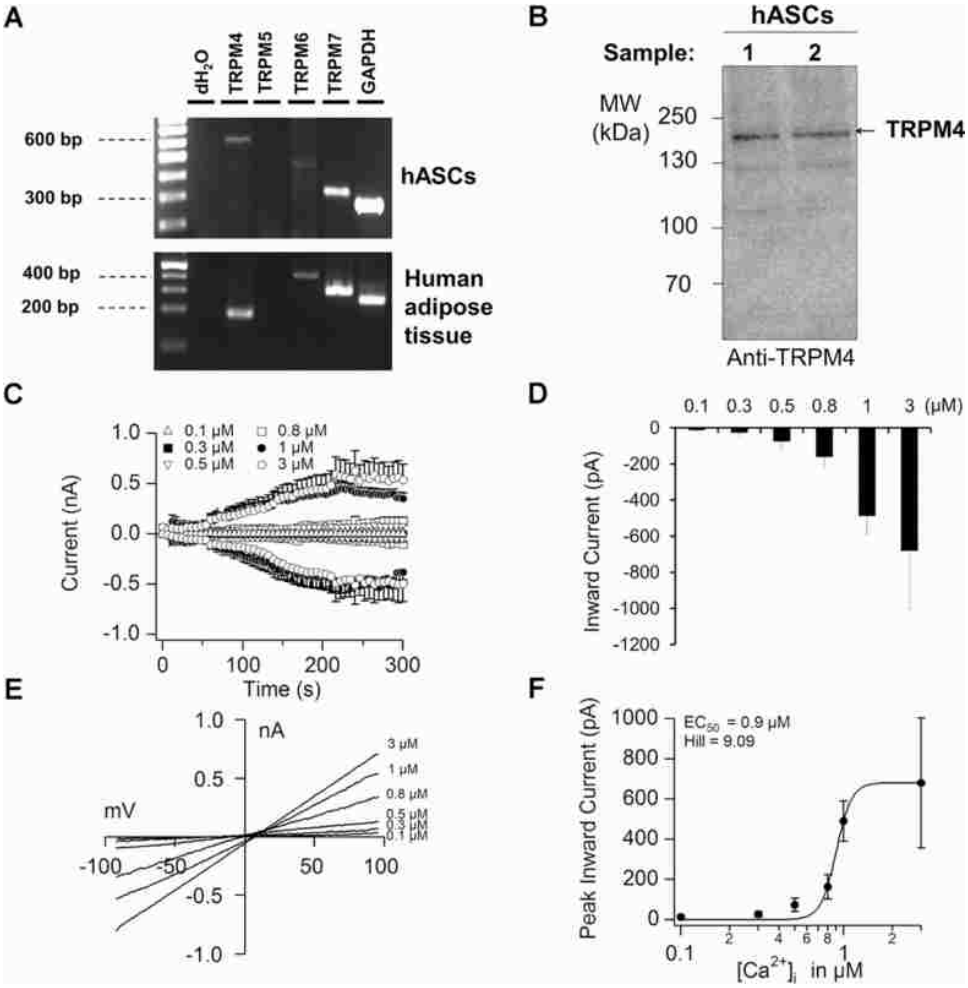

Figure 3.1 TRPM4 expression and functionality in hASCs. (A) Expression of the TRPM4 gene in hASCs and human adipose tissue. In addition, we have detected the presence of TRPM6 and TRPM7. RT–PCR was performed with specific TRPM4, TRPM5, TRPM6 and TRPM7 primers. Distilled water and glyceraldehyde-3-phosphate dehydrogenase (GAPDH) served as negative and positive controls respectively. (B) Western blot analysis confirmed the presence of TRPM4 protein in two different hASC lines. (C) Increases in the intracellular Ca^{2+} activated TRPM4 currents in a concentration-dependent manner. Average inward and outward currents during perfusion of single cells with increasing intracellular buffered Ca^{2+} concentrations. Traces represent the means±S.E.M. (n=5–10 cells per concentration) extracted at −80 mV and +80 mV from a holding potential of 0 mV. (D) Average peak inward currents from cells represented in (C). (E) *I–V* relationship under experimental conditions described in (C) taken from representative cells at 300 s into the recordings. (F) The calculated EC_{50} value and Hill coefficient for different Ca^{2+} concentrations.

dependency, where positive potentials increase its open probability and negative potentials decreases it [2]. Hence, we have performed patch-clamp recordings with holding potentials from −80 mV to +60 mV while perfusing cells with 1 μM intracellular buffered Ca^{2+} concentration. Under these conditions, we have obtained the greatest current amplitude at +60 mV and the smallest at −80 mV (Figure 3.2,A). The *I–V* relationship obtained from representative cells at 300 s is shown in Figure 3.2,B. To investigate TRPM4's ionic conductivity, we have replaced NaCl in the extracellular solution with an equimolar concentration of NMDG and performed recordings with 1 μM intracellular buffered Ca^{2+} concentration at +60 mV holding potential, which gave the maximum current amplitude. Replacement of Na^+ from the extracellular solution abolished TRPM4 currents compared with cells maintained under Na^+ containing buffer, even under high Ca^{2+} and positive holding potential conditions (Figure 3.2,C). The *I–V* relationship confirmed the lack of channel activity in the absence of Na^+ (Figure 3.2,D).

3.3.3 Inhibition of TRPM4 activity by 9-phenanthrol

Next, we have performed patch-clamp recordings using the specific TRPM4 blocker 9-phenanthrol [38–40] to further confirm its presence in hASCs. Pre-treatment of cells with 0.3–10 nM 9-phenanthrol inhibited TRPM4 currents in a concentration-dependent manner during perfusion with 1 μM intracellular buffered Ca^{2+} concentration and 0 mV holding potential (Figures 3.3,A and 3.3,B). The *I–V* relationship showed the reduction in TRPM4 activity with increased 9-phenanthrol concentration (Figure 3.3,C). The calculated IC_{50} and Hill coefficient in hASCs were 1.75 nM and 1.61 respectively (Figure 3.3,D).

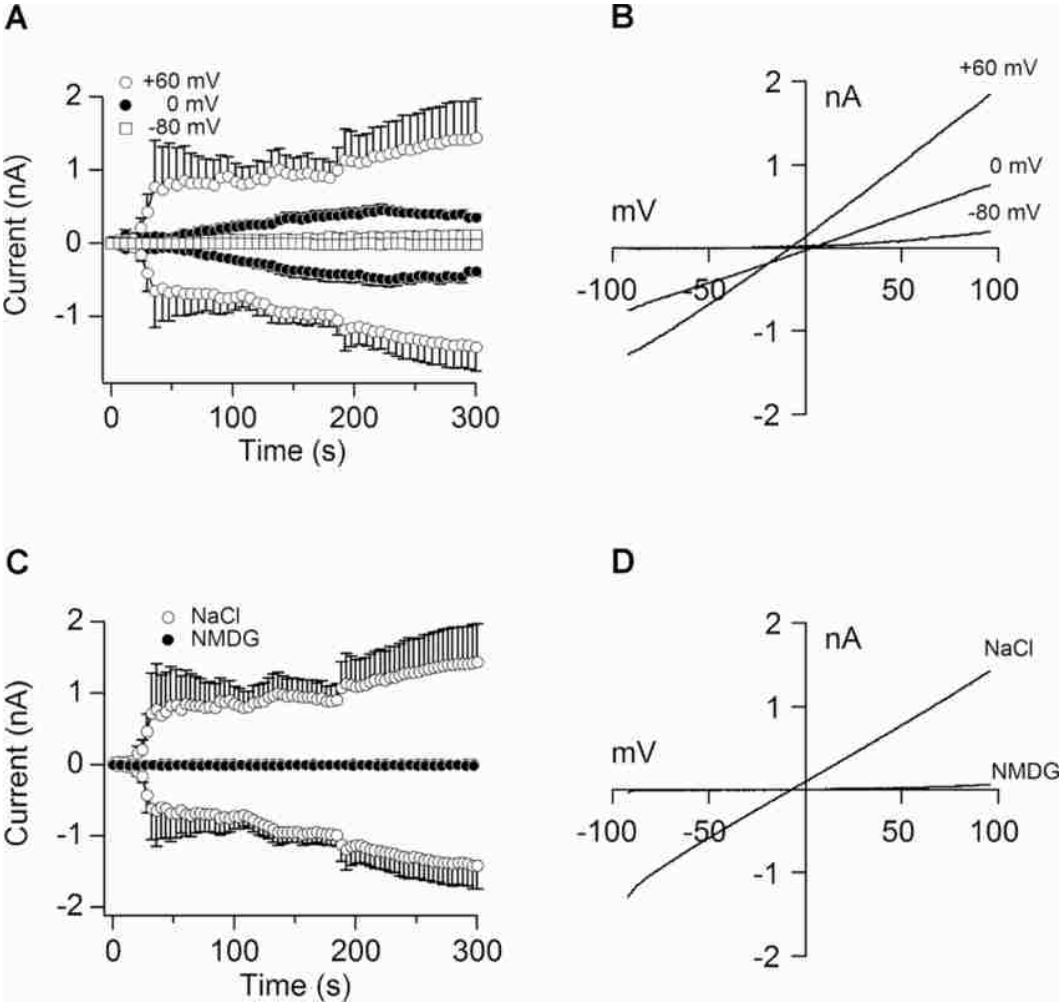

Figure 3.2 Voltage-dependency and ionic conductivity of TRPM4. (A) Average inward and outward currents under −80 mV, 0 mV and +60 mV holding potentials during perfusion of cells with 1 μM intracellular buffered Ca^{2+} concentration. Traces are means±S.E.M. (*n*=3–8 cells per holding potential). (B) *I–V* relationship under experimental conditions described in (A) obtained from representative cells at 300 s. (C) Replacement of NaCl by NMDG in the extracellular buffer solution inhibited TRPM4 currents. Average inward and outward currents from hASCs maintained in control NaCl solution compared with NMDG solution during perfusion with 1 μM intracellular buffered Ca^{2+} concentration at +60 mV holding potential. Traces are means±S.E.M. (*n*=3–8 cells per condition). (D) *I–V* relationship under experimental conditions described in (C) taken from representative cells at 300 s.

3.3.4 Molecular suppression of TRPM4 inhibits channel activity

To determine the importance of TRPM4 for adipogenesis and Ca^{2+} signalling, we have generated stable knockdown cells using shRNA and a

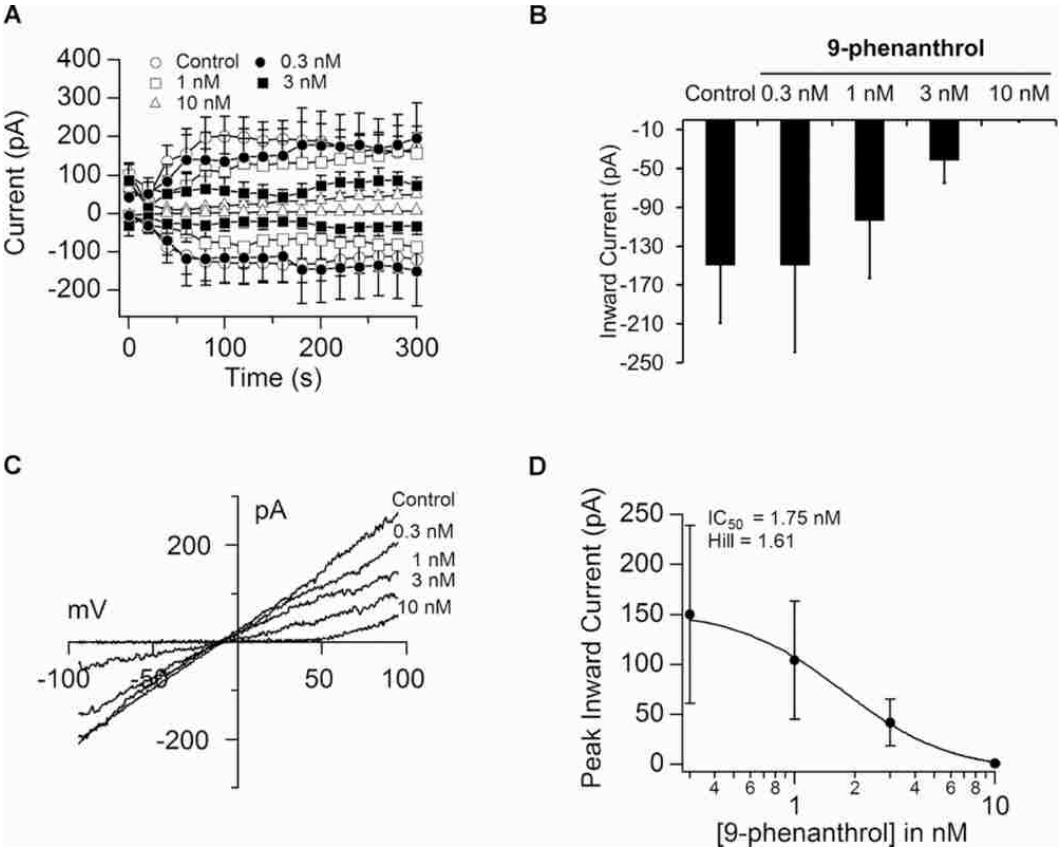

Figure 3.3 Pharmacological suppression of TRPM4 by 9-phenanthrol. (A) Pre-treatment of cells with the specific TRPM4 blocker 9-phenanthrol inhibited channel currents in a concentration-dependent manner during perfusion of cells with 1 μM buffered Ca^{2+} concentration and 0 mV holding potential. (B) Average peak inward currents from cells represented in (A) and compared with control cells without blocker. (C) *I–V* relationship under experimental condition described in (A) obtained from representative cells at 300 s. (D) Calculated IC_{50} and Hill coefficient for different 9-phenanthrol concentrations. Traces represent means±S.E.M. (*n*=6–18 cells per concentration).

lentiviral vector as a delivery agent. The goal of this approach is to obtain cells with reduced TRPM4 activity, which is confirmed by the current amplitude during electrophysiological recordings. We have compared TRPM4 currents between control cells transduced with a scramble sequence shRNA and specific TRPM4 shRNA cells during perfusion with 1 μM intracellular buffered Ca^{2+} concentration at +60 mV holding potential. The currents under these conditions were reduced

significantly with TRPM4 knockdown (Figures 3.4,A and 3.4,B). This confirmed the inhibitory effect of shRNA on channel activity.

3.3.5 TRPM4 suppression decreases lipid droplet accumulation and adipocyte gene expression during adipogenesis

Lipid droplet accumulation is a well-accepted marker for adipocyte differentiation [41]. Hence, we have performed a differentiation assay using Oil Red O staining to determine whether there were differences between control shRNA and TRPM4 knockdown cells after 21 days in adipogenic medium. In accordance with our previous findings in rDFSCs, molecular suppression of TRPM4 significantly reduced lipid droplet accumulation over a 21-day period of differentiation (Figure 3.4,C). In addition, TRPM4 knockdown with two different sets of shRNAs decreased the expression of CCAAT/enhancer-binding protein α (C/EBPα), C/EBPβ, PPARγ2, adipocyte fatty acid-binding protein (aP2) and adiponectin, which are adipocyte marker genes (Figure 3.4,D).

3.3.6 TRPM4 affects Ca^{2+} signalling in response to histamine stimulation

An increase in intracellular Ca^{2+} signals is often seen during stem cell differentiation and is important for this process. Therefore, we have tested whether inhibition of TRPM4 activity in hASCs affected Ca^{2+} signals upon agonist stimulation. We have selected histamine due to its ability to increase intracellular Ca^{2+} and stimulate differentiation of stem cells [42–44]. Stimulation of control wild type cells with 1–300 μM histamine resulted in a concentration-dependent increase in the $[Ca^{2+}]_i$ with maximum responses at 300 μM (Figures 3.5,A and 3.5,B). Next, we examined the histamine receptor mediating the increases using the 300 μM. Pre-treatment of wild-type cells with 10 μM chlorpheniramine, a histamine receptor 1

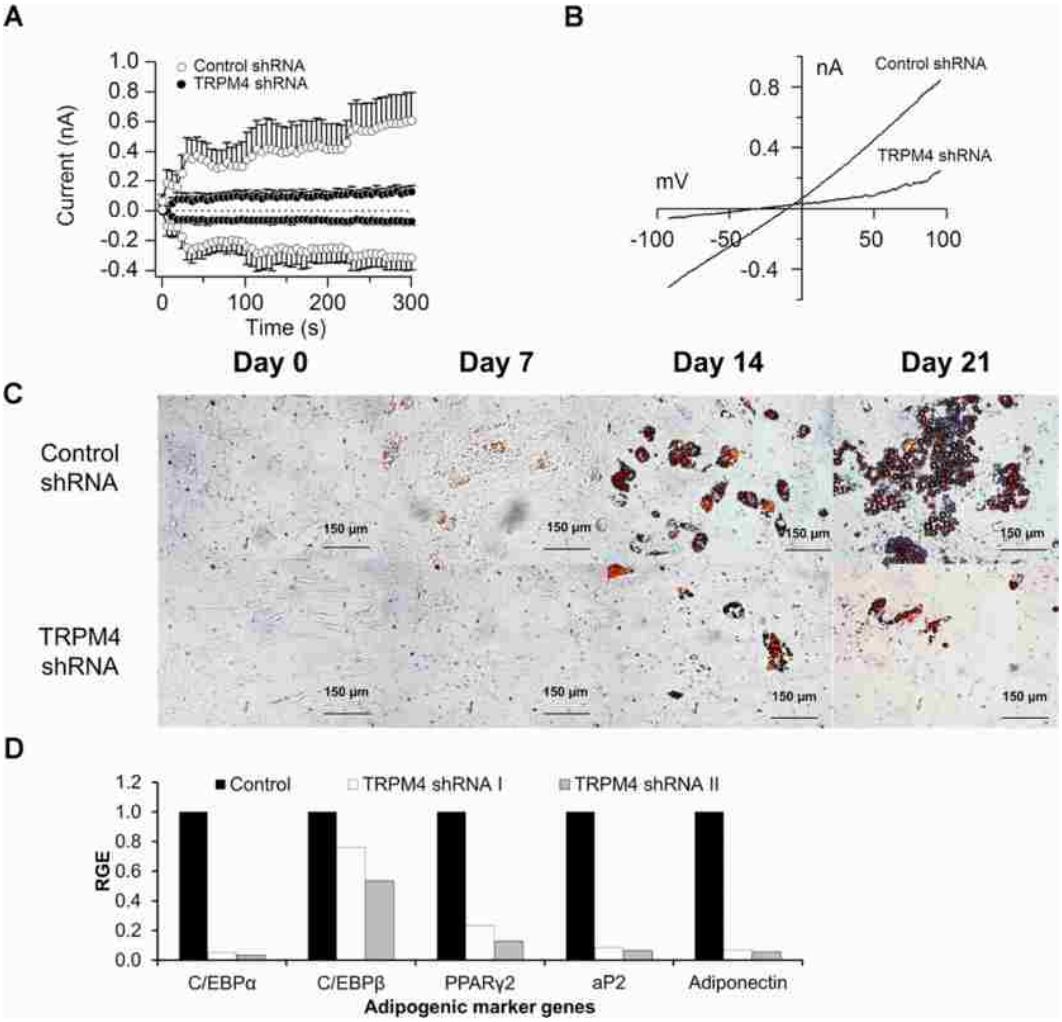

Figure 3.4 TRPM4 knockdown by shRNA inhibits adipocyte differentiation. (A) Inhibition of TRPM4 activity was confirmed by the decrease in the current amplitude under 1 µM intracellular buffered Ca^{2+} concentration and +60 mV holding potential and compared with control shRNA cells. (B) *I–V* relationship under experimental conditions described in (A) obtained from representative cells at 300 s. Traces represent means±S.E.M. [*n*=5 (control shRNA) and 6 (TRPM4 shRNA) cells]. (C) Control shRNA and knockdown cells differentiated into adipocytes for 21 days and stained with Oil Red O for the presence of lipid droplets (×20 magnification). Note the reduction in lipid droplet accumulation with TRPM4 suppression. (D) Molecular suppression of TRPM4 with two different sets of shRNAs decreased adipocyte marker gene expression compared with control cells after 14 days in adipocyte differentiation medium.

(H1) receptor antagonist, completely abolished the Ca^{2+} signals generated by histamine, but not 100 µM cimetidine, an H2 antagonist (Figures 3.5,C–3.5,E). Because TRPM4 is reported to control Ca^{2+} signals in both excitable and non-

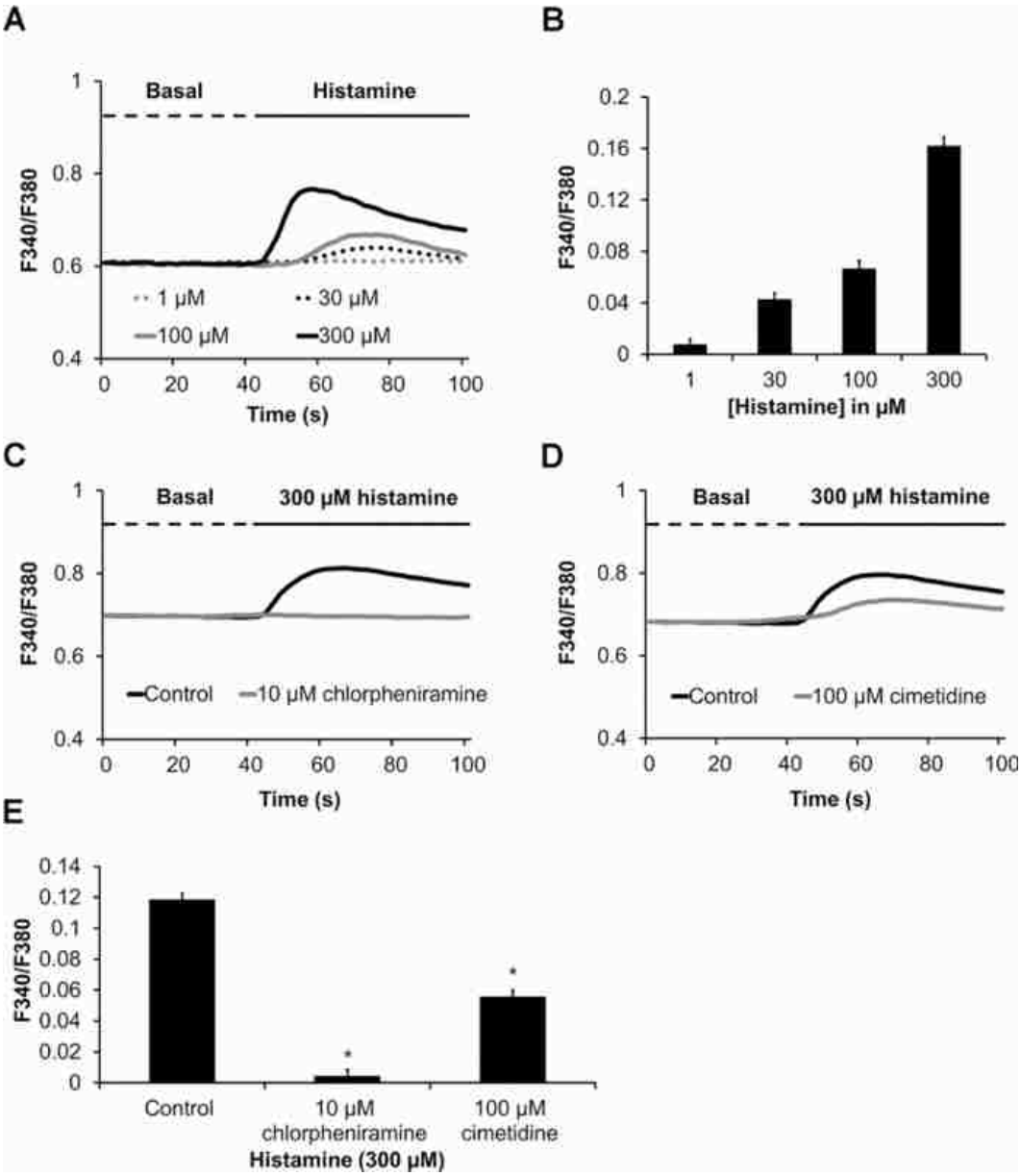

Figure 3.5 Histamine-induced increases in intracellular Ca^{2+} concentration. (A) Average Ca^{2+} signals during stimulation of hASCs with increasing histamine concentrations. (B) Average peak increases for each histamine concentration. (C–D) The inhibitory effects of chlorpheniramine and cimetidine on histamine-induced Ca^{2+} signals are shown. (E) Average peak increases after treatment of cells with the respective receptor blocker and compared with control cells without blocker. Values are means±S.E.M.; *n*=49–272 cells per group from three separate experiments; **P*< 0.0001.

excitable cells, we have tested whether channel suppression would alter the signals generated by histamine. Indeed, TRPM4 knockdown significantly decreased the

responses to 300 μM histamine during adipogenic differentiation (Figures 3.6,A–3.6,D).

3.3.7 TRPM4-mediated depolarization facilitates the opening of VDCCs

Inhibition of TRPM4 activity in hASCs decreased the magnitude of the Ca^{2+} signals compared with control shRNA cells (Figure 3.6). This effect was similar to the ones observed in excitable cells of the pancreas [5, 9] that rely on depolarization and the opening of VDCCs for Ca^{2+} influx. Hence, we have examined *VDCC* gene expression in hASCs using RT–PCR analysis. The results revealed that the L-type $Ca_v1.2$ channel was the main VDCC expressed in this stem cell (Figure 3.7,A). We have also detected $Ca_v1.2$ protein along with TRPM4 (Figure 3.7,B). To determine whether it contributed to Ca^{2+} influx, we have performed Ca^{2+} imaging analysis with nimodipine, an L-type Ca^{2+} channel blocker during histamine stimulation. Pre-treatment with 1–30 μM nimodipine decreased the amplitude of the Ca^{2+} signals compared with control wild-type cells without the blocker but did not abolish the signals even at the highest concentration (Figures 3.7,C–3.7,G). Therefore, we have investigated the additional Ca^{2+} source and confirmed the involvement of TRPM4 in VDCC activation by comparing the responses to histamine under extracellular Ca^{2+}-free conditions and after depletion of endoplasmic reticulum (ER) Ca^{2+} with thapsigargin (Figure 3.7,H). Under control conditions with $CaCl_2$ in the extracellular buffer and without thapsigargin, TRPM4-knockdown decreased the magnitude of the Ca^{2+} signals compared with control shRNA cells. When the extracellular Ca^{2+} was removed from the buffer solution, both control shRNA and TRPM4-knockdown cells had reduced but

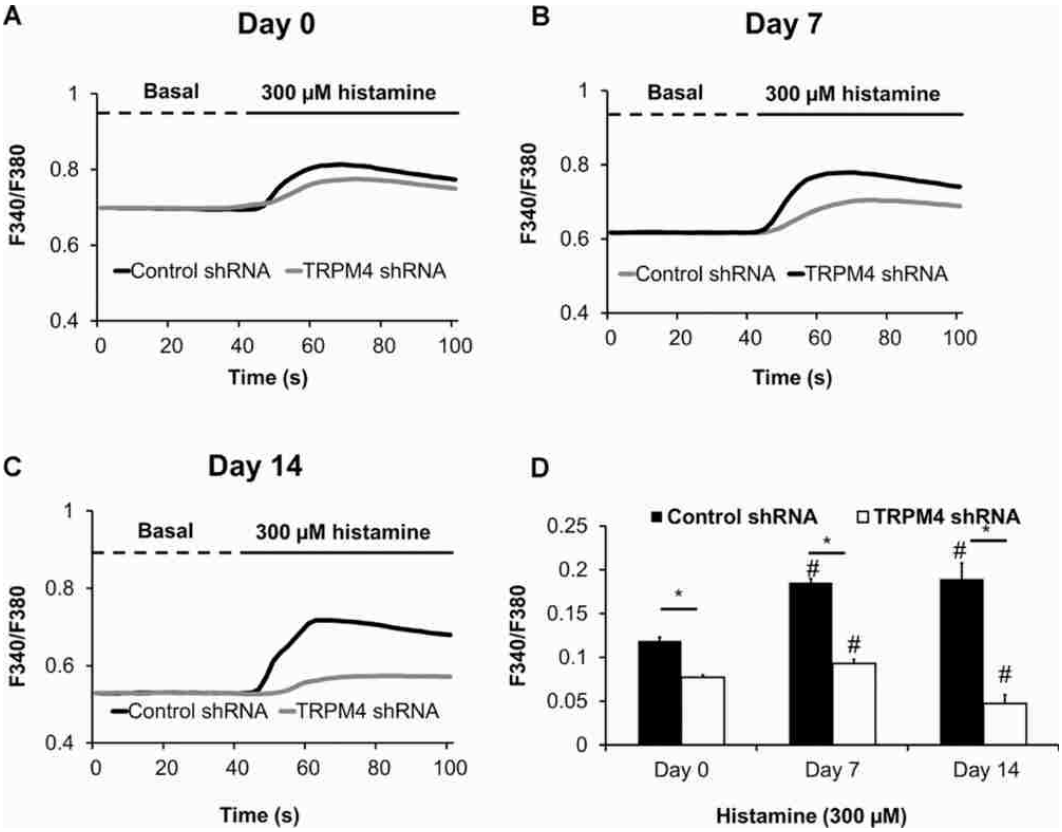

Figure 3.6 TRPM4 knockdown decreases the magnitude of the Ca^{2+} signals by histamine during adipogenesis. (A–C) Average Ca^{2+} signals generated by histamine in control shRNA and TRPM4 knockdown cells at days 0, 7 and 14 of differentiation. (D) Comparison between the average peak Ca^{2+} increases from control shRNA and TRPM4 knockdown cells at the same time point and compared with day 0. Values are means±S.E.M.; *n*=37–338 cells from three separate experiments; **P*<0.05 comparing control and knockdown at the same time point; #*P*<0.05 comparing same group with day 0.

comparable responses. Pre-treatment of cells with thapsigargin almost abolished the responses to histamine in both groups. This indicated that the mechanism by histamine increased intracellular Ca^{2+} was initiated by ER release followed by influx, and the opening of VDCCs was facilitated by TRPM4.

3.3.8 Histamine stimulates adipocyte differentiation

Since histamine stimulates the differentiation of other types of stem cells [42–44], we have examined whether it would affect adipogenesis in hASCs.

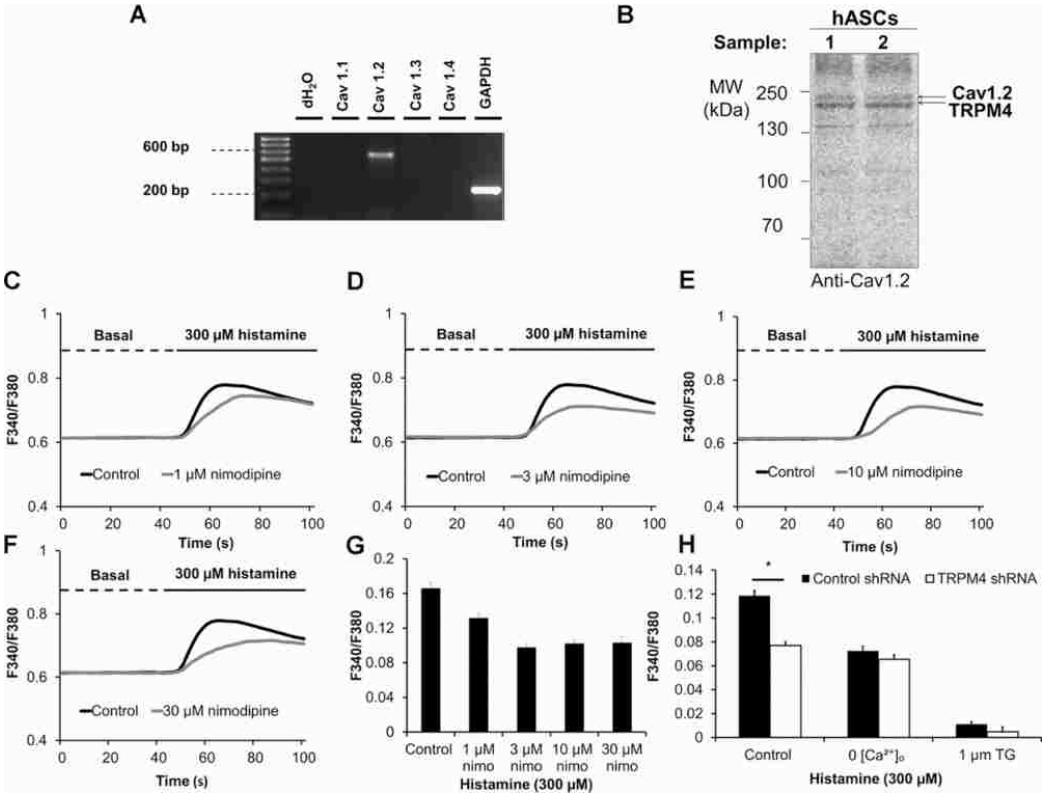

Figure 3.7 hASCs express VDCCs and utilize different Ca^{2+} sources for histamine responses. (A) We have detected $Ca_v1.2$ gene expression in wild-type hASCs, an L-type VDCC, but not $Ca_v1.1$, $Ca_v1.3$ or $Ca_v1.4$. Distilled water and glyceraldehyde-3-phosphate dehydrogenase (GAPDH) served as negative and positive controls respectively. (B) In addition to TRPM4 protein, we have also detected $Ca_v1.2$ protein in two different hASC lines using Western blot analysis. (C–F) Pre-treatment of wild-type cells with increasing nimodipine concentrations, an L-type VDCC blocker, reduced the magnitude of the Ca^{2+}signals in response to histamine stimulation but did not abolished them. (G) Average peak Ca^{2+} increases by histamine after VDCC channel blockage with different nimodipine concentrations and compared with controls cells without the blocker. (H) Comparison between peak Ca^{2+} signals from control shRNA and TRPM4 knockdown cells during histamine stimulation under extracellular free Ca^{2+} condition and after depletion of intracellular Ca^{2+} stores with thapsigargin. Values are means±S.E.M.; *n*=132–338 cells from three separate experiments; **P*<0.001 comparing control shRNA and TRPM4 shRNA cells under same experimental condition.

Histamine (200 nM) supplementation to the adipogenic medium significantly increased lipid droplet accumulation and the number of adipocytes after 14 days of

differentiation compared with control medium without histamine (Figures 3.8,A–3.8,C). These results confirmed its stimulatory effect on the differentiation process.

3.4 DISCUSSION

In a recent report, we have described the presence of TRPM4 in rDFSCs and demonstrated that the channel is required for adipogenesis [6]. Since hASCs are the normal precursors for adipocytes, we have investigated TRPM4 in this type of stem cell. We have identified TRPM4 gene expression and protein in hASCs and human adipose tissue. We have also ruled out the possibility of TRPM5 affecting differentiation and functioning of these cells since hASCs and adipocytes did not express this particular channel. Our findings that adipose tissue expresses TRPM4 suggest a potential role in adipocytes. In fact, white and brown adipocytes have Ca^{2+}-activated non-selective cation (CAN) channels with similar characteristics of TRPM4, such as Ca^{2+}-dependent activation, conductivity, reversal potential and voltage-dependency [45–47]. However, none of these CANs have been recognized until now and it is possible that some might be TRPM4. Furthermore, perfusion of hASCs with increasing buffered Ca^{2+}concentrations activated TRPM4 in a concentration-dependent manner. The calculated EC_{50} value and Hill coefficient of 0.9 μM and 9.09 are very similar to the ones in rDFSCs. Additional characterization of TRPM4 in other stem cells is needed to determine whether there are differences in biophysical properties. In hASCs, we have confirmed TRPM4's voltage-dependency, where negative holding potential inhibited and positive holding potential facilitated channel activity [5, 9]. The channel also conducted Na^+ as the main ion since its replacement by NMDG

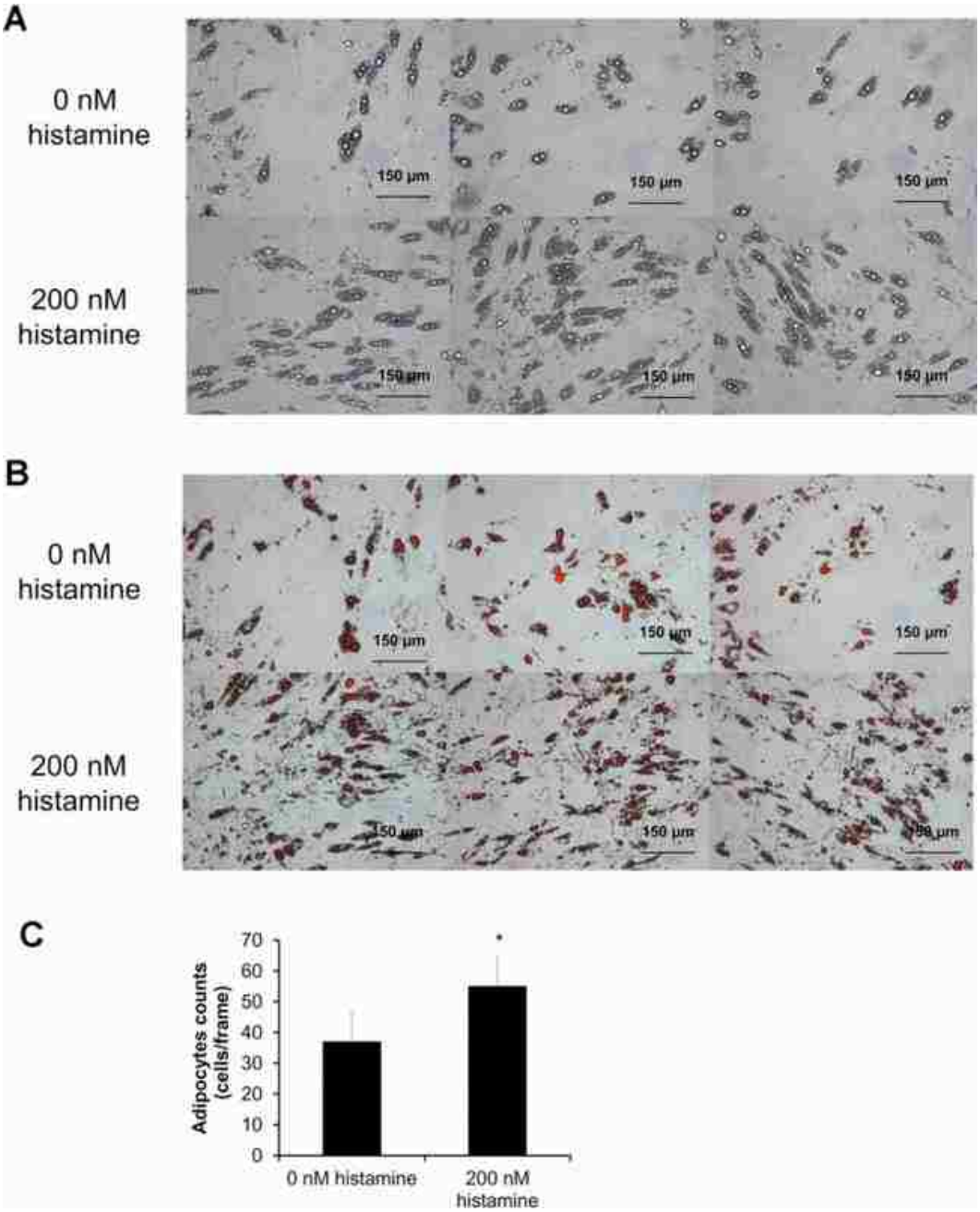

Figure 3.8 Histamine stimulates adipogenesis in hASCs. Wild-type cells were differentiated into adipocytes for 14 days with and without 200 nM histamine in the adipogenic medium and stained with Oil Red O for the presence of lipid droplets (×20 magnification). Note the increase in lipid droplet accumulation with histamine supplementation. (A) Brightfield. (B) Oil Red O staining. (C) Average adipocytes counted from a total of 18 frames taken at ×10 magnification. Values are means±S.E.M.; n=667 (− histamine) and 991 (+ histamine) cells; *P<0.0001.

resulted in complete current suppression. The specific blocker 9-phenanthrol inhibited TRPM4 activity in a concentration-dependent manner. These results showed that the channel is not only is expressed in hASCs but also is functionally active.

To investigate TRPM4's impact on adipogenesis, we have generated stable knockdown cells with the use of shRNA. This approach significantly reduced channel activity as confirmed by patch-clamp recordings. When TRPM4-knockdown cells were cultured in adipogenic medium, there was decreased lipid droplet accumulation and expression of adipocyte marker genes. As with rDFSCs, this is evidence that adipogenesis in hASCs is dependent on functional TRPM4 channels. This process may require TRPM4 activity alone or in combination with other proteins. Heteromultimerization of TRPM4 with sulfonylurea receptor 1 (SUR1) increases channel sensitivity to intracellular Ca^{2+} and affinity to calmodulin [48]. These Ca^{2+} signals are reported to activate transcription factors and enzymes involved in adipogenesis [e.g. PPARγ and fatty acid synthase (FAS)] and to suppress adipolysis [49–51]. Other TRPM family members such as TRPM7 are important for proliferation and conversion of pre-adipocyte cells into the mature adipocyte [52]. Using RT–PCR, we have identified *TRPM6* and *TRPM7* gene expressions in hASCs and human adipose tissue; however, their roles remain to be determined.

One of the goals of the present study was to provide insight into the Ca^{2+} signalling mechanism controlling adipogenesis in hASCs. Using histamine, a well-known activator of Ca^{2+} signals and regulator of stem cell differentiation, we

have found that TRPM4 suppression reduced the magnitude of the signals compared with control shRNA cells. This was an unexpected finding since TRPM4 knockdown in rDFSCs enhances Ca^{2+} signalling. From this observation, we have reasoned that hASCs use VDCCs as their main pathway for Ca^{2+} influx (excitable cells) instead of SOCs (non-excitable cells) [53]. This is supported by findings in pancreatic α- and β-cells, where TRPM4 suppression decreases the magnitude of Ca^{2+} signals generated by agonist stimulation [5, 9]. In non-excitable cells, the opposite occurs when TRPM4 is inhibited because depolarization decreases the driving force for Ca^{2+} entry via SOCs [6, 7, 54]. In support of our excitable cell hypothesis, we have found that hASCs expressed the $Ca_v1.2$ channel, a main type of VDCC. Furthermore, the VDCC blocker (nimodipine) decreased the magnitude of the Ca^{2+}signals generated by histamine. These findings suggested that Ca^{2+} influx via the $Ca_v1.2$ channel is a component of the Ca^{2+} signals. Experiments under extracellular Ca^{2+}-free conditions and after depletion of the intracellular Ca^{2+}stores were performed to examine additional Ca^{2+} sources. From our data, it was clear that TRPM4 is required for the full histamine response since channel knockdown reduced the magnitude of the Ca^{2+} signals. Experiments in the absence of extracellular Ca^{2+} had a similar effect to TRPM4 knockdown. This can be explained by the fact that TRPM4 depolarization opens VDCCs resulting in Ca^{2+} influx. Without Ca^{2+} in the extracellular buffer or TRPM4 activity there is no influx. When the intracellular Ca^{2+} stores were depleted using thapsigargin, the Ca^{2+} signals were abolished regardless of whether or not TRPM4 was suppressed. These Ca^{2+} signals generated by histamine in hASCs are typical of G_q-coupled receptors that increase

inositol 1,4,5-trisphosphate (IP_3) formation and mobilize intracellular Ca^{2+} from the ER. This initial Ca^{2+} release is likely to activate TRPM4, which depolarizes the cell leading to the opening of VDCCs to further increase the magnitude of the Ca^{2+} signals and stimulate PPARγ and FAS during adipogenesis according to the proposed mechanism shown in Figure 3.9. This would explain in part why TRPM4 knockdown inhibited adipogenesis in hASCs. Despite the differences in the Ca^{2+} signalling pattern between rDFSCs and hASCs, both showed decreased lipid droplet accumulation and expression of adipocyte marker genes with channel knockdown. This raises the possibility that other factors that are not Ca^{2+}-dependent but are linked to TRPM4 may control adipogenesis.

Another interesting finding was the presence of two histamine receptors (H1 and H2) in hASCs as determined using chlorpheniramine and cimetidine. From our results, H1 receptors seem to be the most predominant since chlorpheniramine completely inhibited the Ca^{2+} signals, whereas cimetidine reduced the responses by 50%. Both receptors, especially H1, are critical for differentiation. For example, H1 receptors are up-regulated during 3T3-L1 fibroblast differentiation and antagonists or receptor knockdown inhibits insulin-induced adipogenesis [51]. Histamine increases dendritic cell differentiation via H1 and H2 receptors becausereceptor blockage reduces the expression of differentiation markers [42]. In another study, H1 is the most important for monocyte differentiation despite the expression of H2 [55]. Histamine also increases the expression of receptor activator of nuclear factor κB ligand during osteoclastogenesis via H1 receptors [56]. Both

receptor types are critical for histamine-induced neural stem cell proliferation and differentiation [44].

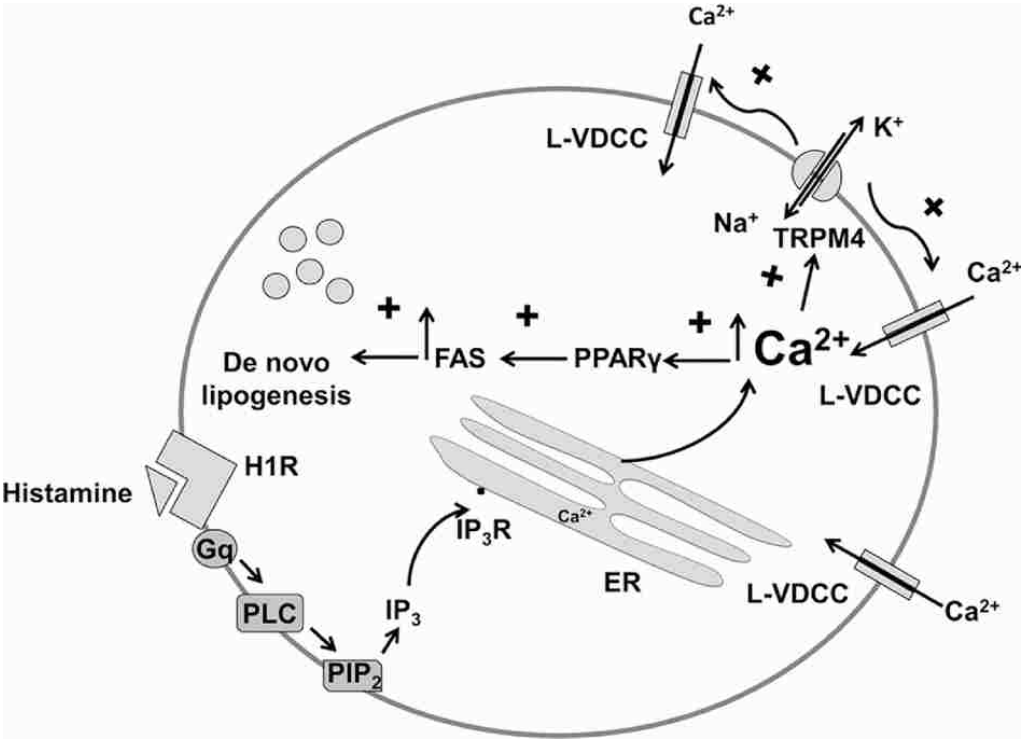

Figure 3.9 Proposed mechanism for histamine and TRPM4 control of Ca^{2+} signalling and adipogenesis in hASCs. Activation of histamine receptors, mainly the H1 type, increases intracellular Ca^{2+} via G_q-proteins and the phospholipase C (PLC)/IP_3 pathway. The initial Ca^{2+} release from the ER activates TRPM4, which depolarizes cells leading to the opening of VDCCs and Ca^{2+} influx. The Ca^{2+} release and influx are the sources for the Ca^{2+} signals that could control the activation of transcription factors and enzymes involved in adipogenesis.

In addition to H1/H2, the H4 receptor is described in bone marrow mesenchymal stem cells; however, only H1 mediates the Ca^{2+} signals [57]. Based on our findings and reports by other laboratories, we have found that the increases in intracellular Ca^{2+} mainly via H1 receptors are essential for adipocyte differentiation and/or function.

Conclusions

We have characterized for the first time TRPM4 in hASCs and demonstrated its importance for histamine-induced Ca^{2+} signalling and adipogenesis. The mechanism appears to involve in part Ca^{2+} release from the ER and influx via VDCCs with TRPM4 providing the depolarization necessary to activate the channel. The excitable cell characteristic of hASCs was a surprising finding since most undifferentiated stem cells are known to be of the non-excitable type.

3.5 REFERENCES

1 Nelson, P. L., Beck, A. and Cheng, H. (2011) Transient receptor proteins illuminated: current views on TRPs and disease. Vet. J. **187**, 153-164.

2 Launay, P., Fleig, A., Perraud, A. L., Scharenberg, A. M., Penner, R. and Kinet, J. P. (2002) TRPM4 is a Ca2+-activated nonselective cation channel mediating cell membrane depolarization. Cell. **109**, 397-407.

3 Prawitt, D., Monteilh-Zoller, M. K., Brixel, L., Spangenberg, C., Zabel, B., Fleig, A. and Penner, R. (2003) TRPM5 is a transient Ca2+-activated cation channel responding to rapid changes in [Ca2+]i. Proc. Natl. Acad. Sci. U. S. A. **100**, 15166-15171.

4 Cheng, H., Beck, A., Launay, P., Gross, S. A., Stokes, A. J., Kinet, J. P., Fleig, A. and Penner, R. (2007) TRPM4 controls insulin secretion in pancreatic beta-cells. Cell Calcium. **41**, 51-61.

5 Nelson, P. L., Zolochevska, O., Figueiredo, M. L., Soliman, A., Hsu, W. H., Feng, J. M., Zhang, H. and Cheng, H. (2011) Regulation of Ca(2+)-entry in pancreatic alpha-cell line by transient receptor potential melastatin 4 plays a vital role in glucagon release. Mol. Cell. Endocrinol. **335**, 126-134.

6 Nelson, P., Ngoc Tran, T. D., Zhang, H., Zolochevska, O., Figueiredo, M., Feng, J. M., Gutierrez, D. L., Xiao, R., Yao, S., Penn, A., Yang, L. J. and Cheng, H. (2013) Transient receptor potential melastatin 4 channel controls calcium signals and dental follicle stem cell differentiation. Stem Cells. **31**, 167-177.

7 Launay, P., Cheng, H., Srivatsan, S., Penner, R., Fleig, A. and Kinet, J. P. (2004) TRPM4 regulates calcium oscillations after T cell activation. Science. **306**, 1374-1377.

8 Vennekens, R., Olausson, J., Meissner, M., Bloch, W., Mathar, I., Philipp, S. E., Schmitz, F., Weissgerber, P., Nilius, B., Flockerzi, V. and Freichel, M. (2007) Increased IgE-dependent mast cell activation and anaphylactic responses in mice lacking the calcium-activated nonselective cation channel TRPM4. Nat. Immunol. **8**, 312-320.

9 Marigo, V., Courville, K., Hsu, W. H., Feng, J. M. and Cheng, H. (2009) TRPM4 impacts on Ca2+ signals during agonist-induced insulin secretion in pancreatic beta-cells. Mol. Cell. Endocrinol. **299**, 194-203.

10 Mironov, S. L. (2008) Metabotropic glutamate receptors activate dendritic calcium waves and TRPM channels which drive rhythmic respiratory patterns in mice. J. Physiol. **586**, 2277-2291.

11 Dolmetsch, R. E., Xu, K. and Lewis, R. S. (1998) Calcium oscillations increase the efficiency and specificity of gene expression. Nature. **392**, 933-936.

12 Kawano, S., Otsu, K., Kuruma, A., Shoji, S., Yanagida, E., Muto, Y., Yoshikawa, F., Hirayama, Y., Mikoshiba, K. and Furuichi, T. (2006) ATP autocrine/paracrine signaling induces calcium oscillations and NFAT activation in human mesenchymal stem cells. Cell Calcium. **39**, 313-324.

13 Sun, S., Liu, Y., Lipsky, S. and Cho, M. (2007) Physical manipulation of calcium oscillations facilitates osteodifferentiation of human mesenchymal stem cells. FASEB J. **21**, 1472-1480.

14 Kapur, N., Mignery, G. A. and Banach, K. (2007) Cell cycle-dependent calcium oscillations in mouse embryonic stem cells. Am. J. Physiol. Cell Physiol. **292**, C1510-1518.

15 Todorova, M. G., Fuentes, E., Soria, B., Nadal, A. and Quesada, I. (2009) Lysophosphatidic acid induces Ca2+ mobilization and c-Myc expression in mouse embryonic stem cells via the phospholipase C pathway. Cell. Signal. **21**, 523-528.

16 Resende, R. R., Adhikari, A., da Costa, J. L., Lorencon, E., Ladeira, M. S., Guatimosim, S., Kihara, A. H. and Ladeira, L. O. (2010) Influence of spontaneous calcium events on cell-cycle progression in embryonal carcinoma and adult stem cells. Biochim. Biophys. Acta. **1803**, 246-260.

17 Shi, H., Halvorsen, Y. D., Ellis, P. N., Wilkison, W. O. and Zemel, M. B. (2000) Role of intracellular calcium in human adipocyte differentiation. Physiological genomics. **3**, 75-82.

18 Cheng, H., Feng, J. M., Figueiredo, M. L., Zhang, H., Nelson, P. L., Marigo, V. and Beck, A. (2010) Transient receptor potential melastatin type 7 channel is critical for the survival of bone marrow derived mesenchymal stem cells. Stem Cells Dev. **19**, 1393-1403.

19 Jin, J., Wu, L. J., Jun, J., Cheng, X., Xu, H., Andrews, N. C. and Clapham, D. E. (2012) The channel kinase, TRPM7, is required for early embryonic development. Proc. Natl. Acad. Sci. U. S. A. **109**, E225-233.

20 Tao, R., Sun, H. Y., Lau, C. P., Tse, H. F., Lee, H. C. and Li, G. R. (2011) Cyclic ADP ribose is a novel regulator of intracellular Ca2+ oscillations in human bone marrow mesenchymal stem cells. J. Cell. Mol. Med. **15**, 2684-2696.

21 Deng, X. L., Sun, H. Y., Lau, C. P. and Li, G. R. (2006) Properties of ion channels in rabbit mesenchymal stem cells from bone marrow. Biochem. Biophys. Res. Commun. **348**, 301-309.

22 Wang, S. P., Wang, J. A., Luo, R. H., Cui, W. Y. and Wang, H. (2008) Potassium channel currents in rat mesenchymal stem cells and their possible roles in cell proliferation. Clin. Exp. Pharmacol. Physiol. **35**, 1077-1084.

23 Hu, H., He, M. L., Tao, R., Sun, H. Y., Hu, R., Zang, W. J., Yuan, B. X., Lau, C. P., Tse, H. F. and Li, G. R. (2009) Characterization of ion channels in human preadipocytes. J. Cell. Physiol. **218**, 427-435.

24 Bai, X., Ma, J., Pan, Z., Song, Y. H., Freyberg, S., Yan, Y., Vykoukal, D. and Alt, E. (2007) Electrophysiological properties of human adipose tissue-derived stem cells. Am. J. Physiol. Cell Physiol. **293**, C1539-1550.

25 Sukumar, P., Sedo, A., Li, J., Wilson, L. A., O'Regan, D., Lippiat, J. D., Porter, K. E., Kearney, M. T., Ainscough, J. F. and Beech, D. J. (2012) Constitutively active TRPC channels of adipocytes confer a mechanism for sensing dietary fatty acids and regulating adiponectin. Circ. Res. **111**, 191-200.

26 Zhang, L. L., Yan Liu, D., Ma, L. Q., Luo, Z. D., Cao, T. B., Zhong, J., Yan, Z. C., Wang, L. J., Zhao, Z. G., Zhu, S. J., Schrader, M., Thilo, F., Zhu, Z. M. and Tepel, M. (2007) Activation of transient receptor potential vanilloid type-1 channel prevents adipogenesis and obesity. Circ. Res. **100**, 1063-1070.

27 Iwasaki, Y., Tamura, Y., Inayoshi, K., Narukawa, M., Kobata, K., Chiba, H., Muraki, E., Tsunoda, N. and Watanabe, T. (2011) TRPV1 agonist monoacylglycerol increases UCP1 content in brown adipose tissue and suppresses accumulation of visceral fat in mice fed a high-fat and high-sucrose diet. Biosci. Biotechnol. Biochem. **75**, 904-909.

28 Motter, A. L. and Ahern, G. P. (2008) TRPV1-null mice are protected from diet-induced obesity. FEBS Lett. **582**, 2257-2262.

29 Ma, S., Yu, H., Zhao, Z., Luo, Z., Chen, J., Ni, Y., Jin, R., Ma, L., Wang, P., Zhu, Z., Li, L., Zhong, J., Liu, D., Nilius, B. and Zhu, Z. (2012) Activation of the cold-sensing TRPM8 channel triggers UCP1-dependent thermogenesis and prevents obesity. J. Mol. Cell. Biol. **4**, 88-96.

30 Bourin, P., Bunnell, B. A., Casteilla, L., Dominici, M., Katz, A. J., March, K. L., Redl, H., Rubin, J. P., Yoshimura, K. and Gimble, J. M. (2013) Stromal cells from the adipose tissue-derived stromal vascular fraction and culture expanded adipose tissue-derived stromal/stem cells: a joint statement of the International Federation for Adipose Therapeutics and Science (IFATS) and the International Society for Cellular Therapy (ISCT). Cytotherapy. **15**, 641-648.

31 Yu, G., Floyd, Z. E., Wu, X., Halvorsen, Y. D. and Gimble, J. M. (2011) Isolation of human adipose-derived stem cells from lipoaspirates. Methods Mol. Biol. **702**, 17-27.

32 Zuk, P. A., Zhu, M., Mizuno, H., Huang, J., Futrell, J. W., Katz, A. J., Benhaim, P., Lorenz, H. P. and Hedrick, M. H. (2001) Multilineage cells from human adipose tissue: implications for cell-based therapies. Tissue Eng. **7**, 211-228.

33 Zuk, P. A., Zhu, M., Ashjian, P., De Ugarte, D. A., Huang, J. I., Mizuno, H., Alfonso, Z. C., Fraser, J. K., Benhaim, P. and Hedrick, M. H. (2002) Human adipose tissue is a source of multipotent stem cells. Mol. Biol. Cell. **13**, 4279-4295.

34 Guilak, F., Lott, K. E., Awad, H. A., Cao, Q., Hicok, K. C., Fermor, B. and Gimble, J. M. (2006) Clonal analysis of the differentiation potential of human adipose-derived adult stem cells. J. Cell. Physiol. **206**, 229-237.

35 Gimble, J. M., Katz, A. J. and Bunnell, B. A. (2007) Adipose-derived stem cells for regenerative medicine. Circ. Res. **100**, 1249-1260.

36 Mitchell, J. B., McIntosh, K., Zvonic, S., Garrett, S., Floyd, Z. E., Kloster, A., Di Halvorsen, Y., Storms, R. W., Goh, B., Kilroy, G., Wu, X. and Gimble, J. M. (2006) Immunophenotype of human adipose-derived cells: temporal changes in stromal-associated and stem cell-associated markers. Stem Cells. **24**, 376-385.

37 Yu, G., Floyd, Z. E., Wu, X., Hebert, T., Halvorsen, Y. D., Buehrer, B. M. and Gimble, J. M. (2011) Adipogenic differentiation of adipose-derived stem cells. Methods Mol. Biol. **702**, 193-200.

38 Grand, T., Demion, M., Norez, C., Mettey, Y., Launay, P., Becq, F., Bois, P. and Guinamard, R. (2008) 9-phenanthrol inhibits human TRPM4 but not TRPM5 cationic channels. Br. J. Pharmacol. **153**, 1697-1705.

39 Gonzales, A. L., Garcia, Z. I., Amberg, G. C. and Earley, S. (2010) Pharmacological inhibition of TRPM4 hyperpolarizes vascular smooth muscle. Am. J. Physiol. Cell Physiol. **299**, C1195-1202.

40 Guinamard, R., Hof, T. and Del Negro, C. A. (2014) The TRPM4 channel inhibitor 9-phenanthrol. Br. J. Pharmacol. **171**, 1600–1613.

41 Nagayama, M., Uchida, T. and Gohara, K. (2007) Temporal and spatial variations of lipid droplets during adipocyte division and differentiation. J. Lipid Res. **48**, 9-18.

42 Szeberenyi, J. B., Pallinger, E., Zsinko, M., Pos, Z., Rothe, G., Orso, E., Szeberenyi, S., Schmitz, G., Falus, A. and Laszlo, V. (2001) Inhibition of effects of endogenously synthesized histamine disturbs in vitro human dendritic cell differentiation. Immunol. Lett. **76**, 175-182.

43 Kawano, S., Otsu, K., Shoji, S., Yamagata, K. and Hiraoka, M. (2003) Ca(2+) oscillations regulated by Na(+)-Ca(2+) exchanger and plasma membrane Ca(2+) pump induce fluctuations of membrane currents and potentials in human mesenchymal stem cells. Cell Calcium. **34**, 145-156.

44 Molina-Hernandez, A. and Velasco, I. (2008) Histamine induces neural stem cell proliferation and neuronal differentiation by activation of distinct histamine receptors. J. Neurochem. **106**, 706-717.

45 Koivisto, A., Dotzler, E., Russ, U., Nedergaard, J. and Siemen, D. (1993) Nonselective cation channels in brown and white fat cells. EXS. **66**, 201-211.

46 Koivisto, A. and Nedergaard, J. (1995) Modulation of calcium-activated non-selective cation channel activity by nitric oxide in rat brown adipose tissue. J. Physiol. **486 (Pt 1)**, 59-65.

47 Halonen, J. and Nedergaard, J. (2002) Adenosine 5'-monophosphate is a selective inhibitor of the brown adipocyte nonselective cation channel. J. Membr. Biol. **188**, 183-197.

48 Woo, S. K., Kwon, M. S., Ivanov, A., Gerzanich, V. and Simard, J. M. (2013) The sulfonylurea receptor 1 (Sur1)-transient receptor potential melastatin 4 (Trpm4) channel. J. Biol. Chem. **288**, 3655-3667.

49 Shi, H., Moustaid-Moussa, N., Wilkison, W. O. and Zemel, M. B. (1999) Role of the sulfonylurea receptor in regulating human adipocyte metabolism. FASEB J. **13**, 1833-1838.

50 Gabrielsson, B. G., Karlsson, A. C., Lonn, M., Olofsson, L. E., Johansson, J. M., Torgerson, J. S., Sjostrom, L., Carlsson, B., Eden, S. and Carlsson, L. M. (2004) Molecular characterization of a local sulfonylurea system in human adipose tissue. Mol. Cell. Biochem. **258**, 65-71.

51 Kawazoe, Y., Tanaka, S. and Uesugi, M. (2004) Chemical genetic identification of the histamine H1 receptor as a stimulator of insulin-induced adipogenesis. Chem. Biol. **11**, 907-913.

52 Chen, K. H., Xu, X. H., Liu, Y., Hu, Y., Jin, M. W. and Li, G. R. (2014) TRPM7 channels regulate proliferation and adipogenesis in 3T3-L1 preadipocytes. J. Cell. Physiol. **229**, 60-67.

53 Kawano, S., Shoji, S., Ichinose, S., Yamagata, K., Tagami, M. and Hiraoka, M. (2002) Characterization of Ca(2+) signaling pathways in human mesenchymal stem cells. Cell Calcium. **32**, 165-174.

54 Weber, K. S., Hildner, K., Murphy, K. M. and Allen, P. M. (2010) Trpm4 differentially regulates Th1 and Th2 function by altering calcium signaling and NFAT localization. J. Immunol. **185**, 2836-2846.

55 Triggiani, M., Petraroli, A., Loffredo, S., Frattini, A., Granata, F., Morabito, P., Staiano, R. I., Secondo, A., Annunziato, L. and Marone, G. (2007) Differentiation of monocytes into macrophages induces the upregulation of histamine H1 receptor. J. Allergy Clin. Immunol. **119**, 472-481.

56 Ikawa, Y., Yonekawa, T., Ohkuni, Y., Kuribayashi, M., Fukino, K. and Ueno, K. (2007) A comparative study of histamine activities on differentiation of osteoblasts and osteoclasts. J. Toxicol. Sci. **32**, 555-564.

57 Nemeth, K., Wilson, T., Rada, B., Parmelee, A., Mayer, B., Buzas, E., Falus, A., Key, S., Masszi, T., Karpati, S. and Mezey, E. (2012) Characterization and function of histamine receptors in human bone marrow stromal cells. Stem Cells. **30**, 222-231.

CHAPTER 4: ARGININE VASOPRESSIN INHIBITS ADIPOGENESIS IN HUMAN ADIPOSE-DERIVED STEM CELLS*

4.1 INTRODUCTION

Arginine vasopressin (AVP) is synthesized in the paraventricular and supraoptic nucleus of the hypothalamus and is secreted from the posterior pituitary gland mainly in response to dehydration. It is also detected in ovaries, adrenal gland, testis, thymus and pancreas [1-5]. AVP mediates its effects via three G protein-coupled receptors, the V1a, V1b, and V2. The V1a receptor can be found in lymphocytes, smooth muscle and mesangial cells [6-8]. The V1b receptor is present in pancreatic α and β cells, astrocytes and adrenal medulla [9-12]. In addition, AVP binds to V2 receptors in the renal distal tubule and collecting duct cells to promote water reabsorption during dehydration by activating the cAMP pathway [13]. Important physiological roles for AVP include platelet aggregation, liver glycogenolysis, uterine motility, vasoconstriction, cell proliferation and growth. It stimulates protein synthesis via V1a receptors and insulin, glucagon, catecholamine, ACTH secretion via V1b receptors [14]. Activation of V1 receptors has a significant impact on intracellular Ca^{2+} signals because they are coupled to Gq-proteins and the phospholipase C-β (PLC-β) and inositol triphosphate (IP_3) pathway. Increases in IP_3 result in Ca^{2+} release from the endoplasmic reticulum (ER) and influx from the extracellular space [15]. Calcium oscillations are required for cell proliferation and differentiation, because it activates transcription factors,

---

* Reprinted with permission from Elsevier Ltd. Authors: Tran Doan Ngoc Tran, Shaomian Yao, Walter H. Hsu, Jeffrey M. Gimble, Bruce A. Bunnell and Henrique Cheng. Molecular and Cellular Endocrinology 2015; 406: 1–9.

such as nuclear factor of activated T-cells (NFAT) [16]. Translocation of NFAT adipogenic and into the nucleus is observed during stem cell differentiation, but ends at terminal stages of osteogenic differentiation [17, 18]. Elevation in intracellular Ca^{2+} inhibits adipocyte formation during early stages of differentiation, but facilitates it at later stages [19, 20]. An increase in Ca^{2+} influx activates the mitogen-activated protein kinase (MAPK) pathway to stimulate osteogenic differentiation in mesenchymal stem cells [18]. Calcium signaling is essential for embryonic and mesenchymal stem cell cycle progression via the G_1/S phase [21-23]. They up-regulate peroxisome proliferator-activated receptor γ (PPARγ) gene expression, a master transcription factor for adipogenesis. PPARγ increases fatty acid synthase activity and triacylglycerol production in lipid droplets [19]. Other studies revealed a stimulatory effect of AVP on myoblast and T-cell differentiation via V1 receptors [8, 24, 25]. However, AVP inhibits osteoclast differentiation [26].

Other physiological functions for AVP include control of thermogenesis by increasing UCP-1 protein expression for uncoupling oxidative phosphorylation during heat production from brown fat [27]. Studies in V1a receptor knockout mice show enhanced lipid metabolism, muscle proteolysis and insulin signaling suppression that is supported by observations of impaired glucose tolerance in these animals [28]. The anti-lipolytic effect is mediated by Ca^{2+} signals and the MAPK pathway [27, 29]. A reduction in adiponectin mRNA is detected after adipocyte stimulation with AVP [27]. This hormone also inhibits ketogenesis by suppressing β-oxidation of fatty acid [30]. Pathophysiological conditions such as hypertension and obesity are associated with reduced plasma AVP [31, 32]. Obese and sedentary

individuals have lower AVP levels compared to lean ones, whereas exercise increases hormone secretion [33, 34]. This observation is confirmed in patients before and after weight loss [35]. The same study reported an inverse correlation between AVP and insulin that is consistent with the knowledge that obese nondiabetic individuals have increased insulin and adipose tissue but low AVP levels. Patients with multiple symmetric lipomatosis due to alcohol abuse exhibit large symmetrical accumulation of non-capsulated fat tissue that is associated with reduced AVP secretion caused by alcohol [36]. Interestingly, nicotine stimulates AVP secretion and may in part explain why cigarette smokers gain weight after they stop smoking [37]. Although Ca^{2+} signals are reported in hASCs [38], the mechanism by which AVP increases intracellular Ca^{2+} and its role on adipogenesis is unknown. In this study, we characterized the AVP receptor subtype, its signaling pathway and impact on adipocyte differentiation.

4.2 MATERIALS AND METHODS

4.2.1 Reagents

All reagents were purchased from Sigma Chemical Co. (St. Louis, MO, USA), except that fura-2 acetoxymethyl ester (Fura-2AM) was from Anaspec (Fremont, CA, USA), d-calcium pantothenate was from Fisher Scientific (Pittsburgh, PA, USA), [Arg8] vasopressin (AVP) from American Peptide Co. (Sunnyvale, CA, USA) and 2-APB from Cayman Chemical Co. **(**Ann Arbor, MI, USA).

4.2.2 Cell culture

Human adipose-derived stem cells were isolated from lipoaspirates of abdomen, breast adipose tissues, right knee and right scapula donated by consenting two Caucasian females and a male, age from 34 to 66 years old, BMI from 23.5 to 33.78 under a protocol reviewed and approved by the Pennington Biomedical Institutional Review Board (#PBRC23040) and maintained in Dulbecco's modified Eagles medium (DMEM)/Ham's F-12 medium with 10% fetal bovine serum (FBS) (Atlanta Biologicals, Lawrenceville, GA, USA) and aerated with 5% CO_2 at 37°C. All experiments were performed with cells from passages 3-8.

4.2.3 RT-PCR

Total RNA was extracted using the RNAqueous-4PCR® kit according to the manufacturer's instructions (Ambion, Austin, TX, USA). The RNA was treated with DNase 1 to remove DNA contamination. Reverse transcription and PCR were performed using Ambion's RETROscript® kit. The human PCR primers (forward/reverse [5'–3']) are listed in Table 4.1. Human glyceraldehyde-3-phosphate dehydrogenase (GAPDH) and dH_2O were used as positive and negative controls, respectively.

Table 4.1 List of primers of AVP receptor genes for RT-PCR

Gene	Forward primer (5'-3')	Reverse primer (5'-3')	Size (bp)
C/EBPα	CGGTGGACAAGAACAGCAAC	CGGAATCTCCTAGTCCTGGC	365
C/EBPβ	CACAGCGACGACTGCAAGATCC	CTTGAACAAGTTCCGCAGGGTG	188
PPARγ2	GCTGTTATGGGTGAAACTCTG	ATAAGGTGGAGATGCAGGTTC	325
aP2	TGGTTGATTTTCCATCCCAT	TACTGGGCCAGGAATTTGAT	150

(Table 4.1 continued)

Gene	Forward primer (5'-3')	Reverse primer (5'-3')	Size (bp)
Adiponectin	GGCCGTGATGGCAG AGAT	TTTCACCGATGTCTCC CTTAGG	88
LPL	GAGATTTCTCTGTAT GGCACC	CTGCAAATGAGACACT TTCTC	276
Leptin	GGCTTTGGCCCTATC TTTTC	GCTCTTAGAGAAGGCC AGCA	325
Cyclophilin B	GGAGATGGCACAGG AGGAAA	CGTAGTGCTTCAGTTT GAAGTTCTCA	72

4.2.4 Quantitative RT-PCR

From each sample, 2μg of total RNA was reverse-transcribed into 20μl of cDNA. Each PCR was prepared by mixing 2μl of the cDNA with 2x SYBR Green PCR master mix (Bio-Rad, Hercules, CA, USA) and gene-specific primers (Table 4.2). The PCR was carried out with ABI 7300 real-time PCR system (Life Technologies, Grand Island, NY, USA) to obtain the C_T value. Relative gene expression (RGE) was calculated by the delta C_T method using β-actin as the endogenous control for normalization and cyclophilin B as the reference control with an RGE of 1.

Table 4.2 List of primers of adipogenic marker genes for quantitative RT-PCR

Gene	Forward primer (5'-3')	Reverse primer (5'-3')	Size (bp)
AVP V1a receptor	CAGGTGTTCGGCATG TTTG	ACCAGATGTTGTAGCA GATGAA	343
AVP V1b receptor	CTCATCTGCCATGAG ATCTGTAA	CCACATCTGGACACTG AAGAA	249
AVP V2 receptor	ATTCATGCCAGTCTG GTGC	TCACGATGAAGTGTCC TTGG	422
GAPDH	AACAGCGACACCCA CTCCTC	GGAGGGGAGATTCAG TGTGGT	258

4.2.5 Calcium imaging analysis

Cells were loaded with 2μM Fura-2AM for 30 min at 37°C. The imaging buffer containing (in mM): NaCl 136, KCl 4.8, $CaCl_2$ 1.2, $MgSO_4$ 1.2, HEPES 10, glucose 4, and 0.1% BSA, pH 7.3 was used for Fura-2AM loading and perfusion throughout the experiments. Calcium measurements were obtained using a dual excitation fluorometric imaging system (TILL-Photonics, Gräfefingen, Germany) controlled by TILLvisION software. Fura-2AM loaded cells in perfusion chamber were excited by 340nm and 380nm wavelengths. Fluorescence emissions were sampled at a frequency of 1 Hz and computed into relative ratio units of the fluorescence intensity of the difference of wavelengths (F340/F380). Data were expressed as averages from several cells from three separate experiments.

4.2.6 Induction and detection of lipid droplets

Cells reaching between 80% and 90% were induced with differentiation medium containing DMEM/Ham's F-12 supplemented with 3% FBS, 0.25mM 3-isobutyl-1-methylxanthine (IBMX), 33μM biotin, 17μM d-calcium panthothenate, 100nM human insulin, 1μM dexamethasone and 5μM rosiglitazone for 3 days. Adipocyte medium having the same composition as differentiation medium except for IBMX and rosiglitazone was changed every 3 days from day 3 to day 21 [39]. To test the effect of AVP on adipogenesis, 100nM AVP was supplemented to the adipogenic medium and changed every 2 days until day 14 of differentiation. Adipogenesis was determined by Oil Red O (ORO) staining. Briefly, cells were washed with PBS, fixed with 10% formalin for 10 min, washed twice with dH_2O, and incubated with 60% isopropanol for 5 min. Cells were then stained with ORO

solution for 5 min and washed again to remove excess dye. The presence of lipid droplets was visualized by phase contrast microscopy using an inverted microscope (Zeiss, Thornwood, NY, USA).

4.2.7 Data analysis

Adipocyte count was performed from a total of 36 or 18 frames taken at 10x magnification from each group using software ImageJ (1.47v; http://imagej.nih.gov/ij). The peak Ca^{2+} signals and adipocyte counts are shown as means ± S.E.M. and were analyzed using a two-tailed and unpaired Student's *t*-test (GraphPad *Software Inc.*, La Jolla, CA, USA). Statistical significance was established at $P<0.05$.

4.3 RESULTS

4.3.1 hASCs differentiate into adipocytes and express the V1a receptor gene

In order to demonstrate that hASCs can differentiate into adipocytes, we cultured the cells in adipogenic media and examined the differentiated cells with ORO staining at the end of 14 days. Adipogenesis was confirmed by the presence of lipid droplet accumulation (Figure 4.1,A). Next, we examined the type of AVP receptor in hASCs at day 0 and 14 of differentiation. RT-PCR analysis revealed V1a receptor gene expression, but not V1b or V2 (Figure 4.1,B).

4.3.2 AVP increases intracellular Ca^{2+} in hASCs under growth and adipogenic conditions

Since hASCs expressed the V1a receptor before and after differentiation, we performed real-time Ca^{2+} imaging analysis to investigate the responses to AVP. Stimulation of cells with 1μM AVP increased intracellular Ca^{2+} at days 0, 7, 14 and 21 of differentiation (Figure 4.2,A). However, there was a greater response to AVP

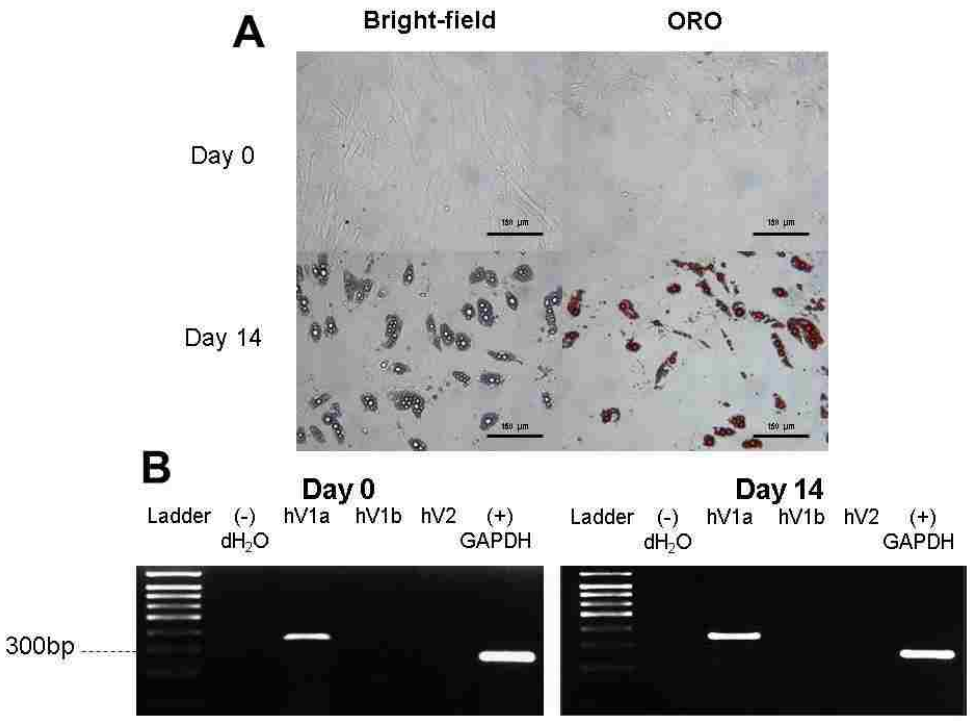

Figure 4.1 hASCs differentiation into adipocytes and expression of the V1a receptor gene. (A) hASCs were differentiated into adipocytes for 14 days and stained with Oil Red O (ORO) for the presence of lipid droplets (20x magnification). (B) hASCs expressed the V1a receptor gene at day 0 and day 14 of differentiation. RT-PCR was performed with specific human V1a, V1b, V2 primers. dH_2O and GAPDH served as negative and positive controls, respectively.

at day 14 compared to day 21 of differentiation (Figure 4.2,B). Therefore, we chose day 14 for our experiments since at this time period, we also detected adipocyte differentiation. To confirm the AVP responses in hASCs, cells were stimulated with 0.003-1µM AVP that resulted in a concentration-dependent increase in $[Ca^{2+}]_i$ with a peak at 1µM concentration (Figure 4.2,C and D). In order to test whether the V1a receptor indeed mediated the effect of AVP, cells were pretreated with 0.0001-1µM V2255, a selective V1a receptor antagonist. V2255 inhibited the Ca^{2+} signals in a concentration-dependent manner in both undifferentiated and differentiated cells (Figure 4.3,A-D).

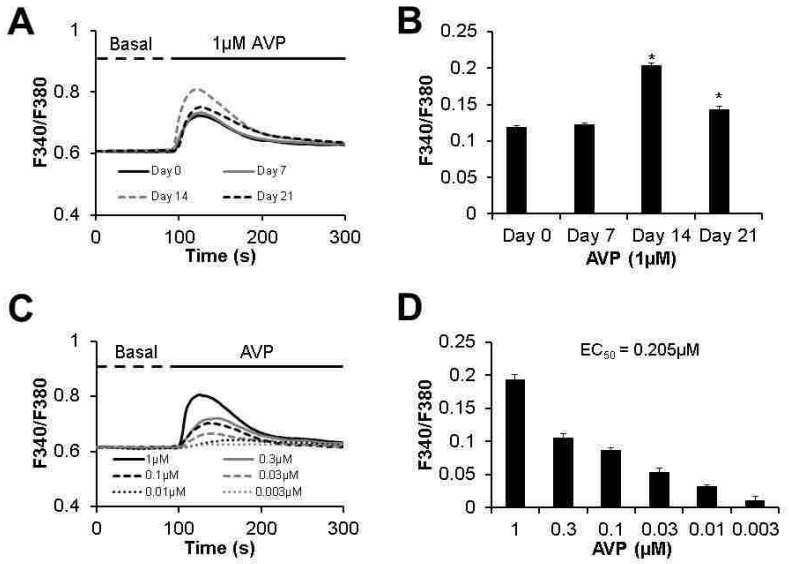

Figure 4.2 hASCs are responsive to AVP prior to and during adipogenesis**.** (A) Average Ca^{2+} signals in response to AVP from day 0 to day 21 of differentiation. (B) The AVP response increased until day 14, but decreased at day 21. (C) Average Ca^{2+} signals in response to increasing AVP concentration. (D) Average peak responses to different AVP concentrations. Values are means ± S.E.M.; n = 86-705 cells; * P<0.0001 compared to day 0.

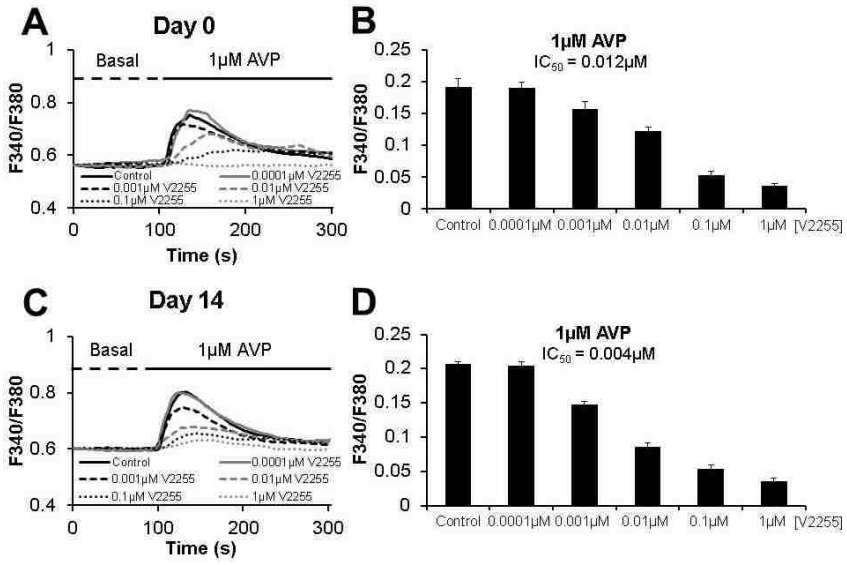

Figure 4.3 The V1a receptor mediates AVP signaling in hASCs. (A, B) Average traces and peak Ca^{2+} signals generated by AVP after V2255, a selective V1a blocker pretreatment at day 0. (C, D) Same experiments as in A and B, except at day 14 of adipogenic differentiation. Values are means ± S.E.M.; n = 51-433 cells/concentration.

4.3.3 AVP increases intracellular Ca^{2+} via the PLC-IP_3 pathway

AVP stimulates Ca^{2+} signals via the V1a receptor in smooth muscle and intestinal epithelial cells by activating the phospholipase C enzyme (PLC) [40, 41].Therefore, we utilized the PLC blocker, U73122 to test whether it could inhibit AVP signaling. U73122 (2-12µM) pretreatment for 5 min inhibited the responses to AVP in a concentration-dependent manner (Figure 4.4,A and B). Pretreatment of cells with U73343, an inactive analog of U73122 did not alter the responses to AVP (Figure 4.4,C and D). Since IP_3 is a downstream second messenger to PLC,

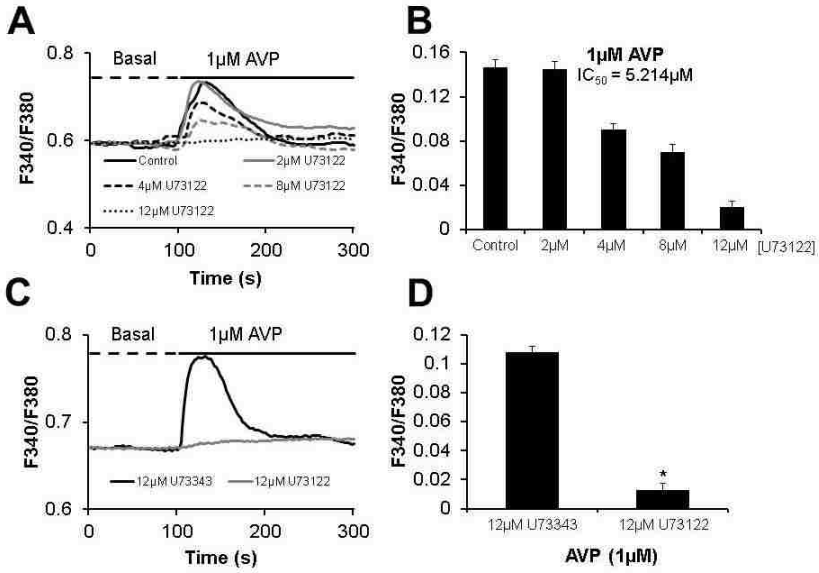

Figure 4.4 Involvement of PLC in the AVP mechanism in hASCs. (A, B) Averages and peak Ca^{2+} signals generated by AVP after pretreatment of cells with the PLC inhibitor, U73122. (C, D) Averages and peak Ca^{2+} signals after pretreatment with U73343, an inactive analog of U73122. Values are means ± S.E.M.; n = 59-81 cells/concentration; * P<0.0001.

we utilized 2-APB, an IP_3 receptor blocker. Pretreatment of cells for 5 min with 10-300µM 2-APB inhibited the responses to AVP in a concentration-dependent manner (Figure 4.5,A and B). In addition, we compared the maximum AVP

response in hASCs to those of 2μM ionomycin and 100μM ATP, another Gq-coupled receptor agonist (Figure 4.5,C and D).

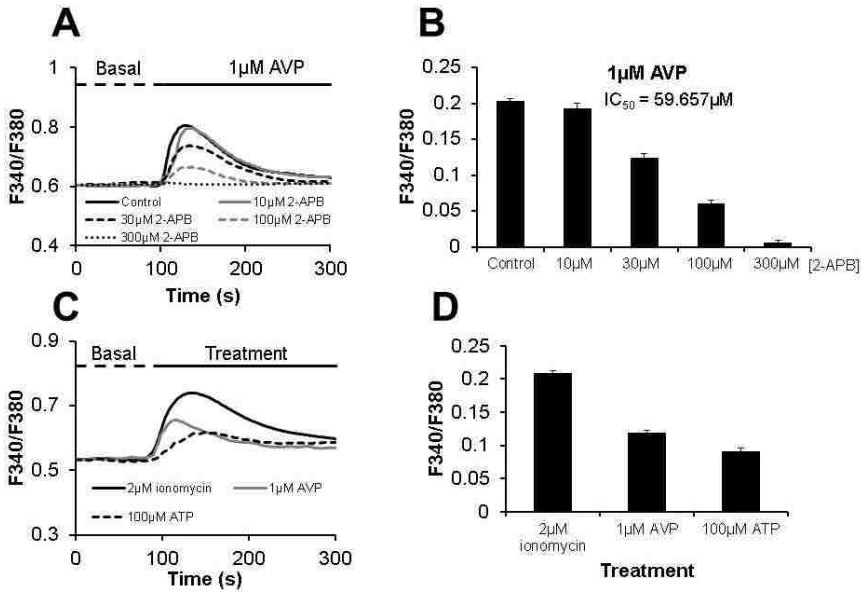

Figure 4.5 IP_3 binding to its receptor initiates the Ca^{2+} signals. (A, B) Average Ca^{2+} signals and peak responses after pretreatment of cells with 2-ABP, a selective IP_3 receptor blocker. Values are means ± S.E.M.; n = 77-705 cells/concentration. (C, D) Average Ca^{2+} signals and peak responses induced by ionomycin, AVP and ATP in hASCs. Values are means ± S.E.M.; n = 102-131 cells/concentration.

4.3.4 Sources of Ca^{2+} for AVP signals

In bone marrow-derived stem cells, Ca^{2+} influx and release from the ER generate the Ca^{2+} signals [42]. Hence, we tested in hASCs the contribution of extracellular Ca^{2+} on AVP signaling by performing experiments under Ca^{2+} free buffer condition. Removal of extracellular Ca^{2+} significantly reduced the Ca^{2+} signals compared to control cells in Ca^{2+} containing buffer (Figure 4.6,A). Next, we pretreated cells with thapsigargin (TG) for 20 min, a Ca^{2+}-ATPase pump inhibitor in the ER to investigate the impact of intracellular Ca^{2+} on AVP signals. Depletion of Ca^{2+} stores with TG completely abolished the responses to AVP (Figure 4.6,B).

Under extracellular free Ca^{2+} and TG conditions, AVP also failed to increase intracellular Ca^{2+} (Figure 4.6,C and D).

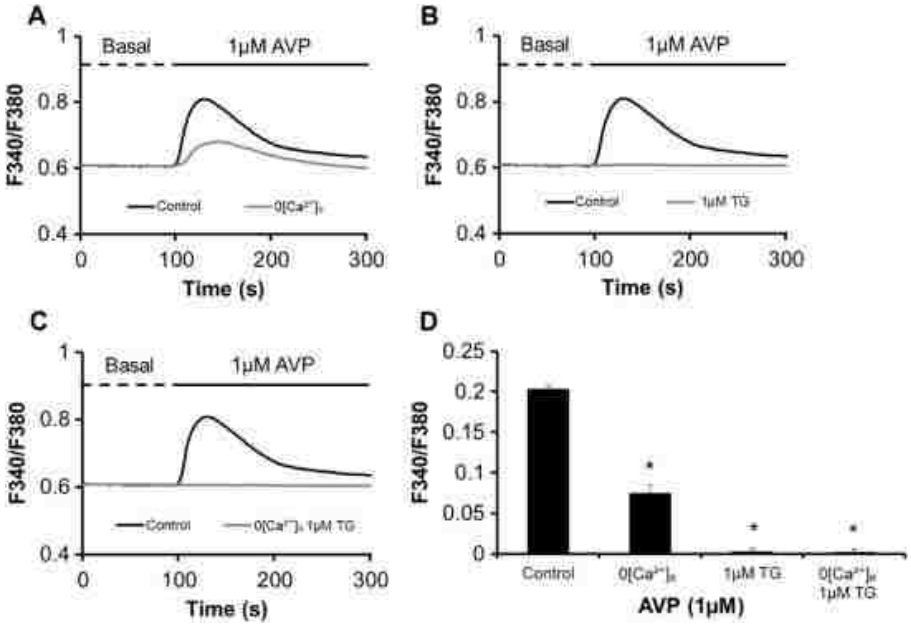

Figure 4.6 Intracellular Ca^{2+} release and influx are sources for the Ca^{2+} signals. (A) Average Ca^{2+} signals during AVP stimulation under extracellular Ca^{2+} and Ca^{2+} free conditions. (B) Depletion of ER Ca^{2+} stores with thapsigargin (TG) abolished the AVP responses. (C) Experiments performed under extracellular Ca^{2+} free condition and TG simultaneously. (D) Average peak responses from experiments in A–C. Values are means ± S.E.M; n = 63-705 cells/treatment; * P<0.0001 compared to peak control group.

4.3.5 AVP inhibits adipogenesis during hASC differentiation

To investigate the effect of AVP on adipogenesis, we supplemented the differentiation medium with 100nM AVP which enhances differentiation of other cell types [24, 43, 44]. AVP supplementation reduced lipid droplet accumulation as determined by ORO staining (Figure 4.7,A-C) and decreased adipocyte formation compared to control cells without AVP (Figure 4.7,D). The hormone also decreased the expression of adipocyte marker genes: CCAAT/enhancer-binding protein α (C/EBPα), CCAAT/ enhancer-binding protein β (C/EBPβ), peroxisome proliferator-activated receptor γ 2 (PPARγ2), adipocyte protein 2 (aP2),

adiponectin, lipoprotein lipase (LPL) and leptin compared to control group without AVP after 14 days of differentiation (Figure 4.8).

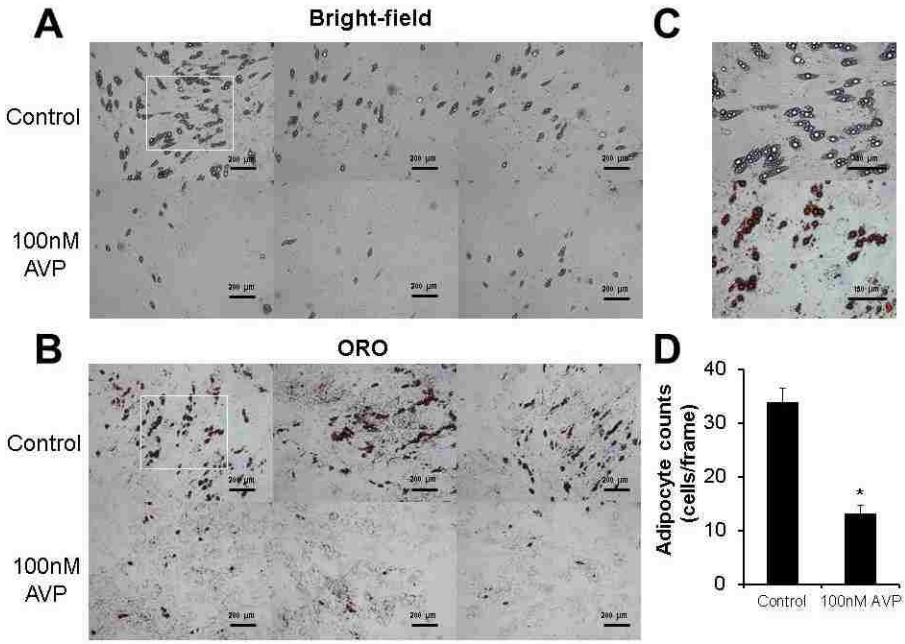

Figure 4.7 AVP inhibits adipogenesis during hASC differentiation. (A, B) Bright-field and ORO staining images taken at day 14 of differentiation from AVP treated and control group without AVP (10x magnification). (C) Adipocyte morphology shown at 20x magnification from cells in A and B. (D) Adipocyte count per frame from a total of 36 frames from each group. Values are means ± S.E.M; n = 471 (+AVP) and 1213 (-AVP) cells; * P<0.0001.

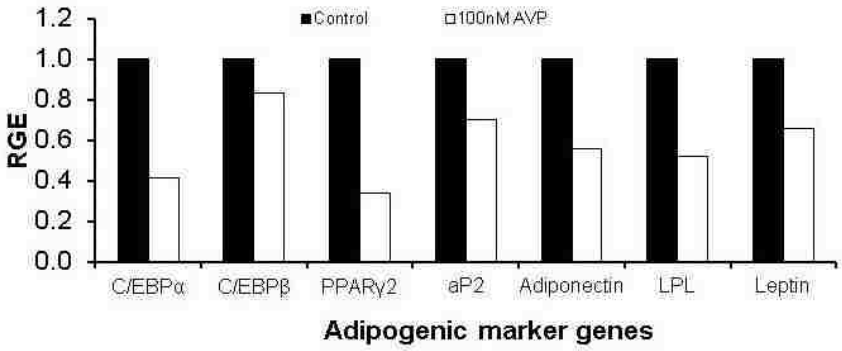

Figure 4.8 AVP down-regulates adipocyte marker genes in hASCs. Stimulation of cells with AVP during 14 days of adipogenic differentiation decreased the expression of adipocyte marker genes compared to control cells in the absence of AVP.

4.3.6 V1a receptor blocker V2255 reverses the effect of AVP on adipogenesis

Finally, to confirm the effect of AVP on adipocyte differentiation we performed adipogenic experiments with the V1a receptor blocker V2255. AVP (100nM) supplementation significantly reduced the number of adipocytes as indicated by lipid droplet accumulation and ORO staining. When V2255 (100μM) was added to the differentiation medium along with AVP, it reversed the inhibitory effect of AVP on adipogenesis (Figure 4.9,A and B). In the study, V2255 alone did not alter adipocyte formation.

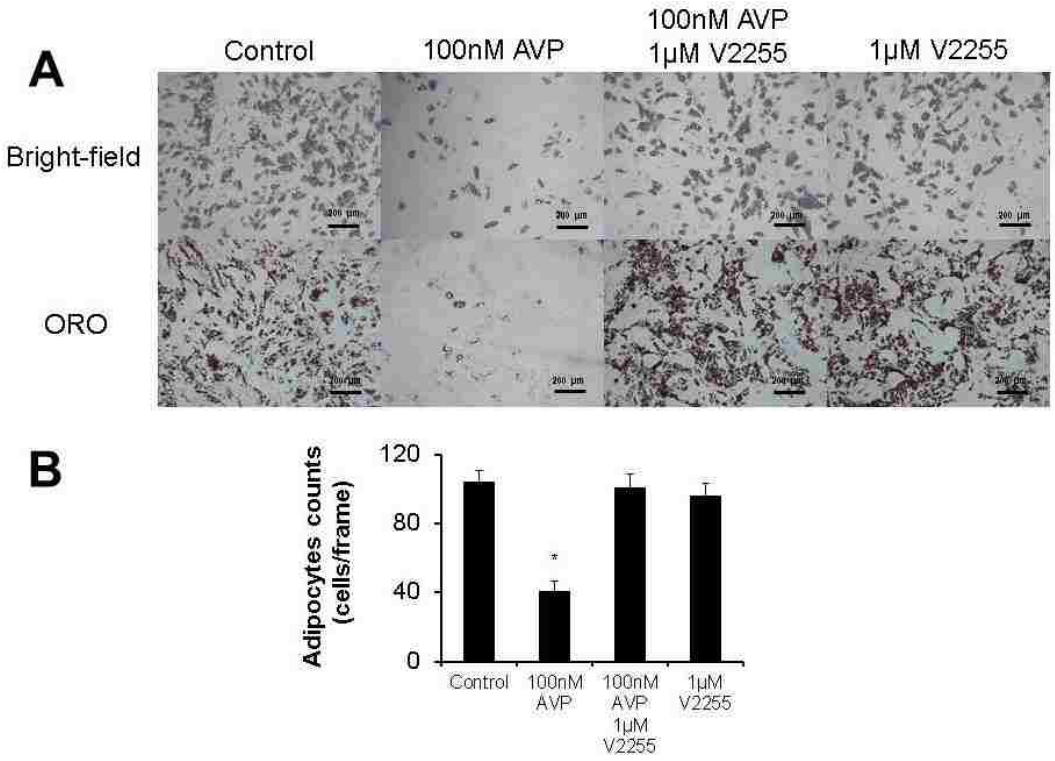

Figure 4.9 V1a receptor blocker reverses the effect of AVP on adipogenesis. (A) Bright-field and ORO staining images taken at day 10 of differentiation from control adipogenic medium alone and AVP, AVP+V2255 or V2255 supplemented groups (10x magnification). (B) Adipocyte count per frame from a total of 18 frames from each group. Values are means ± S.E.M; n = 1869 (control adipogenic medium), 725 (+AVP), 1805 (+AVP and V2255), and 1723 (+V2255) cells; * $P<0.001$.

4.4 DISCUSSION

The role of AVP (a.k.a. anti-diuretic hormone) in water conservation during dehydration is well established. It acts by promoting translocation into the plasma membrane of tubular cells to allow water reabsorption [45]. Other studies revealed that the hormone is capable of stimulating cellular growth and proliferation. Despite the identification of AVP receptors in stem cells [44], its function in Ca^{2+} signaling and differentiation remains largely unexplored. We investigated the mechanism of AVP signaling and its impact on adipocyte differentiation in hASCs, which is a well-accepted stem cell type for adipogenic studies [46]. When placed in adipogenic medium, accumulation of lipid droplets can be evidenced within the cell population that resembles the characteristics of mature adipocytes. We demonstrated that undifferentiated hASCs and differentiated adipocytes express the V1a receptor, but not the V1b or V2. This observation differs from mouse embryonic stem cells that express all three receptor subtypes [44]. It is possible that the pluripotent nature of embryonic stem cells compared to multipotent adult stem cells may be accountable for this variation. The possibility of AVP receptor variation among species also needs to be considered. Since V1a receptors are coupled to Gq-proteins that utilize the PLC-IP3 pathway and Ca^{2+} signaling [47-49], we examined whether the Ca^{2+} signals observed in hASCs during AVP stimulation was a result of this mechanism. In addition, we investigated the impact of the hormone on adipocyte differentiation.

Initial experiments demonstrated that hASCs are responsive to AVP throughout the differentiation process, with a peak Ca^{2+} increase at day 14, but

decreases at day 21. Other types of adult stem cells (e.g. bone marrow derived) exhibit similar Ca^{2+} signaling pattern during the terminal stages of osteoblast and adipocyte differentiation [17, 18]. It is reasoned that these signals are important for directing and terminating the differentiation process. Furthermore, we confirmed the V1a receptor as the type mediating the effect of AVP before and after differentiation. The V1a receptor blocker V2255 inhibited the responses to AVP in a concentration-dependent manner, which is consistent with the RT-PCR data showing V1a gene expression in hASCs. Since receptors coupled to Gq proteins in hASCs activate the PLC enzyme [38], we utilized U73122, a PLC inhibitor to test whether it mediated the effects of AVP. Indeed, pretreatment of cells with U73122 inhibited the Ca^{2+} signals, but not U73343, an inactive analog. Next, we examined the effect of IP_3 a downstream second messenger to PLC on ER Ca^{2+} release. Pretreatment of cells with 2-APB, an IP3 receptor blocker inhibited the AVP responses in a concentration-dependent manner. These findings revealed that the mechanism by which AVP signals in hASCs is by activating V1a receptors and the PLC-IP3 pathway. In view that 2-APB abolished the AVP response, it indicated that ER Ca^{2+} release was a source for the Ca^{2+} signals. To test this hypothesis and to determine whether extracellular Ca^{2+} was involved, we performed experiments with TG and under extracellular Ca^{2+} free conditions. Depletion of Ca^{2+} stores by TG resulted in a complete suppression of the AVP responses, but not in the absence of extracellular Ca^{2+}. Under both conditions, AVP also failed to increase intracellular Ca^{2+}. From these results, it is clear that both Ca^{2+} release and influx are required for AVP signaling in hASCs. While most of the Ca^{2+} appears to come

from the extracellular space, the ER release is needed to initiate the process. These observations are consistent with those reported for Gq-coupled receptor hormones that utilize the PLC-IP_3 pathway. This mechanism involves both Ca^{2+} release from the ER followed by the opening of store-operated Ca^{2+} channels in the plasma membrane via the Ca^{2+} sensor STIM-1 and Orai1 [50, 51]. One important question that needed to be addressed was the effect of AVP on adipogenesis. This was determined by supplementing the adipogenic differentiation medium with AVP followed by adipocyte quantification and marker gene expression in the cell population. The data demonstrated an inhibitory effect of AVP on adipogenesis since the number of adipocytes was significantly reduced. In addition, key adipogenic marker genes (e.g. C/EBPα, C/EBPβ, PPARγ2) were down-regulated. It is possible that AVP's effect on adipogenesis may involve MAPK/Erk signaling since this pathway is activated by the hormone and V1a receptors [52, 53]. This is supported by findings in bone marrow-derived stem cells where inhibition of MAPK/Erk facilitates adipocyte differentiation [54, 55]. Furthermore, MAPK/Erk signaling phosphorylates PPARγ leading to decreased transcriptional activity and suppression of adipogenesis [56]. Most importantly, Ca^{2+} signals inhibit adipogenesis by down-regulating C/EBPα, C/EBPβ, C/EBPγ and PPARγ genes in preadipocytes via MAPK/Erk [57].

Based on our results and those presented by others, it appears that AVP exerts mainly an inhibitory effect on adipocyte metabolism and differentiation. This is based on the fact that the absence of V1a receptor in knockout mice enhances lipolysis but decreases glucose uptake by adipocytes [28, 58]. AVP also inhibits β-

oxidation of fatty acid as an alternative energy source for the body [30]. The inhibitory effect of AVP on adipocyte differentiation could be reversed by the V1a receptor blocker V2255 which confirms its role on adipogenesis. It is tempting to speculate that the reduction in plasma AVP levels during obesity or multiple symmetric lipomatosis might be one of the factors responsible for adipose tissue accumulation/formation. Additional studies in V1a receptor knockout mice and humans with V1a receptor mutation show a tendency to develop obesity and diabetes [59, 60]. A link between AVP and body weight gain in cigarette smokers after quitting has been established due to the stimulatory action of nicotine on AVP secretion [37]. These observations together with our findings in hASCs could provide insights into new therapies for obesity.

In conclusion, we have identified the V1a receptor as the only type for AVP in hASCs. This receptor mediates the effect of AVP on intracellular Ca^{2+} signaling by activating Gq-proteins and the PLC-IP_3 pathway. This mechanism appears to exert an inhibitory effect on adipogenesis by down-regulating the expression of key adipogenic genes.

4.5 REFERENCES

1 Schaeffer, J. M., Liu, J., Hsueh, A. J. and Yen, S. S. (1984) Presence of oxytocin and arginine vasopressin in human ovary, oviduct, and follicular fluid. J. Clin. Endocrinol. Metab. **59**, 970-973.

2 Ang, V. T. and Jenkins, J. S. (1984) Neurohypophysial hormones in the adrenal medulla. J. Clin. Endocrinol. Metab. **58**, 688-691.

3 Kasson, B. G., Meidan, R. and Hsueh, A. J. (1985) Identification and characterization of arginine vasopressin-like substances in the rat testis. J. Biol. Chem. **260**, 5302-5307.

4 Markwick, A. J., Lolait, S. J. and Funder, J. W. (1986) Immunoreactive arginine vasopressin in the rat thymus. Endocrinology. **119**, 1690-1696.

5 Yibchok-anun, S., Abu-Basha, E. A., Yao, C. Y., Panichkriangkrai, W. and Hsu, W. H. (2004) The role of arginine vasopressin in diabetes-associated increase in glucagon secretion. Regul. Pept. **122**, 157-162.

6 Serradeil-Le Gal, C., Herbert, J. M., Delisee, C., Schaeffer, P., Raufaste, D., Garcia, C., Dol, F., Marty, E., Maffrand, J. P. and Le Fur, G. (1995) Effect of SR-49059, a vasopressin V1a antagonist, on human vascular smooth muscle cells. Am. J. Physiol. **268**, H404-410.

7 Tahara, A., Tsukada, J., Tomura, Y., Yatsu, T. and Shibasaki, M. (2008) Vasopressin increases type IV collagen production through the induction of transforming growth factor-beta secretion in rat mesangial cells. Pharmacol. Res. **57**, 142-150.

8 Jessop, D. S., Murphy, D. and Larsen, P. J. (1995) Thymic vasopressin (AVP) transgene expression in rats: a model for the study of thymic AVP hyper-expression in T cell differentiation. J. Neuroimmunol. **62**, 85-90.

9 Syed, N., Martens, C. A. and Hsu, W. H. (2007) Arginine vasopressin increases glutamate release and intracellular Ca2+ concentration in hippocampal and cortical astrocytes through two distinct receptors. J. Neurochem. **103**, 229-237.

10 Yibchok-Anun, S., Cheng, H., Heine, P. A. and Hsu, W. H. (1999) Characterization of receptors mediating AVP- and OT-induced glucagon release from the rat pancreas. Am. J. Physiol. **277**, E56-62.

11 Lee, B., Yang, C., Chen, T. H., al-Azawi, N. and Hsu, W. H. (1995) Effect of AVP and oxytocin on insulin release: involvement of V1b receptors. Am. J. Physiol. **269**, E1095-1100.

12 Grazzini, E., Lodboerer, A. M., Perez-Martin, A., Joubert, D. and Guillon, G. (1996) Molecular and functional characterization of V1b vasopressin receptor in rat adrenal medulla. Endocrinology. **137**, 3906-3914.

13 Laycock, J. F. (2010) Perspectives on Vasopressin. Imperial College Press.

14 Koshimizu, T. A., Nakamura, K., Egashira, N., Hiroyama, M., Nonoguchi, H. and Tanoue, A. (2012) Vasopressin V1a and V1b receptors: from molecules to physiological systems. Physiol. Rev. **92**, 1813-1864.

15 Thibonnier, M., Berti-Mattera, L. N., Dulin, N., Conarty, D. M. and Mattera, R. (1998) Signal transduction pathways of the human V1-vascular, V2-renal, V3-pituitary vasopressin and oxytocin receptors. Prog. Brain Res. **119**, 147-161.

16 Dolmetsch, R. E., Xu, K. and Lewis, R. S. (1998) Calcium oscillations increase the efficiency and specificity of gene expression. Nature. **392**, 933-936.

17 Kawano, S., Otsu, K., Kuruma, A., Shoji, S., Yanagida, E., Muto, Y., Yoshikawa, F., Hirayama, Y., Mikoshiba, K. and Furuichi, T. (2006) ATP autocrine/paracrine signaling induces calcium oscillations and NFAT activation in human mesenchymal stem cells. Cell Calcium. **39**, 313-324.

18 Sun, S., Liu, Y., Lipsky, S. and Cho, M. (2007) Physical manipulation of calcium oscillations facilitates osteodifferentiation of human mesenchymal stem cells. FASEB J. **21**, 1472-1480.

19 Shi, H., Halvorsen, Y. D., Ellis, P. N., Wilkison, W. O. and Zemel, M. B. (2000) Role of intracellular calcium in human adipocyte differentiation. Physiological genomics. **3**, 75-82.

20 Draznin, B., Sussman, K. E., Eckel, R. H., Kao, M., Yost, T. and Sherman, N. A. (1988) Possible role of cytosolic free calcium concentrations in mediating insulin resistance of obesity and hyperinsulinemia. J. Clin. Invest. **82**, 1848-1852.

21 Kapur, N., Mignery, G. A. and Banach, K. (2007) Cell cycle-dependent calcium oscillations in mouse embryonic stem cells. Am. J. Physiol. Cell Physiol. **292**, C1510-1518.

22 Todorova, M. G., Fuentes, E., Soria, B., Nadal, A. and Quesada, I. (2009) Lysophosphatidic acid induces Ca2+ mobilization and c-Myc expression in mouse embryonic stem cells via the phospholipase C pathway. Cell. Signal. **21**, 523-528.

23 Resende, R. R., Adhikari, A., da Costa, J. L., Lorencon, E., Ladeira, M. S., Guatimosim, S., Kihara, A. H. and Ladeira, L. O. (2010) Influence of spontaneous calcium events on cell-cycle progression in embryonal carcinoma and adult stem cells. Biochim. Biophys. Acta. **1803**, 246-260.

24 Gutkowska, J., Miszkurka, M., Danalache, B., Gassanov, N., Wang, D. and Jankowski, M. (2007) Functional arginine vasopressin system in early heart maturation. Am. J. Physiol. Heart Circ. Physiol. **293**, H2262-2270.

25 Toschi, A., Severi, A., Coletti, D., Catizone, A., Musaro, A., Molinaro, M., Nervi, C., Adamo, S. and Scicchitano, B. M. (2011) Skeletal muscle regeneration in mice is stimulated by local overexpression of V1a-vasopressin receptor. Mol. Endocrinol. **25**, 1661-1673.

26 Lagumdzija, A., Bucht, E., Stark, A., Hulting, A. L. and Petersson, M. (2004) Arg-vasopressin increases proliferation of human osteoblast-like cells and decreases production of interleukin-6 and macrophage colony-stimulating factor. Regul. Pept. **121**, 41-48.

27 Kuchler, S., Perwitz, N., Schick, R. R., Klein, J. and Westphal, S. (2010) Arginine-vasopressin directly promotes a thermogenic and pro-inflammatory adipokine expression profile in brown adipocytes. Regul. Pept. **164**, 126-132.

28 Nakamura, K., Aoyagi, T., Hiroyama, M., Kusakawa, S., Mizutani, R., Sanbe, A., Yamauchi, J., Kamohara, M., Momose, K. and Tanoue, A. (2009) Both V(1A) and V(1B) vasopressin receptors deficiency result in impaired glucose tolerance. Eur. J. Pharmacol. **613**, 182-188.

29 Boston, B. A. and Cone, R. D. (1996) Characterization of melanocortin receptor subtype expression in murine adipose tissues and in the 3T3-L1 cell line. Endocrinology. **137**, 2043-2050.

30 Sugden, M. C., Ball, A. J., Ilic, V. and Williamson, D. H. (1980) Stimulation of [1-14C]oleate oxidation to 14CO2 in isolated rat hepatocytes by vasopressin: effects of Ca2+. FEBS Lett. **116**, 37-40.

31 Kotchen, T. A. (2008) Obesity-related hypertension?: weighing the evidence. Hypertension. **52**, 801-802.

32 Sukhonthachit, P., Aekplakorn, W., Hudthagosol, C. and Sirikulchayanonta, C. (2014) The association between obesity and blood pressure in Thai public school children. BMC Public Health. **14**, 729.

33 Inder, W. J., Hellemans, J., Swanney, M. P., Prickett, T. C. and Donald, R. A. (1998) Prolonged exercise increases peripheral plasma ACTH, CRH, and AVP in male athletes. Journal of applied physiology (Bethesda, Md.: 1985). **85**, 835-841.

34 Hew-Butler, T., Noakes, T. D., Soldin, S. J. and Verbalis, J. G. (2010) Acute changes in arginine vasopressin, sweat, urine and serum sodium concentrations in exercising humans: does a coordinated homeostatic relationship exist? Br. J. Sports Med. **44**, 710-715.

35 Coiro, V. and Chiodera, P. (1987) Effect of obesity and weight loss on the arginine vasopressin response to insulin-induced hypoglycaemia. Clin. Endocrinol. (Oxf.). **27**, 253-258.

36 Angelini, C. (2014) Multiple Symmetric Lipomatosis. In Genetic Neuromuscular Disorders. pp. 251-254, Springer.

37 Thorgeirsson, T. E., Gudbjartsson, D. F., Sulem, P., Besenbacher, S., Styrkarsdottir, U., Thorleifsson, G., Walters, G. B., Furberg, H., Sullivan, P. F., Marchini, J., McCarthy, M. I., Steinthorsdottir, V., Thorsteinsdottir, U. and Stefansson, K. (2013) A common biological basis of obesity and nicotine addiction. Translational psychiatry. **3**, e308.

38 Kotova, P. D., Sysoeva, V. Y., Rogachevskaja, O. A., Bystrova, M. F., Kolesnikova, A. S., Tyurin-Kuzmin, P. A., Fadeeva, J. I., Tkachuk, V. A. and Kolesnikov, S. S. (2014) Functional expression of adrenoreceptors in mesenchymal stromal cells derived from the human adipose tissue. Biochim. Biophys. Acta. **1843**, 1899-1908.

39 Yu, G., Floyd, Z. E., Wu, X., Hebert, T., Halvorsen, Y. D., Buehrer, B. M. and Gimble, J. M. (2011) Adipogenic differentiation of adipose-derived stem cells. Methods Mol. Biol. **702**, 193-200.

40 Chiu, T., Wu, S. S., Santiskulvong, C., Tangkijvanich, P., Yee, H. F., Jr. and Rozengurt, E. (2002) Vasopressin-mediated mitogenic signaling in intestinal epithelial cells. Am. J. Physiol. Cell Physiol. **282**, C434-450.

41 Thibonnier, M., Bayer, A. L., Simonson, M. S. and Kester, M. (1991) Multiple signaling pathways of V1-vascular vasopressin receptors of A7r5 cells. Endocrinology. **129**, 2845-2856.

42 Kawano, S., Shoji, S., Ichinose, S., Yamagata, K., Tagami, M. and Hiraoka, M. (2002) Characterization of Ca(2+) signaling pathways in human mesenchymal stem cells. Cell Calcium. **32**, 165-174.

43 Nervi, C., Benedetti, L., Minasi, A., Molinaro, M. and Adamo, S. (1995) Arginine-vasopressin induces differentiation of skeletal myogenic cells and up-regulation of myogenin and Myf-5. Cell Growth Differ. **6**, 81-89.

44 Gassanov, N., Jankowski, M., Danalache, B., Wang, D., Grygorczyk, R., Hoppe, U. C. and Gutkowska, J. (2007) Arginine vasopressin-mediated cardiac differentiation: insights into the role of its receptors and nitric oxide signaling. J. Biol. Chem. **282**, 11255-11265.

45 Yu, L., Moriguchi, T., Souma, T., Takai, J., Satoh, H., Morito, N., Engel, J. D. and Yamamoto, M. (2014) GATA2 regulates body water homeostasis through maintaining aquaporin 2 expression in renal collecting ducts. Mol. Cell. Biol. **34**, 1929-1941.

46 Bourin, P., Bunnell, B. A., Casteilla, L., Dominici, M., Katz, A. J., March, K. L., Redl, H., Rubin, J. P., Yoshimura, K. and Gimble, J. M. (2013) Stromal cells from the adipose tissue-derived stromal vascular fraction and culture expanded adipose tissue-derived stromal/stem cells: a joint statement of the International Federation for Adipose Therapeutics and Science (IFATS) and the International Society for Cellular Therapy (ISCT). Cytotherapy. **15**, 641-648.

47 Pequeux, C., Breton, C., Hendrick, J. C., Hagelstein, M. T., Martens, H., Winkler, R., Geenen, V. and Legros, J. J. (2002) Oxytocin synthesis and oxytocin receptor expression by cell lines of human small cell carcinoma of the lung stimulate tumor growth through autocrine/paracrine signaling. Cancer Res. **62**, 4623-4629.

48 Nakamura, Y., Haneda, T., Osaki, J., Miyata, S. and Kikuchi, K. (2000) Hypertrophic growth of cultured neonatal rat heart cells mediated by vasopressin V(1A) receptor. Eur. J. Pharmacol. **391**, 39-48.

49 Tahara, A., Tsukada, J., Tomura, Y., Suzuki, T., Yatsu, T. and Shibasaki, M. (2008) Effect of vasopressin on type IV collagen production in human mesangial cells. Regul. Pept. **147**, 60-66.

50 Peinelt, C., Vig, M., Koomoa, D. L., Beck, A., Nadler, M. J., Koblan-Huberson, M., Lis, A., Fleig, A., Penner, R. and Kinet, J. P. (2006) Amplification of CRAC current by STIM1 and CRACM1 (Orai1). Nat. Cell Biol. **8**, 771-773.

51 Prakriya, M., Feske, S., Gwack, Y., Srikanth, S., Rao, A. and Hogan, P. G. (2006) Orai1 is an essential pore subunit of the CRAC channel. Nature. **443**, 230-233.

52 Keegan, B. P., Akerman, B. L., Pequeux, C. and North, W. G. (2006) Provasopressin expression by breast cancer cells: implications for growth and novel treatment strategies. Breast Cancer Res. Treat. **95**, 265-277.

53 He, Y. P., Zhao, L. Y., Zheng, Q. S., Liu, S. W., Zhao, X. Y., Lu, X. L. and Niu, X. L. (2008) Arginine vasopressin stimulates proliferation of adult rat cardiac fibroblasts via protein kinase C-extracellular signal-regulated kinase 1/2 pathway. Sheng li xue bao: [Acta physiologica Sinica]. **60**, 333-340.

54 Liu, Q., Cen, L., Zhou, H., Yin, S., Liu, G., Liu, W., Cao, Y. and Cui, L. (2009) The role of the extracellular signal-related kinase signaling pathway in osteogenic differentiation of human adipose-derived stem cells and in adipogenic transition initiated by dexamethasone. Tissue engineering. Part A. **15**, 3487-3497.

55 Jaiswal, R. K., Jaiswal, N., Bruder, S. P., Mbalaviele, G., Marshak, D. R. and Pittenger, M. F. (2000) Adult human mesenchymal stem cell differentiation to the osteogenic or adipogenic lineage is regulated by mitogen-activated protein kinase. J. Biol. Chem. **275**, 9645-9652.

56 Camp, H. S. and Tafuri, S. R. (1997) Regulation of peroxisome proliferator-activated receptor gamma activity by mitogen-activated protein kinase. J. Biol. Chem. **272**, 10811-10816.

57 Lin, F., Ribar, T. J. and Means, A. R. (2011) The Ca2+/calmodulin-dependent protein kinase kinase, CaMKK2, inhibits preadipocyte differentiation. Endocrinology. **152**, 3668-3679.

58 Hiroyama, M., Aoyagi, T., Fujiwara, Y., Birumachi, J., Shigematsu, Y., Kiwaki, K., Tasaki, R., Endo, F. and Tanoue, A. (2007) Hypermetabolism of fat in V1a vasopressin receptor knockout mice. Mol. Endocrinol. **21**, 247-258.

59 Aoyagi, T., Birumachi, J., Hiroyama, M., Fujiwara, Y., Sanbe, A., Yamauchi, J. and Tanoue, A. (2007) Alteration of glucose homeostasis in V1a vasopressin receptor deficient mice. Endocrinology. **148**, 2075-2084.

60 Enhorning, S., Leosdottir, M., Wallstrom, P., Gullberg, B., Berglund, G., Wirfalt, E. and Melander, O. (2009) Relation between human vasopressin 1a gene variance, fat intake, and diabetes. Am. J. Clin. Nutr. **89**, 400-406.

CHAPTER 5: CONCLUDING REMARKS

5.1 SUMMARY OF FINDINGS AND SIGNIFICANCE OF THE RESEARCH

Calcium signaling plays an important role in many cell functions such as differentiation, proliferation, apoptosis, and muscle contraction [1]. Chapter 1 of this dissertation summarizes the different types of stem cells, the Ca^{2+} signaling mechanisms, the TRPM4 channel and AVP's impact on Ca^{2+} signals. We utilized rDFSCs and hASCs to investigate the role of TRPM4 and AVP on stem cell differentiation. Chapter 2 describes our findings on the role of TRPM4 in rDFSCs. We generated TRPM4 knockdown cells to investigate its effect on osteogenesis and adipogenesis. After 14 days in differentiation media, TRPM4 knockdown showed enhanced mineralization and decreased lipid droplet accumulation. Microarray analysis revealed upregulation of critical genes for bone formation such as LUM and MEPE, and downregulation of ASPN, which inhibits differentiation and mineralization [2]. Several adipogenic genes, for example, TRIB3 and SFRP1, decreased in expression; TRIB3 is crucial for adipocyte formation and SFRP1 enhances adipogenesis in human and mice [3, 4]. The Ca^{2+} signals generated by ATP changed from a biphasic pattern to a gradual and sustained increase with TRPM4 inhibition. Therefore, we identified for the first time TRPM4 in stem cells and demonstrated that it is a key regulator of Ca^{2+} signals that facilitates adipogenesis but inhibits osteogenesis in rDFSCs.

As hASCs are a more suitable model for adipogenic studies, we investigated the role of TRPM4 in these cells in Chapter 3. We identified TRPM4 gene expression in hASCs and human adipose tissue. We also characterized the channel

in these cells. Our findings from the adipogenic studies were similar to those in rDFSCs since TRPM4 knockdown inhibited adipocyte formation and decreased adipocyte marker genes (PPARγ2, C/EBPα, C/EBPβ, aP2 and adiponectin). However, the Ca^{2+} signals with TRPM4 knockdown were different from rDFSCs and resembles those observed in pancreatic α and β cells which are excitable cells. We found that hASC gene expressed the L-type VDCCs ($Ca_v1.2$) which contributed to Ca^{2+} signals stimulated by histamine. This is important since undifferentiated stem cells are considered as non-excitable cells with SOCs as their main Ca^{2+} entry pathway [5]. The difference in the Ca^{2+} pattern between rDFSCs and hASCs may be due to the type of MSCs, species or impact of other pathways during differentiation.

In Chapter 4, we investigated the effect of AVP on adipogenesis of hASCs. We showed for the first time V1a receptor gene expression in hASCs. AVP in this stem cell type inhibited adipogenesis. This is in accordance to V1a receptor mutation or knockout that leads to obesity and diabetes [6, 7]. Our result provides insight into the mechanism of AVP on adipogenesis.

The decrease in intracellular Ca^{2+} during histamine stimulation in hASCs after TRPM4 suppression inhibited adipogenesis and was similar to our findings with AVP supplementation to the adipogenic medium. Therefore, it is likely that other signaling pathways may contribute to this process. In fact, Ca^{2+} signaling can crosstalk with other pathways such as cAMP because Ca^{2+} release from the ER activates STIM1 and increases cAMP signaling [8]. Activation of the V1a receptor by AVP also stimulates phosphatidylcholine hydrolysis by phospholipase A2. This

results in arachidonic acid production, increased phospholipase D and Na^+/H^+ exchanger activity. These effects control gene expression and protein synthesis during the differentiation process [9].

5.2 FUTURE STUDIES

TRPM4 facilitates adipogenesis, but inhibits osteogenesis in rDFSCs. To confirm these observations, we will rescue TRPM4 expression and perform a differentiation experiment to determine if the effect can be reversed in TRPM4 knockdown cells. To do that, we will design TRPM4 siRNA against the 3′-untranslated regions (UTR) of the endogenous TRPM4 gene. Then, we will transfect a vector containing the coding sequence for TRPM4 without the 3'-UTR. Therefore, TRPM4 overexpression from the vector construct will not be affected by the siRNA whereas the endogenous TRPM4 mRNA will be degraded. We will confirm TRPM4 expression by RT-PCR and Western blot. Functional studies will be performed with patch-clamp, ARS and ORO staining, Ca^{2+} imaging analysis, and quantitative RT-PCR. By patch-clamp, we will compare the amplitude of TRPM4 currents to those of control cells. ARS and ORO staining, Ca^{2+} imaging analysis, and quantitative RT-PCR will be performed during differentiation at days 0, 7, 14, 21 to determine whether the effect of TRPM4 knockdown can be reversed.

Furthermore, we will investigate the effect of TRPM4 *in vivo*. We plan to examine the ability of TRPM4 knockdown rDFSCs in bone repair of critical-size calvarial defects in the rat model. We will use micro-CT imaging, perform histologic analysis, and confirm osteogenic marker gene expression for new bone formation [10]. Regarding a pharmacological approach, 9-phenanthrol, a TRPM4

selective blocker can be toxic to the cells; therefore, it has limited potential in clinical therapy [11]. Other TRPM4 blockers such as flufenamic acid, an anti-inflammatory drug, and glibenclamide, the antidiabetic drug; both have been approved by the FDA [11, 12]. However, they also interact with other ion channels which can cause many side effects. As a consequence, more research needs to be done to identify specific TRPM4 blockers to control obesity and osteoporosis in the future. In conclusion, our results provided insights into the molecular mechanisms controlling stem cell differentiation by the TRPM4 ion channel and the hormone AVP. These findings could potentially lead to new therapies for the treatment of obesity and bone defects.

5.3 REFERENCES

1 Berridge, M. J., Lipp, P. and Bootman, M. D. (2000) The versatility and universality of calcium signalling. Nat. Rev. Mol. Cell Biol. **1**, 11-21.

2 Yamada, S., Tomoeda, M., Ozawa, Y., Yoneda, S., Terashima, Y., Ikezawa, K., Ikegawa, S., Saito, M., Toyosawa, S. and Murakami, S. (2007) PLAP-1/asporin, a novel negative regulator of periodontal ligament mineralization. J. Biol. Chem. **282**, 23070-23080.

3 Ti, Y., Xie, G. L., Wang, Z. H., Bi, X. L., Ding, W. Y., Wang, J., Jiang, G. H., Bu, P. L., Zhang, Y., Zhong, M. and Zhang, W. (2011) TRB3 gene silencing alleviates diabetic cardiomyopathy in a type 2 diabetic rat model. Diabetes. **60**, 2963-2974.

4 Lagathu, C., Christodoulides, C., Tan, C. Y., Virtue, S., Laudes, M., Campbell, M., Ishikawa, K., Ortega, F., Tinahones, F. J., Fernandez-Real, J. M., Oresic, M., Sethi, J. K. and Vidal-Puig, A. (2010) Secreted frizzled-related protein 1 regulates adipose tissue expansion and is dysregulated in severe obesity. Int. J. Obes. (Lond.). **34**, 1695-1705.

5 Kawano, S., Shoji, S., Ichinose, S., Yamagata, K., Tagami, M. and Hiraoka, M. (2002) Characterization of Ca(2+) signaling pathways in human mesenchymal stem cells. Cell Calcium. **32**, 165-174.

6 Aoyagi, T., Birumachi, J., Hiroyama, M., Fujiwara, Y., Sanbe, A., Yamauchi, J. and Tanoue, A. (2007) Alteration of glucose homeostasis in V1a vasopressin receptor-deficient mice. Endocrinology. **148**, 2075-2084.

7 Enhorning, S., Leosdottir, M., Wallstrom, P., Gullberg, B., Berglund, G., Wirfalt, E. and Melander, O. (2009) Relation between human vasopressin 1a gene variance, fat intake, and diabetes. Am. J. Clin. Nutr. **89**, 400-406.

8 Lefkimmiatis, K., Srikanthan, M., Maiellaro, I., Moyer, M. P., Curci, S. and Hofer, A. M. (2009) Store-operated cyclic AMP signalling mediated by STIM1. Nat. Cell Biol. **11**, 433-442.

9 Thibonnier, M. (1992) Signal transduction of V1-vascular vasopressin receptors. Regul. Pept. **38**, 1-11.

10 Levi, B., James, A. W., Nelson, E. R., Vistnes, D., Wu, B., Lee, M., Gupta, A. and Longaker, M. T. (2010) Human adipose derived stromal cells heal critical size mouse calvarial defects. PLoS One. **5**, e11177.

11 Guinamard, R., Hof, T. and Del Negro, C. A. (2014) The TRPM4 channel inhibitor 9-phenanthrol. Br. J. Pharmacol. **171**, 1600-1613.

12 Guinamard, R., Simard, C. and Del Negro, C. (2013) Flufenamic acid as an ion channel modulator. Pharmacol. Ther. **138**, 272-284.

APPENDIX: LETTERS OF PERMISSION

JOHN WILEY AND SONS LICENSE TERMS AND CONDITIONS

Nov 02, 2014

This is a License Agreement between Tran Doan Ngoc Tran ("You") and John Wiley and Sons ("John Wiley and Sons") provided by Copyright Clearance Center ("CCC"). The license consists of your order details, the terms and conditions provided by John Wiley and Sons, and the payment terms and conditions.

All payments must be made in full to CCC. For payment instructions, please see information listed at the bottom of this form.

License Number	3498860724979
License date	Oct 30, 2014
Licensed content publisher	John Wiley and Sons
Licensed content publication	Stem Cells
Licensed content title	Transient Receptor Potential Melastatin 4 Channel Controls Calcium Signals and Dental Follicle Stem Cell Differentiation
Licensed copyright line	Copyright © 2012 AlphaMed Press
Licensed content author	Piper Nelson,Tran Doan Ngoc Tran,Hanjie Zhang,Olga Zolochevska,Marxa Figueiredo,Ji-Ming Feng,Dina L. Gutierrez,Rui Xiao,Shaomian Yao,Arthur Penn,Li-Jun Yang,Henrique Cheng
Licensed content date	Dec 19, 2012
Start page	167
End page	177
Type of use	Dissertation/Thesis
Requestor type	Author of this Wiley article
Format	Print and electronic
Portion	Full article
Will you be translating?	No
Title of your thesis / dissertation	Mechanisms controlling stem cell differentiation
Expected completion date	May 2015
Expected size (number of pages)	150
Total	0.00 USD
Terms and Conditions	

TERMS AND CONDITIONS

This copyrighted material is owned by or exclusively licensed to John Wiley & Sons, Inc. or one of its group companies (each a"Wiley Company") or handled on behalf of a society with which a Wiley Company has exclusive publishing rights in relation to a particular work (collectively

"WILEY"). By clicking "accept" in connection with completing this licensing transaction, you agree that the following terms and conditions apply to this transaction (along with the billing and payment terms and conditions established by the Copyright Clearance Center Inc., ("CCC's Billing and Payment terms and conditions"), at the time that you opened your RightsLink account (these are available at any time at http://myaccount.copyright.com).

Terms and Conditions

- The materials you have requested permission to reproduce or reuse (the "Wiley Materials") are protected by copyright.

- You are hereby granted a personal, non-exclusive, non-sub licensable (on a stand-alone basis), non-transferable, worldwide, limited license to reproduce the Wiley Materials for the purpose specified in the licensing process. This license is for a one-time use only and limited to any maximum distribution number specified in the license. The first instance of republication or reuse granted by this licence must be completed within two years of the date of the grant of this licence (although copies prepared before the end date may be distributed thereafter). The Wiley Materials shall not be used in any other manner or for any other purpose, beyond what is granted in the license. Permission is granted subject to an appropriate acknowledgement given to the author, title of the material/book/journal and the publisher. You shall also duplicate the copyright notice that appears in the Wiley publication in your use of the Wiley Material. Permission is also granted on the understanding that nowhere in the text is a previously published source acknowledged for all or part of this Wiley Material. Any third party content is expressly excluded from this permission.

- With respect to the Wiley Materials, all rights are reserved. Except as expressly granted by the terms of the license, no part of the Wiley Materials may be copied, modified, adapted (except for minor reformatting required by the new Publication), translated, reproduced, transferred or distributed, in any form or by any means, and no derivative works may be made based on the Wiley Materials without the prior permission of the respective copyright owner. You may not alter, remove or suppress in any manner any copyright, trademark or other notices displayed by the Wiley Materials. You may not license, rent, sell, loan, lease, pledge, offer as security, transfer or assign the Wiley Materials on a stand-alone basis, or any of the rights granted to you hereunder to any other person.

- The Wiley Materials and all of the intellectual property rights therein shall at all times remain the exclusive property of John Wiley & Sons Inc, the Wiley Companies, or their respective licensors, and your interest therein is only that of having possession of and the right to reproduce the Wiley Materials pursuant to Section 2 herein during the continuance of this Agreement. You agree that you own no right, title or interest in or to the Wiley Materials or any of the intellectual property rights therein. You shall have no rights hereunder other than the license as provided for above in Section 2. No right, license or interest to any trademark, trade name, service mark or other branding ("Marks") of WILEY or its licensors is granted hereunder, and you agree that you shall not assert any such right, license or interest with respect thereto.

- NEITHER WILEY NOR ITS LICENSORS MAKES ANY WARRANTY OR REPRESENTATION OF ANY KIND TO YOU OR ANY THIRD PARTY, EXPRESS, IMPLIED OR STATUTORY, WITH RESPECT TO THE MATERIALS OR THE ACCURACY OF ANY INFORMATION CONTAINED IN THE MATERIALS, INCLUDING, WITHOUT LIMITATION, ANY IMPLIED WARRANTY OF MERCHANTABILITY, ACCURACY, SATISFACTORY QUALITY, FITNESS FOR A PARTICULAR PURPOSE, USABILITY, INTEGRATION OR NON-INFRINGEMENT AND ALL SUCH WARRANTIES ARE HEREBY EXCLUDED BY WILEY AND ITS LICENSORS AND WAIVED BY YOU

- WILEY shall have the right to terminate this Agreement immediately upon breach of this Agreement by you.

- You shall indemnify, defend and hold harmless WILEY, its Licensors and their respective directors, officers, agents and employees, from and against any actual or threatened claims, demands, causes of action or proceedings arising from any breach of this Agreement by you.

- IN NO EVENT SHALL WILEY OR ITS LICENSORS BE LIABLE TO YOU OR ANY OTHER PARTY OR ANY OTHER PERSON OR ENTITY FOR ANY SPECIAL, CONSEQUENTIAL, INCIDENTAL, INDIRECT, EXEMPLARY OR PUNITIVE DAMAGES, HOWEVER CAUSED, ARISING OUT OF OR IN CONNECTION WITH THE DOWNLOADING, PROVISIONING, VIEWING OR USE OF THE MATERIALS REGARDLESS OF THE FORM OF ACTION, WHETHER FOR BREACH OF CONTRACT, BREACH OF WARRANTY, TORT, NEGLIGENCE, INFRINGEMENT OR OTHERWISE (INCLUDING, WITHOUT LIMITATION, DAMAGES BASED ON LOSS OF PROFITS, DATA, FILES, USE, BUSINESS OPPORTUNITY OR CLAIMS OF THIRD PARTIES), AND WHETHER OR NOT THE PARTY HAS BEEN ADVISED OF THE POSSIBILITY OF SUCH DAMAGES. THIS LIMITATION SHALL APPLY NOTWITHSTANDING ANY FAILURE OF ESSENTIAL PURPOSE OF ANY LIMITED REMEDY PROVIDED HEREIN.

- Should any provision of this Agreement be held by a court of competent jurisdiction to be illegal, invalid, or unenforceable, that provision shall be deemed amended to achieve as nearly as possible the same economic effect as the original provision, and the legality, validity and enforceability of the remaining provisions of this Agreement shall not be affected or impaired thereby.

- The failure of either party to enforce any term or condition of this Agreement shall not constitute a waiver of either party's right to enforce each and every term and condition of this Agreement. No breach under this agreement shall be deemed waived or excused by either party unless such waiver or consent is in writing signed by the party granting such waiver or consent. The waiver by or consent of a party to a breach of any provision of this Agreement shall not operate or be construed as a waiver of or consent to any other or subsequent breach by such other party.

- This Agreement may not be assigned (including by operation of law or otherwise) by you without WILEY's prior written consent.

- Any fee required for this permission shall be non-refundable after thirty (30) days from receipt by the CCC.

- These terms and conditions together with CCC's Billing and Payment terms and conditions (which are incorporated herein) form the entire agreement between you and WILEY concerning this licensing transaction and (in the absence of fraud) supersedes all prior agreements and representations of the parties, oral or written. This Agreement may not be amended except in writing signed by both parties. This Agreement shall be binding upon and inure to the benefit of the parties' successors, legal representatives, and authorized assigns.

- In the event of any conflict between your obligations established by these terms and conditions and those established by CCC's Billing and Payment terms and conditions, these terms and conditions shall prevail.

- WILEY expressly reserves all rights not specifically granted in the combination of (i) the license details provided by you and accepted in the course of this licensing transaction, (ii) these terms and conditions and (iii) CCC's Billing and Payment terms and conditions.

- This Agreement will be void if the Type of Use, Format, Circulation, or Requestor Type was misrepresented during the licensing process.

- This Agreement shall be governed by and construed in accordance with the laws of the State of New York, USA, without regards to such state's conflict of law rules. Any legal action, suit or proceeding arising out of or relating to these Terms and Conditions or the breach thereof shall be instituted in a court of competent jurisdiction in New York County in the State of New York in the United States of America and each party hereby consents and submits to the personal jurisdiction of such court, waives any objection to venue in such court and consents to service of process by registered or certified mail, return receipt requested, at the last known address of such party.

WILEY OPEN ACCESS TERMS AND CONDITIONS

Wiley Publishes Open Access Articles in fully Open Access Journals and in Subscription journals offering Online Open. Although most of the fully Open Access journals publish open access articles under the terms of the Creative Commons Attribution (CC BY) License only, the subscription journals and a few of the Open Access Journals offer a choice of Creative Commons Licenses:: Creative Commons Attribution (CC-BY) license Creative Commons Attribution Non-Commercial (CC-BY-NC) license and Creative Commons Attribution Non-Commercial-NoDerivs (CC-BY-NC-ND) License. The license type is clearly identified on the article.

Copyright in any research article in a journal published as Open Access under a Creative Commons License is retained by the author(s). Authors grant Wiley a license to publish the article

and identify itself as the original publisher. Authors also grant any third party the right to use the article freely as long as its integrity is maintained and its original authors, citation details and publisher are identified as follows: [Title of Article/Author/Journal Title and Volume/Issue. Copyright (c) [year] [copyright owner as specified in the Journal]. Links to the final article on Wiley's website are encouraged where applicable.

The Creative Commons Attribution License

The Creative Commons Attribution License (CC-BY) allows users to copy, distribute and transmit an article, adapt the article and make commercial use of the article. The CC-BY license permits commercial and non-commercial re-use of an open access article, as long as the author is properly attributed.

The Creative Commons Attribution License does not affect the moral rights of authors, including without limitation the right not to have their work subjected to derogatory treatment. It also does not affect any other rights held by authors or third parties in the article; including without limitation the rights of privacy and publicity. Use of the article must not assert or imply, whether implicitly or explicitly, any connection with, endorsement or sponsorship of such use by the author, publisher or any other party associated with the article.

For any reuse or distribution, users must include the copyright notice and make clear to others that the article is made available under a Creative Commons Attribution license, linking to the relevant Creative Commons web page.

To the fullest extent permitted by applicable law, the article is made available as is and without representation or warranties of any kind whether express, implied, statutory or otherwise and including, without limitation, warranties of title, merchantability, fitness for a particular purpose, non-infringement, absence of defects, accuracy, or the presence or absence of errors.

Creative Commons Attribution Non-Commercial License

The Creative Commons Attribution Non-Commercial (CC-BY-NC) License permits use, distribution and reproduction in any medium, provided the original work is properly cited and is not used for commercial purposes.(see below)

Creative Commons Attribution-Non-Commercial-NoDerivs License

The Creative Commons Attribution Non-Commercial-NoDerivs License (CC-BY-NC-ND) permits use, distribution and reproduction in any medium, provided the original work is properly cited, is not used for commercial purposes and no modifications or adaptations are made. (see below)

Use by non-commercial users

For non-commercial and non-promotional purposes, individual users may access, download, copy, display and redistribute to colleagues Wiley Open Access articles, as well as adapt, translate, text- and data-mine the content subject to the following conditions:

- The authors' moral rights are not compromised. These rights include the right of "paternity" (also known as "attribution" – the right for the author to be identified as such) and "integrity" (the right for the author not to have the work altered in such a way that the author's reputation or integrity may be impugned).

- Where content in the article is identified as belonging to a third party, it is the obligation of the user to ensure that any reuse complies with the copyright policies of the owner of that content.

- If article content is copied, downloaded or otherwise reused for non-commercial research and education purposes, a link to the appropriate bibliographic citation (authors, journal, article title, volume, issue, page numbers, DOI and the link to the definitive published version on **Wiley Online Library**) should be maintained. Copyright notices and disclaimers must not be deleted.

- Any translations, for which a prior translation agreement with Wiley has not been agreed, must prominently display the statement: "This is an unofficial translation of an article that appeared in a Wiley publication. The publisher has not endorsed this translation."

Use by commercial "for-profit" organisations

Use of Wiley Open Access articles for commercial, promotional, or marketing purposes requires further explicit permission from Wiley and will be subject to a fee. Commercial purposes include:

- Copying or downloading of articles, or linking to such articles for further redistribution, sale or licensing;

- Copying, downloading or posting by a site or service that incorporates advertising with such content;

- The inclusion or incorporation of article content in other works or services (other than normal quotations with an appropriate citation) that is then available for sale or licensing, for a fee (for example, a compilation produced for marketing purposes, inclusion in a sales pack)

- Use of article content (other than normal quotations with appropriate citation) by for-profit organisations for promotional purposes

- Linking to article content in e-mails redistributed for promotional, marketing or educational purposes;

- Use for the purposes of monetary reward by means of sale, resale, licence, loan, transfer or other form of commercial exploitation such as marketing products

- Print reprints of Wiley Open Access articles can be purchased from: corporatesales@wiley.com

ELSEVIER LICENSE
TERMS AND CONDITIONS

Jan 14, 2015

This is a License Agreement between Tran Doan Ngoc Tran ("You") and Elsevier ("Elsevier") provided by Copyright Clearance Center ("CCC"). The license consists of your order details, the terms and conditions provided by Elsevier, and the payment terms and conditions.

All payments must be made in full to CCC. For payment instructions, please see information listed at the bottom of this form.

Supplier	Elsevier Limited The Boulevard,Langford Lane Kidlington,Oxford,OX5 1GB,UK
Registered Company Number	1982084
Customer name	Tran Doan Ngoc Tran
Customer address	3950 Dulcito Ave BATON ROUGE, LA 70820
License number	3547800552137
License date	Jan 14, 2015
Licensed content publisher	Elsevier
Licensed content publication	The Veterinary Journal
Licensed content title	Transient receptor proteins illuminated: Current views on TRPs and disease
Licensed content author	Piper L. Nelson,Andreas Beck,Henrique Cheng
Licensed content date	February 2011
Licensed content volume number	187
Licensed content issue number	2
Number of pages	12
Start Page	153
End Page	164
Type of Use	reuse in a thesis/dissertation
Intended publisher of new work	other
Portion	figures/tables/illustrations
Number of figures/tables/illustrations	1
Format	both print and electronic
Are you the author of this Elsevier article?	No

Will you be translating?	No
Original figure numbers	Figure 1
Title of your thesis/dissertation	Mechanisms controlling stem cell differentiation
Expected completion date	May 2015
Estimated size (number of pages)	150
Elsevier VAT number	GB 494 6272 12
Permissions price	0.00 USD
VAT/Local Sales Tax	0.00 USD / 0.00 GBP
Total	0.00 USD
Terms and Conditions	

INTRODUCTION

1. The publisher for this copyrighted material is Elsevier. By clicking "accept" in connection with completing this licensing transaction, you agree that the following terms and conditions apply to this transaction (along with the Billing and Payment terms and conditions established by Copyright Clearance Center, Inc. ("CCC"), at the time that you opened your Rightslink account and that are available at any time at http://myaccount.copyright.com).

GENERAL TERMS

2. Elsevier hereby grants you permission to reproduce the aforementioned material subject to the terms and conditions indicated.

3. Acknowledgement: If any part of the material to be used (for example, figures) has appeared in our publication with credit or acknowledgement to another source, permission must also be sought from that source. If such permission is not obtained then that material may not be included in your publication/copies. Suitable acknowledgement to the source must be made, either as a footnote or in a reference list at the end of your publication, as follows:

"Reprinted from Publication title, Vol /edition number, Author(s), Title of article / title of chapter, Pages No., Copyright (Year), with permission from Elsevier [OR APPLICABLE SOCIETY COPYRIGHT OWNER]." Also Lancet special credit - "Reprinted from The Lancet, Vol. number, Author(s), Title of article, Pages No., Copyright (Year), with permission from Elsevier."

4. Reproduction of this material is confined to the purpose and/or media for which permission is hereby given.

5. Altering/Modifying Material: Not Permitted. However figures and illustrations may be altered/adapted minimally to serve your work. Any other abbreviations, additions, deletions and/or any other alterations shall be made only with prior written authorization of Elsevier Ltd. (Please contact Elsevier at permissions@elsevier.com)

6. If the permission fee for the requested use of our material is waived in this instance, please be advised that your future requests for Elsevier materials may attract a fee.

7. Reservation of Rights: Publisher reserves all rights not specifically granted in the combination of (i) the license details provided by you and accepted in the course of this licensing transaction, (ii) these terms and conditions and (iii) CCC's Billing and Payment terms and conditions.

8. License Contingent Upon Payment: While you may exercise the rights licensed immediately upon issuance of the license at the end of the licensing process for the transaction, provided that you have disclosed complete and accurate details of your proposed use, no license is finally effective unless and until full payment is received from you (either by publisher or by CCC) as provided in CCC's Billing and Payment terms and conditions. If full payment is not received on a timely basis, then any license preliminarily granted shall be deemed automatically revoked and shall be void as if never granted. Further, in the event that you breach any of these terms and conditions or any of CCC's Billing and Payment terms and conditions, the license is automatically revoked and shall be void as if never granted. Use of materials as described in a revoked license, as well as any use of the materials beyond the scope of an unrevoked license, may constitute copyright infringement and publisher reserves the right to take any and all action to protect its copyright in the materials.

9. Warranties: Publisher makes no representations or warranties with respect to the licensed material.

10. Indemnity: You hereby indemnify and agree to hold harmless publisher and CCC, and their respective officers, directors, employees and agents, from and against any and all claims arising out of your use of the licensed material other than as specifically authorized pursuant to this license.

11. No Transfer of License: This license is personal to you and may not be sublicensed, assigned, or transferred by you to any other person without publisher's written permission.

12. No Amendment Except in Writing: This license may not be amended except in a writing signed by both parties (or, in the case of publisher, by CCC on publisher's behalf).

13. Objection to Contrary Terms: Publisher hereby objects to any terms contained in any purchase order, acknowledgment, check endorsement or other writing prepared by you, which terms are inconsistent with these terms and conditions or CCC's Billing and Payment terms and conditions. These terms and conditions, together with CCC's Billing and Payment terms and conditions (which are incorporated herein), comprise the entire agreement between you and publisher (and CCC) concerning this licensing transaction. In the event of any conflict between your obligations established by these terms and conditions and those established by CCC's Billing and Payment terms and conditions, these terms and conditions shall control.

14. Revocation: Elsevier or Copyright Clearance Center may deny the permissions described in this License at their sole discretion, for any reason or no reason, with a full refund payable to you. Notice of such denial will be made using the contact information provided by you. Failure to receive such notice will not alter or invalidate the denial. In no event will Elsevier or Copyright Clearance Center be responsible or liable for any costs, expenses or damage incurred by you as a result of a denial of your permission request, other than a refund of the amount(s) paid by you to Elsevier and/or Copyright Clearance Center for denied permissions.

LIMITED LICENSE

The following terms and conditions apply only to specific license types:

15. **Translation**: This permission is granted for non-exclusive world **English** rights only unless your license was granted for translation rights. If you licensed translation rights you may only translate this content into the languages you requested. A professional translator must perform all translations and reproduce the content word for word preserving the integrity of the article. If this license is to re-use 1 or 2 figures then permission is granted for non-exclusive world rights in all languages.

16. **Posting licensed content on any Website**: The following terms and conditions apply as follows: Licensing material from an Elsevier journal: All content posted to the web site must maintain the copyright information line on the bottom of each image; A hyper-text must be included to the Homepage of the journal from which you are licensing at http://www.sciencedirect.com/science/journal/xxxxx or the Elsevier homepage for books at http://www.elsevier.com; Central Storage: This license does not include permission for a scanned version of the material to be stored in a central repository such as that provided by Heron/XanEdu.

Licensing material from an Elsevier book: A hyper-text link must be included to the Elsevier homepage at http://www.elsevier.com . All content posted to the web site must maintain the copyright information line on the bottom of each image.

Posting licensed content on Electronic reserve: In addition to the above the following clauses are applicable: The web site must be password-protected and made available only to bona fide students registered on a relevant course. This permission is granted for 1 year only. You may obtain a new license for future website posting.

For journal authors: the following clauses are applicable in addition to the above: Permission granted is limited to the author accepted manuscript version* of your paper.

***Accepted Author Manuscript (AAM) Definition:** An accepted author manuscript (AAM) is the author's version of the manuscript of an article that has been accepted for publication and which may include any author-incorporated changes suggested through the processes of submission processing, peer review, and editor-author communications. AAMs do not include other publisher value-added contributions such as copy-editing, formatting, technical enhancements and (if relevant) pagination.

You are not allowed to download and post the published journal article (whether PDF or HTML, proof or final version), nor may you scan the printed edition to create an electronic version. A hyper-text must be included to the Homepage of the journal from which you are licensing at http://www.sciencedirect.com/science/journal/xxxxx. As part of our normal production process, you will receive an e-mail notice when your article appears on Elsevier's online service ScienceDirect (www.sciencedirect.com). That e-mail will include the article's Digital Object Identifier (DOI). This number provides the electronic link to the published article and should be included in the posting of your personal version. We ask that you wait until you receive this e-mail and have the DOI to do any posting.

Posting to a repository: Authors may post their AAM immediately to their employer's

institutional repository for internal use only and may make their manuscript publically available after the journal-specific embargo period has ended.

Please also refer to Elsevier's Article Posting Policy for further information.

18. **For book authors** the following clauses are applicable in addition to the above: Authors are permitted to place a brief summary of their work online only.. You are not allowed to download and post the published electronic version of your chapter, nor may you scan the printed edition to create an electronic version. **Posting to a repository:** Authors are permitted to post a summary of their chapter only in their institution's repository.

20. **Thesis/Dissertation**: If your license is for use in a thesis/dissertation your thesis may be submitted to your institution in either print or electronic form. Should your thesis be published commercially, please reapply for permission. These requirements include permission for the Library and Archives of Canada to supply single copies, on demand, of the complete thesis and include permission for Proquest/UMI to supply single copies, on demand, of the complete thesis. Should your thesis be published commercially, please reapply for permission.

Elsevier Open Access Terms and Conditions

Elsevier publishes Open Access articles in both its Open Access journals and via its Open Access articles option in subscription journals.

Authors publishing in an Open Access journal or who choose to make their article Open Access in an Elsevier subscription journal select one of the following Creative Commons user licenses, which define how a reader may reuse their work: Creative Commons Attribution License (CC BY), Creative Commons Attribution – Non Commercial - ShareAlike (CC BY NC SA) and Creative Commons Attribution – Non Commercial – No Derivatives (CC BY NC ND)

Terms & Conditions applicable to all Elsevier Open Access articles:

Any reuse of the article must not represent the author as endorsing the adaptation of the article nor should the article be modified in such a way as to damage the author's honour or reputation.

The author(s) must be appropriately credited.

If any part of the material to be used (for example, figures) has appeared in our publication with credit or acknowledgement to another source it is the responsibility of the user to ensure their reuse complies with the terms and conditions determined by the rights holder.

Additional Terms & Conditions applicable to each Creative Commons user license:

CC BY: You may distribute and copy the article, create extracts, abstracts, and other revised versions, adaptations or derivative works of or from an article (such as a translation), to include in a collective work (such as an anthology), to text or data mine the article, including for commercial purposes without permission from Elsevier

CC BY NC SA: For non-commercial purposes you may distribute and copy the article, create extracts, abstracts and other revised versions, adaptations or derivative works of or from an article (such as a translation), to include in a collective work (such as an anthology), to text and data mine the article and license new adaptations or creations under identical terms without permission from Elsevier

CC BY NC ND: For non-commercial purposes you may distribute and copy the article and include it in a collective work (such as an anthology), provided you do not alter or modify the article, without permission from Elsevier

Any commercial reuse of Open Access articles published with a CC BY NC SA or CC BY NC ND license requires permission from Elsevier and will be subject to a fee.

Commercial reuse includes:

- Promotional purposes (advertising or marketing)
- Commercial exploitation (e.g. a product for sale or loan)
- Systematic distribution (for a fee or free of charge)

Please refer to Elsevier's Open Access Policy for further information.

21. **Other Conditions**:

v1.7

Questions? customercare@copyright.com or +1-855-239-3415 (toll free in the US) or +1-978-646-2777.

Gratis licenses (referencing $0 in the Total field) are free. Please retain this printable license for your reference. No payment is required.

ELSEVIER LICENSE
TERMS AND CONDITIONS

Feb 25, 2015

This is a License Agreement between Tran Doan Ngoc Tran ("You") and Elsevier ("Elsevier") provided by Copyright Clearance Center ("CCC"). The license consists of your order details, the terms and conditions provided by Elsevier, and the payment terms and conditions.

All payments must be made in full to CCC. For payment instructions, please see information listed at the bottom of this form.

Supplier	Elsevier Limited The Boulevard,Langford Lane Kidlington,Oxford,OX5 1GB,UK
Registered Company Number	1982084
Customer name	Tran Doan Ngoc Tran
Customer address	3950 Dulcito Ave BATON ROUGE, LA 70820
License number	3575970705551
License date	Feb 25, 2015
Licensed content publisher	Elsevier
Licensed content publication	Molecular and Cellular Endocrinology
Licensed content title	Arginine vasopressin inhibits adipogenesis in human adipose-derived stem cells
Licensed content author	None
Licensed content date	Available online 16 February 2015
Licensed content volume number	n/a
Licensed content issue number	n/a
Number of pages	1
Start Page	None
End Page	None
Type of Use	reuse in a thesis/dissertation
Intended publisher of new work	other
Portion	full article
Format	both print and electronic
Are you the author of this Elsevier article?	Yes
Will you be translating?	No

Title of your thesis/dissertation	Mechanisms controlling stem cell differentiation
Expected completion date	May 2015
Estimated size (number of pages)	
Elsevier VAT number	GB 494 6272 12
Permissions price	0.00 USD
VAT/Local Sales Tax	0.00 USD / 0.00 GBP
Total	0.00 USD
Terms and Conditions	

INTRODUCTION

1. The publisher for this copyrighted material is Elsevier. By clicking "accept" in connection with completing this licensing transaction, you agree that the following terms and conditions apply to this transaction (along with the Billing and Payment terms and conditions established by Copyright Clearance Center, Inc. ("CCC"), at the time that you opened your Rightslink account and that are available at any time at http://myaccount.copyright.com).

GENERAL TERMS

2. Elsevier hereby grants you permission to reproduce the aforementioned material subject to the terms and conditions indicated.

3. Acknowledgement: If any part of the material to be used (for example, figures) has appeared in our publication with credit or acknowledgement to another source, permission must also be sought from that source. If such permission is not obtained then that material may not be included in your publication/copies. Suitable acknowledgement to the source must be made, either as a footnote or in a reference list at the end of your publication, as follows:

"Reprinted from Publication title, Vol /edition number, Author(s), Title of article / title of chapter, Pages No., Copyright (Year), with permission from Elsevier [OR APPLICABLE SOCIETY COPYRIGHT OWNER]." Also Lancet special credit - "Reprinted from The Lancet, Vol. number, Author(s), Title of article, Pages No., Copyright (Year), with permission from Elsevier."

4. Reproduction of this material is confined to the purpose and/or media for which permission is hereby given.

5. Altering/Modifying Material: Not Permitted. However figures and illustrations may be altered/adapted minimally to serve your work. Any other abbreviations, additions, deletions and/or any other alterations shall be made only with prior written authorization of Elsevier Ltd. (Please contact Elsevier at permissions@elsevier.com)

6. If the permission fee for the requested use of our material is waived in this instance, please be advised that your future requests for Elsevier materials may attract a fee.

7. Reservation of Rights: Publisher reserves all rights not specifically granted in the combination of (i) the license details provided by you and accepted in the course of this licensing transaction, (ii)

these terms and conditions and (iii) CCC's Billing and Payment terms and conditions.

8. License Contingent Upon Payment: While you may exercise the rights licensed immediately upon issuance of the license at the end of the licensing process for the transaction, provided that you have disclosed complete and accurate details of your proposed use, no license is finally effective unless and until full payment is received from you (either by publisher or by CCC) as provided in CCC's Billing and Payment terms and conditions. If full payment is not received on a timely basis, then any license preliminarily granted shall be deemed automatically revoked and shall be void as if never granted. Further, in the event that you breach any of these terms and conditions or any of CCC's Billing and Payment terms and conditions, the license is automatically revoked and shall be void as if never granted. Use of materials as described in a revoked license, as well as any use of the materials beyond the scope of an unrevoked license, may constitute copyright infringement and publisher reserves the right to take any and all action to protect its copyright in the materials.

9. Warranties: Publisher makes no representations or warranties with respect to the licensed material.

10. Indemnity: You hereby indemnify and agree to hold harmless publisher and CCC, and their respective officers, directors, employees and agents, from and against any and all claims arising out of your use of the licensed material other than as specifically authorized pursuant to this license.

11. No Transfer of License: This license is personal to you and may not be sublicensed, assigned, or transferred by you to any other person without publisher's written permission.

12. No Amendment Except in Writing: This license may not be amended except in a writing signed by both parties (or, in the case of publisher, by CCC on publisher's behalf).

13. Objection to Contrary Terms: Publisher hereby objects to any terms contained in any purchase order, acknowledgment, check endorsement or other writing prepared by you, which terms are inconsistent with these terms and conditions or CCC's Billing and Payment terms and conditions. These terms and conditions, together with CCC's Billing and Payment terms and conditions (which are incorporated herein), comprise the entire agreement between you and publisher (and CCC) concerning this licensing transaction. In the event of any conflict between your obligations established by these terms and conditions and those established by CCC's Billing and Payment terms and conditions, these terms and conditions shall control.

14. Revocation: Elsevier or Copyright Clearance Center may deny the permissions described in this License at their sole discretion, for any reason or no reason, with a full refund payable to you. Notice of such denial will be made using the contact information provided by you. Failure to receive such notice will not alter or invalidate the denial. In no event will Elsevier or Copyright Clearance Center be responsible or liable for any costs, expenses or damage incurred by you as a result of a denial of your permission request, other than a refund of the amount(s) paid by you to Elsevier and/or Copyright Clearance Center for denied permissions.

LIMITED LICENSE

The following terms and conditions apply only to specific license types:

15. **Translation**: This permission is granted for non-exclusive world **English** rights only unless your license was granted for translation rights. If you licensed translation rights you may only translate this content into the languages you requested. A professional translator must perform all translations and reproduce the content word for word preserving the integrity of the article. If this license is to re-use 1 or 2 figures then permission is granted for non-exclusive world rights in all languages.

16. **Posting licensed content on any Website**: The following terms and conditions apply as follows: Licensing material from an Elsevier journal: All content posted to the web site must maintain the copyright information line on the bottom of each image; A hyper-text must be included to the Homepage of the journal from which you are licensing at http://www.sciencedirect.com/science/journal/xxxxx or the Elsevier homepage for books at http://www.elsevier.com; Central Storage: This license does not include permission for a scanned version of the material to be stored in a central repository such as that provided by Heron/XanEdu.

Licensing material from an Elsevier book: A hyper-text link must be included to the Elsevier homepage at http://www.elsevier.com . All content posted to the web site must maintain the copyright information line on the bottom of each image.

Posting licensed content on Electronic reserve: In addition to the above the following clauses are applicable: The web site must be password-protected and made available only to bona fide students registered on a relevant course. This permission is granted for 1 year only. You may obtain a new license for future website posting.

17. **For journal authors:** the following clauses are applicable in addition to the above: Permission granted is limited to the author accepted manuscript version* of your paper.

***Accepted Author Manuscript (AAM) Definition:** An accepted author manuscript (AAM) is the author's version of the manuscript of an article that has been accepted for publication and which may include any author-incorporated changes suggested through the processes of submission processing, peer review, and editor-author communications. AAMs do not include other publisher value-added contributions such as copy-editing, formatting, technical enhancements and (if relevant) pagination.

You are not allowed to download and post the published journal article (whether PDF or HTML, proof or final version), nor may you scan the printed edition to create an electronic version. A hyper-text must be included to the Homepage of the journal from which you are licensing at http://www.sciencedirect.com/science/journal/xxxxx. As part of our normal production process, you will receive an e-mail notice when your article appears on Elsevier's online service ScienceDirect (www.sciencedirect.com). That e-mail will include the article's Digital Object Identifier (DOI). This number provides the electronic link to the published article and should be included in the posting of your personal version. We ask that you wait until you receive this e-mail and have the DOI to do any posting.

18. **Posting to a repository:** Authors may post their AAM immediately to their employer's institutional repository for internal use only and may make their manuscript publically available after the journal-specific embargo period has ended.

Please also refer to Elsevier's Article Posting Policy for further information.

19. **For book authors** the following clauses are applicable in addition to the above: Authors are permitted to place a brief summary of their work online only.. You are not allowed to download and post the published electronic version of your chapter, nor may you scan the printed edition to create an electronic version. **Posting to a repository:** Authors are permitted to post a summary of their chapter only in their institution's repository.

20. **Thesis/Dissertation**: If your license is for use in a thesis/dissertation your thesis may be submitted to your institution in either print or electronic form. Should your thesis be published commercially, please reapply for permission. These requirements include permission for the Library and Archives of Canada to supply single copies, on demand, of the complete thesis and include permission for Proquest/UMI to supply single copies, on demand, of the complete thesis. Should your thesis be published commercially, please reapply for permission.

Elsevier Open Access Terms and Conditions

Elsevier publishes Open Access articles in both its Open Access journals and via its Open Access articles option in subscription journals.

Authors publishing in an Open Access journal or who choose to make their article Open Access in an Elsevier subscription journal select one of the following Creative Commons user licenses, which define how a reader may reuse their work: Creative Commons Attribution License (CC BY), Creative Commons Attribution – Non Commercial - ShareAlike (CC BY NC SA) and Creative Commons Attribution – Non Commercial – No Derivatives (CC BY NC ND)

Terms & Conditions applicable to all Elsevier Open Access articles:

Any reuse of the article must not represent the author as endorsing the adaptation of the article nor should the article be modified in such a way as to damage the author's honour or reputation.

The author(s) must be appropriately credited.

If any part of the material to be used (for example, figures) has appeared in our publication with credit or acknowledgement to another source it is the responsibility of the user to ensure their reuse complies with the terms and conditions determined by the rights holder.

Additional Terms & Conditions applicable to each Creative Commons user license:

CC BY: You may distribute and copy the article, create extracts, abstracts, and other revised versions, adaptations or derivative works of or from an article (such as a translation), to include in a collective work (such as an anthology), to text or data mine the article, including for commercial purposes without permission from Elsevier

CC BY NC SA: For non-commercial purposes you may distribute and copy the article, create extracts, abstracts and other revised versions, adaptations or derivative works of or from an article

(such as a translation), to include in a collective work (such as an anthology), to text and data mine the article and license new adaptations or creations under identical terms without permission from Elsevier

CC BY NC ND: For non-commercial purposes you may distribute and copy the article and include it in a collective work (such as an anthology), provided you do not alter or modify the article, without permission from Elsevier

Any commercial reuse of Open Access articles published with a CC BY NC SA or CC BY NC ND license requires permission from Elsevier and will be subject to a fee.

Commercial reuse includes:

- Promotional purposes (advertising or marketing)
- Commercial exploitation (e.g. a product for sale or loan)
- Systematic distribution (for a fee or free of charge)

Please refer to Elsevier's Open Access Policy for further information.

21. **Other Conditions**:

v1.7

VITA

Tran Doan Ngoc Tran was born in Ho Chi Minh City, Vietnam to Tran Van Khanh and Doan Thi Phuong Tra in 1983. She received a D.V.M from Nong Lam University in 2006. Tran worked in the National Veterinary Company in Ho Chi Minh City, Vietnam until late 2010. Tran was accepted as a graduate assistant under supervision of Dr. Henrique Cheng for a Ph.D. degree in Department of Comparative Biomedical Sciences in the School of Veterinary Medicine at the Louisiana State University, Baton Rouge from 2011 to present. Her research focused on the mechanisms controlling stem cell differentiation. She is expected to graduate by spring 2015.